IDENTIFYING THE VERSATILE ROLES OF NKX3.1 PHOSPHORYLATION TO EXPLORE NEW CASTRATION-RESISTANT PROSTATE CANCER THERAPY

by

Moloud Aflaki Sooreshjani

A Dissertation

Submitted to the Faculty of Purdue University

In Partial Fulfillment of the Requirements for the degree of

Doctor of Philosophy

Department of Chemistry

West Lafayette, Indiana

May 2021

THE PURDUE UNIVERSITY GRADUATE SCHOOL

STATEMENT OF COMMITTEE APPROVAL

Dr. Kavita Shah, Chair

Department of Chemistry

Dr. Sandra S Rossie

Department of Biochemistry

Dr. Shalini Low-Nam

Department of Chemistry

Dr. Betsy Parkinson

Department of Chemistry

Approved by:

Dr. Christine Hrycyna

ACKNOWLEDGMENTS

I would like to express respect to my research supervisor, Prof. Kavita Shah for allowing me to work in her lab. Her guidance, encouragement, and fruitful criticism have all contributed to the successful completion of this thesis. Her enterprising and enthusiastic approach to research has been a source of inspiration for me. I cordially acknowledge Prof. Shalini Low-Nam for supporting me at professional fronts throughout. She has been very approachable for a productive discussion about work. I would also like to acknowledge Prof. Sandra Rossie and Prof. Betsy Parkinson for their help. I acknowledge Dr. Nikhil Kumar for helping me when I entered the lab. I also acknowledge the friendly support of Dr. Mohini Kamra in the lab. I also acknowledge my lab members Wanzhang Pan, and Humphrey Lotana, and Dung N Nguyen for their all-time support. I also acknowledge Nicolas De Cordoba and Roy Rajeev for helping to review the thesis. I can never thank my family enough who are the source of light and life for me. They have been very understanding and supportive of me and always shown me the best paths to move ahead at different stages of my life.

TABLE OF CONTENTS

LIST OF TABLES

LIST OF FIGURES

ABSTRACT

As reported by the world health organization in 2020, prostate cancer is one of the leading forms of cancer in humans affecting approximately 191,930 men. Studies have shown that castration-resistant prostate cancer (CRPC) could develop even if the patient has undergone surgical procedures and radiotherapy. Thus, understanding the mechanism that causes CRPC could result in promising CRPC therapeutic approaches. Several approaches such as targeting Aurora A kinase, an oncogene overexpressed in multiple cancer types, have not been successful since AURKA is vital for cell survival. LIMK2 is a kinase that directly regulates AURKA and could be a better target. Recently our lab has shown that overexpression of LIMK2 results in the upregulation of AURKA and vice versa. However, five substrates of LIMK2 have been published so far amongst which 3 were identified by Shah *et al*. In this study, we have identified NKX3.1, a transcription factor for cell proliferation and differentiation, as a substrate of both AURKA and LIMK2. Interestingly, we have shown that overexpression of NKX 3.1 leads to downregulation of LIMK2 and AURKA. Herein, we focus on the direct communication between NKX 3.1, AURKA, and LIMK2 to develop a CRPC therapy targeting LIMK2 and NKX 3.1 as direct regulators of AURKA.

CHAPTER 1. LITERATURE REVIEW

1.1 Significance of kinases in cell signaling

Well-regulated intracellular signal transduction is a fundamental feature in noncancerous human cells. Under normal conditions, a cell will receive signals from either neighboring cells or the extracellular environment and then respond appropriately by changing its cellular biochemistry and physiology. One example is cell proliferation (1). Inappropriate intracellular cell signaling can lead to diseases such as cancer; therefore, understanding how cells coordinate signaling networks has important pharmacological implications (2).

Protein kinases modulate signal transduction and help control cell function (3). The scientific community has identified numerous kinases and determined their respective roles in signaling pathways; however, our understanding regarding the mechanisms of signaling pathways and their cellular functions is still limited. Therefore, identifying novel protein kinases and understanding their underlying mechanisms will provide useful insights into how signaling networks function (4).

1.1.1 Aurora kinases: therapeutic targets for cancer therapy

The protein kinase family is one of the largest and most diverse enzyme families. Kinases regulate a variety of biological processes via post-translational phosphorylation of their substrates. Post-translational phosphorylation modulates many cellular functions, such as cell proliferation, cell cycle, apoptosis, motility, and differentiation (5). The deregulation of kinases is oncogenic due to pathophysiological changes in the cell cycle (6). Moreover, kinase deregulation can cause the cell cycle to encounter errors in distributing chromosomes from the parent cell to the daughter cells, resulting in aneuploidy, chromosome instability, and other oncogenic properties (7). One family that has shown to have several significant roles in regulating the cell cycle is the Aurora kinase family (8). Multiple studies have denoted a strong correlation between deregulation of Aurora kinases and tumorigenesis through numerous mechanisms. These mechanisms include defective spindle poles, aneuploidy, and centrosome overgrowth (9).

1.1.2 Discovery of Aurora kinases

Aurora kinases were discovered originally by David Glover in 1989 when investigating the regulatory genes involved in Drosophila's cell cycle (8, 10). The study found that offspring produced by females carrying homozygous mutations of *aurora* had abnormally mitotic phenotypes in neuroblast cells (primitive neural cells) during the larval stage of development (10). More specifically, abnormalities were observed in the mitotic spindles as they were monopolar instead of bipolar (10). Such phenotypic changes suggested lesions affecting the centrosomes segregation. This improper segregation affects cell cycle progression (10). Reverse genetics studies identified Aurora kinases in the cell cycle by investigating the resulting phenotypes when Aurora kinases were mutated, overexpressed, or inhibited. In these studies, overexpression of Aurora-A would lead to centrosome overgrowth, multipolar spindles, aneuploidy, chromosomal separation defects, and tumorigenesis (11). Additionally, these abnormal phenotypes, notably aneuploidy and tumorigenesis, were likewise found to associate with Aurora-B overexpression. However, they could not determine whether the overexpression was the cause of tumorigenesis or vice versa (12). Furthermore, Aurora-C overexpression induces cell transformation and tumorigenesis. (13). These results suggested that the Aurora kinase family has a pivotal role in mitosis.

1.1.3 Evolution of Aurora kinases

Studies regarding homology and sequence similarity of the Aurora kinase family revealed that Aurora genes are evolutionarily conserved. The sequence similarities between human and rodent orthologs of Aurora kinases were 82% for Aurora-A, 84% for Aurora-B, and 78% for Aurora-C (14). Phylogenetic trees denoted that *Aurora* genes evolved from a single ancestral *AURKA* gene called *Ipl1* (Increased-In-Ploidy 1). *AURKA*, first identified in *Saccharomyces cerevisiae* and *Tunicata* (previously named *Urochordata*). *Ipl1* gene in *Saccharomyces cerevisiae* shows 41% sequence identity with the human *AURKA* gene (15).

1.1.4 Aurora kinase family members

Aurora kinases have three members in mammalian cells: Aurora-A, Aurora-B, and Aurora-C. Aurora-A and Aurora-B are both committed to the progression of mitosis in the cell cycle. Aurora-C has a unique function in meiosis (16).

1.2 Structures of Aurora kinase members

The structure of Aurora kinases is composed of three domains: an N-terminal domain, that consists of amino acids from position 39 to 139; a kinase domain, that consists of amino acids from position 250 to 300; a C-terminal domain, that covers amino acid from position 15 to 20 (17). The catalytic domains in aurora kinases are highly conserved; however, the N-terminal domains vary significantly. This variation is crucial as the N-terminal domain is crucial for specific protein-protein interactions(18).

The X-ray crystal structure of the human Aurora-A, when bound to TPX2, was solved at 2.75 A° resolution [Protein Data Bank (PDB) 1OL5]. The results showed that the catalytic domain of Aurora-A contains two lobes found in other kinases (19). The structure indicates that the catalytic domain of Aurora-A contains two lobes found in other kinases. These two lobes, connected by a hinge region, will be referred to as N-lobe and C-lobe. The N-lobe possesses two α-helices and a β-sheet (20). The C-lobe consists of α-helices and loops and is responsible for the active conformation (20, 21). TPX2 binds to the N-lobe of Aurora-A by the residues 7-21 and residues 30-40 (20).

AURKA has a low level of enzymatic activity; however, autophosphorylation of Thr288 enhances AURKA's catalytic activity. Thr288 is an essential residue found in the activation loop of AURKA (22). TPX2 a notable protein cofactor that increases AURKA activity by stabilizing Aurora-A kinase’s active form (22). AURKA interacts directly with TPX2 via the C- terminal that subsequently induces the conformational changes of the activation segment in the kinase. More specifically, TPX2 stabilizes Thr288-phosphorylation by changing the Thr288 position, making it inaccessible from PP1 phosphatase.

The C-terminal domain of Aurora kinases is conserved and has a “destruction box” (D-box). D-box is a short amino-acid peptide motif that is recognized by the anaphase-promoting complex/cyclosome (APC/C) and therefore targets Aurora kinases for proteasomal degradation (23). On the other hand, the N-terminal domain is less conserved, and its function has currently fallen short of a sophisticated understanding. This domain is noted to serve as the targeting site for ubiquitination by the ubiquitin-proteasome pathway (24). AURKA contains the A-box motif (residues 31–66). A-box is required for AURKA degradation by APC/C–Cdh1 (25). Besides, the N-terminal domain also has a KEN motif. The role of this motif remains unclear whether it is required for the AURKA ubiquitination and degradation or not is yet to be determined. In one facet of the discussion, an investigation with regards to the preferred site for ubiquitination has shown the importance of the motif as a ubiquitin acceptor for AURKA degradation (26). On the other hand, a study to identify the required elements for the AURKA degradation showed that the A-box and D-box are needed for the Cdh1-dependent destruction of AURKA. However, the KEN motif is not a prerequisite for AURKA degradation (25).

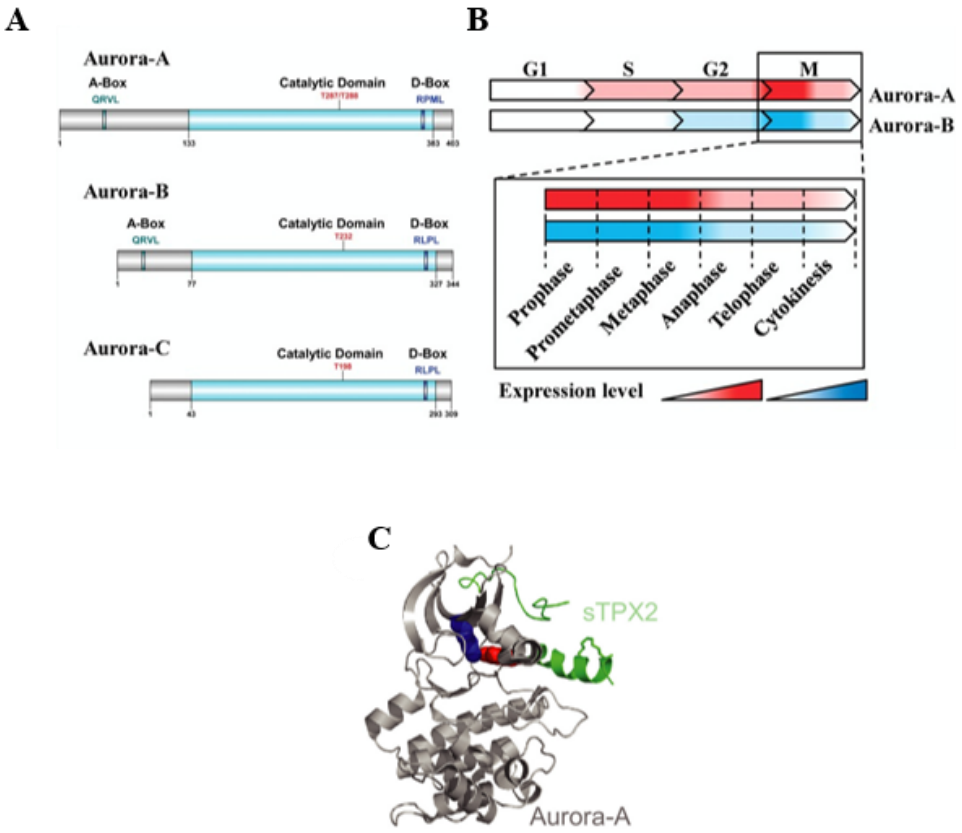

Figure 1-1. Structures and expressions of the Aurora kinase family.

(A) Illustrated Aurora kinases' domains. The catalytic domain of AURKA is highly conserved. D-box is in the carboxy-terminal. Furthermore, Aurora-A and Aurora-B have A-box. **(B)** The Aurora-A level was transitioning from a subtle level during the G1 phase to a more noticeable one during the S phase, particularly at centrosomes. The expression level of Aurora-A became prominent in the late G2-phase. Aurora-A is prominently on spindle poles during prometaphase and metaphase. AURKA expression started to reduce in the metaphase-anaphase transition. In the early anaphase, AURKA localized on the centrosomes and the spindles. During late anaphase and telophase/cytokinesis, AURKA localized to the spindle midzone and centrosomes. Aurora-B was found initially on pericentromeric heterochromatin during the late S phase. The protein kinase's level remained throughout mitosis with a peak in the G2/M phase. During the mitosis, Aurora-B targeted heterochromatin in the prophase, and its expression level increased centromeres during prometaphase. Aurora-B was then relocated to spindle microtubules during the early anaphase and the equatorial cell cortex during cytokinesis(27). **(C)** AURKA has two lobes that are similar to the other kinases (28).

1.3 AURKA as a novel target for cancer treatment

Research substantiates the consensus that AURKA carries a significant contribution to the progression of the cell cycle. Initially, when AURKA was found, its expression was observed to be upregulated in the transition of the G2-M phase and throughout the mitotic stages but downregulated gradually in the anaphase and eventually in the telophase and cytokinesis (29). This led to the hypothesis of a connection between AURKA expression and cell division (17). The

following discussion will focus on explaining in detail the relationship between Aurora-A and the cell cycle, plus how its overexpression could trigger tumorigenesis.

1.3.1 Biological functions of AURKA

Findings have long established that cancer is characterized by centrosome abnormalities, amplification, and aberrations (30). A study, which emphasized centrosome as the potent anti-cancer target, has underlined the coupling between centrosome duplication and DNA replication, mitosis, and cytokinesis (30). Ensuring the normality of cell division is, therefore, heavily reliant on the organization and duplication of centrosomes, which are further under the regulation of centrosome-associated proteins (30, 31). The influential protein among these is Aurora-A kinase, which is considered as one of the most studied centrosome kinases with an oncogenic relationship (30). Researchers found out that Aurora-A asserts its role significantly in the cell cycle by controlling cellular entry into mitosis, regulating centrosome maturation, binding microtubule at spindle poles, directing spindle assembly, and determining spindle polarity (32, 33). For example, AURKA phosphorylates transforming acidic coiled-coil (TACC) and promotes its association with XMAP215. Thus, Aurora-A stabilizes the centrosome microtubule (34). Besides, AURKA phosphorylates polo-like kinase-1 (PLK1) on T210 (35) and leads to PLK1 activation. Active PLK1 then associates with and phosphorylates CDC25C (cell division cycle 25C), which subsequently promotes mitotic entry by activating CDK1/cyclin B (36). AURKA phosphorylates CDC25B on S353 at the centrosome, and this phosphorylation may contribute to the control of mitosis (37). More specifically, CDC25B shows a significant role in the CDK1-cyclin B complex formation in G_2 and mitosis (38).

1.3.2 Expression of AURKA in cancer cells

As previously mentioned, while the causality in tumorigenesis due to the overexpression of Aurora-B and Aurora-C was not observed, AURKA's overexpression was concluded to possess the ability of tumor induction through chromosomal overgrowth and aneuploidy (39). A study investigating the underlying cause of aneuploidy cells in tumors has shown a correlation with centrosome amplification and instability plus chromosomal aberrations (40). A further observation from the study noted that a variety of tumor tissues (colon, pancreatic, ovary, breast, prostate, and

more) were characterized with the chromosome arm 20q's amplification, where the Aurora-A gene is located (39). An examination of the effects of AURKA overexpression has documented that aneuploidy can be triggered. It commonly causes tetraploidization due to centrosome amplification resulting from mitotic aberrations (41). Another quantitative analysis, which investigated the phenotype of cells with overexpressed Aurora-A, has noted observations of vastly abnormal structures, for example, extensive cytoplasmic connections (41). Additionally, 20% of cells that overexpressed AURKA showed manifestation of late mitotic stages and a delay in mitotic exit. Furthermore, the phenotypic consequences could exacerbate in the absence of p53 (also known as TP53), which is strongly linked to cancerous development due to failure in detection for hyperdiploid. Tumor protein 53 (TP53) works as a major tumor suppressor by sensing DNA damage, keeping the pace of the cell cycle under control, and inducing apoptosis. A study revealed that TP53 mutations occur in all cancerous cell types and ranging from 10% (in hematopoietic malignancies) to 100% (in high-grade serous carcinoma of the ovary), which shows how likely the consequences from Aurora-A overexpression can be worsened in tumor tissues (42). Moreover, Aurora-A is found to promote cell proliferation via upregulating mitotic substrates, including PLK1 (polo-kinase-1), TPX2, PP1, and LAST2, which in turn causes cell invasion and metastasis (43).

1.3.3 Aurora-A inhibition as a potential cancer treatment?

As AURKA overexpression is highly associated with tumorigenesis, Aurora-A inhibition may deem to be plausible as a cancer treatment. However, targeting Aurora-A was not successful in the clinical trial. Direct targeting of AURKA results in significant adverse side effects as Aurora-A contribution is important in cell division (28). Researchers likewise studying the consequences from Aurora-A inactivation in normal tissues have revealed that mitotic spindle fragmentation and defects in the formation of mitotic spindles can arise, which could cause unequal chromosome segregation and aneuploidy and trigger tumor formation (44).

1.4 Aurora-A kinase substrates

To gain information on how AURKA modulates signaling in the cells, it is essential to unravel its targets. Ferrari and coworkers conducted a peptide assay experiment to find the

consensus sequence that is phosphorylated by AURKA. Their results indicated that R/K/N-R-X-S/T-B, where B denotes any hydrophobic residue except Pro, is the consensus sequence **(figure1-2)** (45).

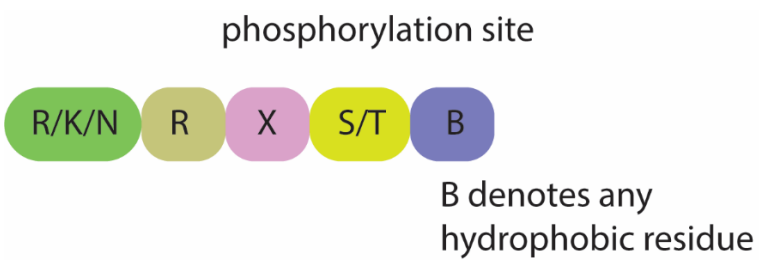

Figure 1-2. AURKA recognition sequence.

AURKA recognizes the consensus of amino acid R/K/N-R-X-S/T-B. B denotes any hydrophobic residue except proline. AURKA substrate specificity was determined by phosphoacceptor peptide following mass spectrometry analysis (45).

A study using a chemical genetic approach to investigate direct substrates for Aurora-A kinase has uncovered that TWIST1 is a direct substrate for AURKA. AURKA phosphorylates Twist1 at S123, T148, and S184 (46). AURKA-mediated Twist1 phosphorylation subsequently inhibits ubiquitin-mediated degradation in Twist1 and induces tumorigenesis *in vivo*. An investigation about uncovering the consequences from the AURKA-Twist1 axis in pancreatic cancer has highlighted an enhancement of epithelial-to-mesenchymal transition (EMT) and chemoresistance. EMT, along with cancer stem cells (CSC), are the underlying cause leading to metastasis, drug resistance, tumor recurrence, and high lethality (46). In other words, AURKA-mediated Twist1 phosphorylation promotes cancer cell growth. Twist1 regulates Aurora-A via a positive feedback loop and reciprocally prevents Aurora-A degradation at the protein level. Hence, ablation or inhibition of Aurora-A or Twist1 would result in an inhibition of EMT. Furthermore, the feedback loop between Aurora-A and Twist1 was observed to facilitate aggressive cancer phenotypes in pancreatic cells (46).

Our lab has recently found an additional novel and direct substrate of Aurora-A kinase in prostate cancer, which is Speckle-type POZ protein (SPOP) known as an E3 ubiquitin ligase substrate-binding adaptor protein (47). SPOP has been observed to be commonly mutated in

prostate cancer. An examination regarding the effects of prostate cancer-associated SPOP mutations has shown an enhancement of cancer cell survival via caprin1 (cell cycle-associated protein 1) (48). Three phosphorylation sites by Aurora-A on SPOP were identified to be at S33, T56, and S105 using a chemical-genetic technique (49). However, a key difference between the AURKA-mediated phosphorylation in SPOP with respect to LIMK2 and Twist1 is that Aurora-A negatively regulates SPOP, in which the ubiquitylation of SPOP was observed due to Aurora-A overexpression. Furthermore, Aurora-A inhibits AR degradation via the depletion of SPOP through phosphorylation. Also, phosphorylation SPOP by AURKA is correlated with oncogenic phenotypes, tumor progression, and EMT *in vivo*. Moreover, our lab has observed a reduction in tumor growth from the overexpression of SPOP in C4-2 cells. Thus, SPOP works as a tumor suppressor (49). An additional direct substrate of Aurora A, ALDH1A1, has been confirmed in our lab using the same method and observed the phosphorylation to occur at three critical residues (T267, T442, and T493). Like how Aurora-A exerts its effect on LIMK2 activity via T505 phosphorylation, Aurora-A regulates ALDH1A1 activity primarily via T267 phosphorylation (50). AURKA-mediated ALDH1A1 phosphorylation positively affects protein stability and dehydrogenase enzymatic activity and prevents ubiquitin-dependent degradation of proteins. The results from our lab suggested that the modulation of ALDH1A1 activity by Aurora-A could potentially be the pivotal path that Aurora-A enhances the phenotypes in EMT and CSC, which subsequently leads to increased cell motility, metastasis, and drug resistance (50). Furthermore, same as LIMK2 and Twist1, ALDH1A1 has also shown a positive regulation on Aurora A and prevents Aurora-A degradation. From the collective results in our lab, it is presumed that Aurora-A triggers highly and aggressively cancerous phenotypes via ALDH1A1-mediated EMT, CSC, motility, and drug resistance (50). Also, our lab has identified YBX1 as a direct substrate for Aurora-A. The group has identified two sites of direct phosphorylation by Aurora-A on YBX1 (T62, and S102). AURKA-mediated YBX1 phosphorylation leads to an inhibition of YBX1 degradation and promotes cancer progression (51). PHLDA1 is an AURKA substrate that is involved in apoptosis. AURKA phosphorates PHLDA1 at S98 and results in its downregulation and cancer progression (52).

Table 1-1. Aurora-A Kinase substrates (53)

This table is a gist of the known substrates and the respective consequence of AURKA-mediated phosphorylation.

Substrates	Substrate function	Targeted residue
Lats2	S83 phosphorylation of Lats2 disturbs its centrosomal localization. S380 phosphorylation regulates appropriate mitotic localization and mitotic progression	S83, S380
NDEL1	NDEL1 phosphorylation by AURKA regulates centrosome maturation.	S251
Cdc25B	Cdc25B phosphorylation activates its phosphatase activity and promotes G2-M transition.	S353
MCAK	MCAK phosphorylation increases bipolar spindle formation.	S196, S719
IκBα	IκBα is phosphorylated upon H_2o_2 stimulation and results in IKK and NF-κB activation.	S32, S36
Gsk3β	Gsk3β phosphorylation results in β-catenin phosphorylation and degradation. Thus, it leads to cancer progression.	S9
ASAP	ASAP phosphorylation by AURKA results in its localization to centrosomes from late G2 to telophase and results in proper mitotic progression.	S625
TACC3	Phosphorylation of TACC3 at S558 results in its localization on mitotic spindles and microtubule stabilization.	S558
CENP-A	Phosphorylation of CENP-A by AURKA modulates AURKB concentration at the centromeres.	S7
RASSF1A	Phosphorylation of RASSF1A inhibits RASSF1A-microtubules interaction and stimulates M-phase arrest.	S203, T202
HURP	AURKA phosphorylates and stabilizes HURP. Thus, HURP is a transforming target of AURKA.	S627, S725, S757, S830
P53	AURKA upregulation results in p53 degradation and contributes to the oncogenic phenotypes.	S215
Plk1	PLK1 phosphorylation by AURKA results in PLK1 activation and leads to mitotic entry.	T210
LDHB (54)	LDHB phosphorylation enhances glycolysis and tumor growth.	S162
KCTD12 (55)	KCTD12 and AURKA regulate each other in a positive feedback loop. This promotes cancer progression.	S243
SPOP (49)	E3 ubiquitin ligase substrate-binding adaptor protein. AURKA modulates SPOP in a negative feedback loop. SPOP downregulation induces oncogenic phenotypes.	S33, T56, S105
YBX1 (51)	Transcription factor in the nucleus, RAN-binding protein in the cytosol. YBX1 and AURKA positive feedback loop promote aggressive cancer phenotype.	T62, S102
TWIST1 (46)	TWIST1 and AURKA positive feedback loop promote aggressive cancer phenotype.	S123, T148, S184
ALDH1A1 (50)	AURKA regulates ALDH1A1 quaternary structure, protein level, and enzymatic action and results in cancer progression.	T267, T442, T493
LIMK2 (56)	AURKA regulates LIMK2 in a positive feedback loop that leads to tumorigenesis.	S283, T494, T505
PHLDA1 (52)	AURKA regulates PHLDA1 in a negative feedback loop that leads to tumorigenesis. PHLDA1 overexpression results in cell death.	S98

1.5 LIMK2: A proposal target for cancer therapy regulated by Aurora-A

AURKA is a ser/threonine kinase, which is engaged in cell cycle progression, proliferation, and survival, and it has an oncogenic property in various cancers. Using a chemical approach to find Aurora-A kinase substrates, our group identified LIMK2 as the new Aurora A kinase substrate (57). *In vitro,* radioactive kinase studies demonstrated that LIMK2 is a direct substrate of Aurora-A kinase. Aurora-A kinase phosphorylates LIMK2 at S283, T494, and T505 positions. Studies have shown that overexpression of LIMK2 results in the upregulation of Aurora A kinase. More specifically, the lab found that Aurora A kinase upregulation is due to stabilization by LIMK2 (56). Thus, it is essential to study the role of LIMK2, a crucial oncogenic target of Aurora-A.

1.6 A Comprehensive review of LIMK

Studies into the mechanism of cytoskeleton remodeling and its role in signaling pathways led to the identification of LIM kinase. It was shown that LIMK phosphorylates cofilin leads to cytoskeleton dynamics regulation. Subsequent studies of LIMK2 function have revealed the importance of LIMK in cancer. Diverse kinases regulate LIMK. This initiates downstream signaling (58).

1.7 Discovery of LIMK

In 1994 Mizonu et al. screened a cDNA library in human hepatoma HepG2 cells to identify novel c-Met/HGF receptor tyrosine kinases (59). However, the subdomain VIB analysis did not indicate whether LIMK can be determined as a serine/threonine or tyrosine kinase. A characteristic short sequence motif in subdomain VIB is used to determine protein kinases and substrate specificity. Tyrosine kinases use DLAARN or DLRAAN as the consensus sequence, while serine/threonine kinases have the consensus sequence of DLK*XX*N in subdomain VIB (60). However, the sequence motif of the LIMK family is DLNSHN which is not in agreement with either the consensus sequence for serine/threonine kinases or tyrosine kinases. Thus, LIM kinases are considered to have dual specificity of serine/threonine and tyrosine kinase (59).

1.8 Members of the LIMK family

LIM kinase 1 (LIMK1) and LIM kinase 2 (LIMK2) are two LIMK family members. LIMK1 was identified in 19941, and LIMK2 was identified in 1995 (61, 62). Human LIMK1 and LIMK2 genes were mapped to 7q11.23 and 22q12.2 chromosomes. LIMK1 contains 16 exons and 39,499 base pairs, whereas LIMK2 has 19 exons and 68,617 base pairs. The LIMK family has been discovered in Xenopus, chicken, rat, mouse, and human. The family has 50% global identity and 70% identity in the catalytic domain. Besides, human and mouse LIMKs have 92% homology (63). Although LIMK1 and LIMK2 have significant structural homology, they show different expression and subcellular localization. LIMK1 is expressed in the skeletal muscle, heart, and brain. However, LIMK2 is detected in all the tissues. LIMK1 is detected at focal adhesions. However, LIMK2 is detected in the cytoplasm. However, LIM kinases share some related roles, like, the role in cancer progression. Different localization and expression levels indicate that LIMK1 and LIMK2 might have unique cellular functions (64).

1.9 LIMK2 structure

LIMK2 is a dual serine/threonine and tyrosine kinase that has two LIM domains. LIM domains are located at the N-terminal region. Besides, LIMK2 has a PDZ domain, a proline/serine-rich, and a kinase domain. The kinase region is located at the carboxy-terminal region (59, 65).

1.9.1 Gene Architecture of LIMK2

Northern blot analysis of rat tissues provided evidence for the existence of a potential LIMK2 spliced variant. The identified spliced variants are LIMK2-1, LIMK2-2a, and LIMK2-2b, each characterized by their boundaries (65, 66). LIMK2-1 (GenBank NM_001031801) is different from the others in the 5′ untranslated regions (UTR) and codes the largest protein. *In silico* analysis indicated that LIMK2-1 is only present in the Hominidae primate. LIMK2-1 is detected in both mRNA and protein levels in the human brain. These data indicate that LIMK2-1 is engaged in neurodevelopment and cognitive disorders. LIMK2-1 has a phosphatase 1 inhibitory domain (PP1i) in its C-terminal. PP1i shows an inhibitory effect on phospho-cofilin and inhibits PP1 partially and therefore increases the phospho-cofilin level **(figure 1-3A).** Thus, cofilin is not being phosphorylated by LIMK2-1 (67, 68).

Two complete LIM domains are present in LIMK2. However, LIMK2b has one and a half LIM domains since 17 amino acids substitute the N-terminal part of the initial LIM domain. LIMK2a and LIMK2b distribute differently in tissue (65, 69). While *LIMK2a* transcripts were present in the stomach, liver, and colon *LIMK2b* was detected mainly in the brain, kidney, and placenta (65). While there is now determined that LIMK2 has different isoforms and has a significant role in cytoskeleton remodeling and cancer development, the mechanism through which this occurs by each isoform is still unclear. Several lines of evidence suggest differences in several respects. LIMK2a and LIMK2b show different subcellular localization: While LIMK2a is found in the nucleus and the cytoplasm, LIMK2b is mainly detected in the cytoplasm and the subcellular localization of LIMK2-1 has not well studied. Stability analysis revealed that LIMK2a is more stable than LIMK2b. LIMK2a turn-over is about 24 hours, LIMK2b turn-over is 6h (70). Unlike LIMK2b and LIMK2-1, LIMK2a is not a target of p53 (71). Most studies on LIMK2 did not specify which isoform was under investigation and functional differences between these isoforms remain a still mystery in the *LIMK2* field.

1.9.2 Protein structure of LIMK2

LIM is named after the initial identification of the motif in three proteins Lin-11, Isl-1, and Mec-3. LIM domains are characterized by a double zinc-finger motif consisting of (C-X2-C-X16-23-H-X2-C)-X2-(C-X2-C-X16-21-C-X2- H/D/C) sequence **(figure1-3B)**. Aspartic acid, cysteine, and histidine form two tetrahedral zinc-binding pockets that stabilize LIMK2's structure (72). The LIM domain is made of a β-sheet. The β-sheet is formed by the β1-IV **(figure1-3C)** (73). LIM domain is involved in protein-protein interactions. Unlike other LIM domains that are engaged in interaction with DNA, the LIM domains of LIMK do not associate with DNA. *In vivo* and *in vitro* binding analysis revealed that the LIM domains of LIMK1 are involved in interaction with proteins. More specifically, the N-terminal LIM domains of LIMK1 binds to the domain and sequesters the kinase activity (74, 75). Association of LIM domains with the other activators might release its inhibitory effect and result in kinase activation. As with LIM domains of LIMK1, the LIM domains of LIMK2 regulates kinase activity, although LIMK2 uses a different mechanism. The LIM domains of LIMK2 masks the NLS and regulates its shuttling. Given the differences between LIMK1 and LIMK2, the LIM domain of LIMK2 might have different mechanisms in kinase activity regulation (74, 75).

PDZ is the initial letter of PSD-95 (PSD-95 is a 95 kDa protein that regulates signaling at the postsynaptic density), DLG (the Drosophila melanogaster Discs Large protein), and ZO-1 (the zonula occludens 1 is a scaffold protein that plays role in epithelial polarity) in which the domain was identified. The PDZ domain has six ß-strands and two α-helices and interacts with binding proteins **(figure1-3D)** (76).

The X-ray crystal structure of LIMK1 has shown a canonical protein kinase domain containing 12 conserved subdomains **(figure1-3E)**. These subdomains fold into two lobes: N-terminal and the C-terminal lobe. The N-terminal lobe is the smaller lobe and has one α helix, which is called the C helix, and a five-stranded β sheet. 20-35 residues in the c lobe made the activation loop and spans between DFG and APE motif and renders a docking site for the substrate (77). Activation loop phosphorylation stabilizes kinase open conformation. A cleft between N and C lobes provides an ATP-binding pocket. P loop is a glycine-rich sequence that allows the loop to turned in toward the phosphates of ATP and stabilize the ATP conformation (73, 78).

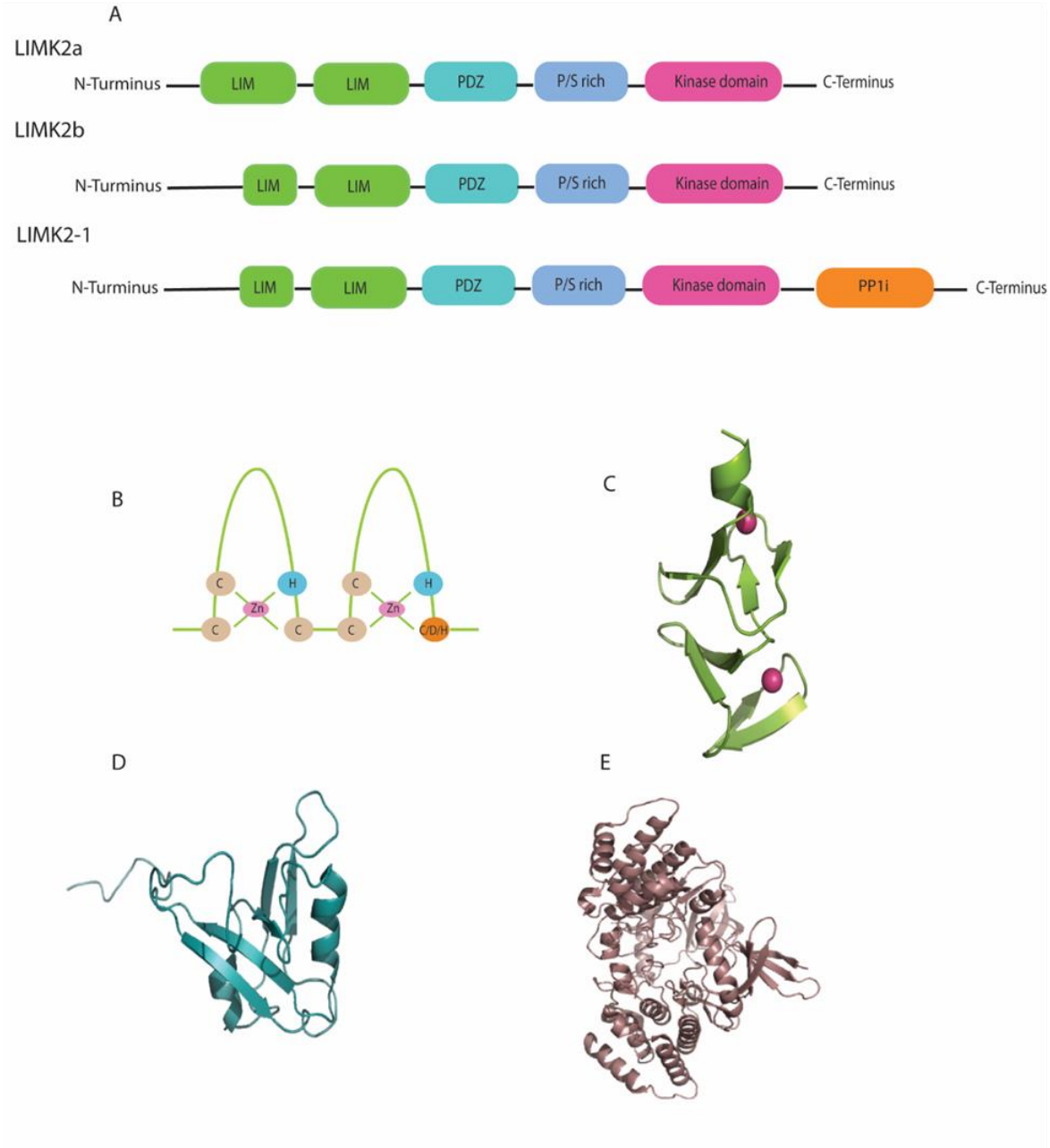

Figure 1-3. LIMK2 structure

LIMK2 isoforms. Two complete LIM domains are present in LIMK2. However, LIMK2b has one and a half LIM domains. LIMK2-1 has a phosphatase 1 inhibitory domain (PP1i) in its C-terminal (67, 68)**. (B)** LIM domain illustration. LIM domains are characterized by a double zinc-finger motif (73)**. (C)** LIM domain structure. The LIM domain is made of a β-sheet. The β-sheet is formed by the β1-IV (73)**. (D)** PDZ domain structure. The PDZ domain has six ß-strands and two α-helices (76). **(E)** Kinase domain structure. These subdomains fold into two lobes: N-terminal and the C-terminal lobe (73, 78).

1.10 Regulation of LIMK2

Protein kinases are activated in the presence of upstream signals. These inputs cause the binding of the kinase to the activator or kinase phosphorylation. LIMK2 activity is modulated positively by multiple upstream stimuli, including Rho-associated kinase, Protein kinase C, Aurora A, and p53. In contrast, as discussed above, N-terminal LIM domains have a suppressive role in LIMK1 activity. LIM domains interact with the kinase domain. Lim domain-kinase interaction results in kinase-inactive conformation stabilization. LIM domains might also prevent kinase catalytic site or substrate-binding site from interacting with the substrate. Association of LIM domain with the other activators can release its inhibitory effect (75). Although the LIM domain acts as a negative regulator of LIMK1 or possibly LIMK2, it is not clear if LIM interaction with the kinase domain is an inter or intramolecular association. It also needs to determine if this inhibition is mediated by any other protein binders. Nevertheless, the LIM domain is an important regulator of LIMKs activity (75).

1.10.1 Post-translational modifications LIMK2

Rho-associated kinase, Protein kinase C, and Aurora-A have a regulatory effect on LIMK2 by post-translational modifications. These modifications affect the behavior of LIMK2, including alterations in its activity, subcellular localization, and protein-protein interaction (75).

1.10.2 ROCK regulates LIMK2 activity by phosphorylation

Phosphorylation of threonine 508 by Rho-kinases, PAK1, and PAK4 activates LIMK1. However, LIMK2 is activated by Rho-kinase and MRCKα at Thr505. Rho-associated kinase (Rho-kinase/ROCK/ROK) is a downstream target of small GTPase and regulates cytoskeleton dynamics. Rho GTPases switches between GDP- and GTP-bound states where the GDP-bound state is the inactive form, and the GTP-bound state is the active form. GTPases recognize target proteins in a GTP-bound state and respond to stimuli until hydrolysis of GTP (79). Sumi *et al.* have shown that ROCK directly phosphorylates LIMK2 at Thr505 and results in cytoskeleton rearrangement (80-82).

1.10.3 PKC regulates LIMK2 localization by phosphorylation

Protein kinase C (PKC) regulates LIMK2 phosphorylation and localization. LIMK2 is mainly found in the cytoplasm. However, tLIMK2 has been detected in the nucleus. tLIMK2 does not have LIM domains. This observation suggested that the LIM domain masking by NLS is not the only mechanism to regulate LIMK2 localization (83). Analysis of LIMK2 by FRAP and FLIP shows that LIMK2 moves between the cytoplasm and the nucleus, where PKC has a significant role in this transportation. PKC is a serine or threonine kinase that targets Ser and Thr in basic sequences. PKC phosphorylates LIMK2 directly at Ser283 and regulates LIMK2 shuttling. The stimulation of PKC with PMA, a potent activator of PKC, results in inhibition of nucleus localization of LIMK2. More specifically, PKC stalls LIMK2 nuclear internalization by phosphorylation of LIMK2 at Ser283 (74). These data support the importance of PKC in LIMK2 phosphorylation and localization.

1.11 Transcriptional regulation of LIMK2

LIMK2 is regulated by P53 and MED12 at the transcriptional level, and this results in tumorigenesis regulation.

1.11.1 LIMK2b is a *p*53-transcriptional target.

P53 is a DNA-associated protein that coordinates the expression of stress response genes. Mutations in *TP53* lead to loss-of-function of P53 and reduces the ability of DNA damage checkpoints and repair mechanisms. Thus, it initiates cancer. Also, some mutant p53 proteins are oncogenic. Recent findings have indicated that p53 targets LIMK2b at the transcriptional level (71).

Alternative splicing produces two main LIMK2 transcripts: LIMK2a and LIMK2b. LIMK2a is a full-length transcript. However, LIMK2b lacks a half portion of the first LIM domain, and instead, a random sequence is substituted. Recent studies have indicated that p53 targets LIMK2b directly following genotoxic stress. The upregulation of LIMK2 by p53 promotes cancer cell survival and contributes to chemoresistance (71).

1.11.2 LIMK2 is a MED12-transcriptional target

The Mediator is a multiprotein complex that has remained conserved during evolution, and it regulates protein-coding genes. One of the subunits of Mediator is MED12, whose upregulation has been observed in prostate cancer (84, 85). Surprisingly, the RNA-seq experiment has shown that the transcript level of LIMK2 was increased in the cells that MED12 is knocked out. It turns out that activated LIMK2 promotes the phosphorylation cofilin, which changed actin-relevant gene expression in NSCLC cells. Cofilin phosphorylation led to multinucleation of the cells and cytokinesis defects. This means MED12 downregulated LIMK2 to affect cytokinesis and promote tumorigenesis (54).

1.12 Downstream effectors of LIMK2

The currently reported targets of LIMK2 appear to be cofilin and TWIST1. We will, therefore, begin with an introduction to these substrates.

1.12.1 LIMK2 Phosphorylation on cofilin and modulation on cytoskeleton dynamics

Cofilin is a small (19 kDa) abundant protein that regulates the dynamics of actin. It binds to G- and F-actin with a preference for ADP-bound actin subunits and decorates the filaments. (86) Then, the filament is severed near boundaries between cofilin-decorated and bare regions (87). LIMK2 phosphorylates cofilin at Ser3 and results in cofilin inactivation (88, 89).

1.12.2 LIMK2 phosphorylation on TWIST1 promoting cancer

Twist1 is a transcription factor, and it is a part of the basic helix-loop-helix (bHLH) family. The family is described by two α-helices linked by a short loop. (90, 91). Twist1 was originally found in Drosophila embryos as a factor for dorso-ventral patterning that leads to mesoderm formation. *Drosophila* embryos deficient in the *Twist1* gene cannot gastrulate, and they die with a ‘twisted’ form (92). Twist1 is also linked with several types of cancer, like prostate cancer. Several studies have revealed that Twist1 promotes EMT and cancer metastasis (90, 91). TWIST1 is phosphorylated by LIMK2 at S199, S95, S78, and S45. LIMK2 stabilizes TWIST1 by inhibiting

its ubiquitination. TWIST1 also stabilizes LIMK2 at the protein level that leads to the upregulation of LIMK2. This positive feedback loop results in cancer progression and development (93).

1.12.3 LIMK2 phosphorylation PTEN

PTEN is a tumor suppressor that is phosphorylated by LIMK2 at S207, S361, S226, S360, and S362. This leads to PTEN downregulation by ubiquitination pathway. Also, LIMK2 sequesters PTEN enzymatic activity. PTEN also regulates LIMK2 in a negative feedback loop. This results in cancer progression (94).

1.12.4 LIMK2 phosphorylation SPOP

SPOP is an E3 ubiquitin ligase adaptor that is phosphorylated by LIMK2 at S59, S226, S171, and S226. This results in SPOP degradation by ubiquitination pathway and tumor progression (95).

Table 1-2. LIMK2 substrates

This table is a gist of the known substrates and the respective consequence of LIMK2-mediated phosphorylation.

Substrates	Substrate function	Targeted residue
Cofilin (88, 89)	Regulation of cytoskeleton dynamics	S3
SPOP (95)	E3 ubiquitin ligase substrate-binding adaptor protein. SPOP and LIMK2 negative feedback loop promote tumorigenesis.	S59, S226, S171, S226
PTEN (94)	LIMK2 regulates PTEN expression and enzymatic function negatively. PTEN also regulates LIMK2 in a negative feedback loop. This results in cancer progression.	S207, S361, S226, S360, S362
TWIST1 (93)	LIMK2 increases the mRNA and protein level of TWIST1. TWIST1 also upregulates LIMK2 protein level. This positive feedback loop promotes cancer aggressive phenotypes.	S199, S95, S78, S45

1.13 MicroRNA and LIMK2 regulation

1.13.1 MicroRNA and cytoskeleton dynamics

MicroRNAs (miRNA) are non-coding RNAs with 22 nucleotides that regulate several biological activities such as cell differentiation and homeostasis. Deregulation of miRNA is linked

to cancer (96). miRNAs regulate Rho GTPase members, their effectors, and their regulators' expression. For example, miR-31 targets Rho A and inhibits cell metastasis (97). Along with Rho, microRNAs regulate cytoskeletal remodeling. For example, miRNA-142, miR-142-3p represses cytoskeleton regulators such as Grlf1, Wasl, Twf1, Cfl2, and Itgav, therefore leading to the proper execution of actin-dependent proplatelet formation (98). MicroRNA-23b is involved in the regulation of cellular architecture by regulation of cytoskeleton dynamics. More specifically, microRNA-23b promotes cell-to-cell interaction and reduces cell motility and invasion (98).

1.13.2 MicroRNA regulation on LIMK2

Single nucleotide polymorphisms (SNPs) in the binding site of microRNA are linked to cancer progression. SNPs could change microRNA-mRNA interaction, thereby change their binding. Consequently, it modulates protein expression (99). For example, SNPrs2073859 changes G to A and decreases MiR-135a binding to the *UTR* regain of *LIMK2* gene. The A allele expression is higher than the G allele in cancer cell lines and tissues. These data indicate that miR-135a binds to the G allele stronger and regulates LIMK2 expression negatively (99). miR-192 is another regulator of LIMK2 phosphorylation. miR-192 is a tumor suppressor and negatively regulated tumor cell initiation and progression. MiR-192-5p inhibits the phosphorylation of LIMK2 (p-LIMK2), which results in cell growth inhibition (100).

1.14 LIMK2 involvement in cancer

Cancer is a complex disease, and dysregulation of cellular signaling pathways underlies most of the characteristics that promote tumorigenesis. Cellular studies have revealed that LIMK2 signaling has a key role in cancer progression (101). As reported, LIMK2 overexpression enhanced multinucleation in the cells and modulate cytoskeleton stability (70). LIMK2 is upregulated in hypoxia and contributes to chemoresistance in neuroblastoma cell lines (71).

1.15 Is LIMK2 inhibition effective in cancer therapy?

Inhibitors of LIM kinases are considered of interest in cancer (102). However, the number of reported LIMK inhibitors remains low compared to other kinase targets, and most reported inhibitors target LIMK1 (103). Two series of LIMK inhibitors have been proposed by Bristol-

Myers-Squibb: 5-thiazolopyrimidine and pyrazolo series (104). Lexicon Pharmaceuticals proposed LX-7101 as the potential inhibitor of LIMK2 to treat glaucoma (105). In 2009, Harrison and coworkers reported pyrrolopyrimidine class as the potential inhibitor of LIMK2 (106). In 2013, Hou and coworkers' theoretical study determined that Ile408, Leu337, Val358, Ala345, and Leu458 are critical residues for the interaction with the inhibitors (107). Goodwin and coworkers used high-throughput screening followed by optimization efforts to identify a sulfonamide as a novel inhibitor (108). They found LIMK2 selective inhibitor by IC_{50} of 0.0039 μM.

1.16 Objectives: To Uncover AURKA and LIMK2-mediated in prostate cancer

Prostate cancer is the second most prevalent cancer in men in the USA (109). it is anticipated that 1 in 6 men will suffer from prostate cancer (110). Different chromosomal alterations have been observed in prostate cancer, including losses of 16q, 10q, 13q, 8p, and gains of Xq, 7p, 8q, and 7q. (111). Tumor susceptibility genes that are linked to these chromosomal alterations are PTEN (phosphatase and tensin homolog), NKX3.1, c-Myc (v-myc myelocytomatosis viral oncogene homolog), AR, and Rb (retinoblastoma 1) (112). NKX3 belongs to the homeobox genes, which are considered transcription factors. They contain 180 nucleotides in the DNA sequence and are involved in embryonic development (113). NKX3.1 is considered a tumor suppressor whose expression is reduced in prostate cancer. Immunohistochemical analysis has revealed the correlation of the progression of prostate cancer with loss of NKX3.1 (114-116).

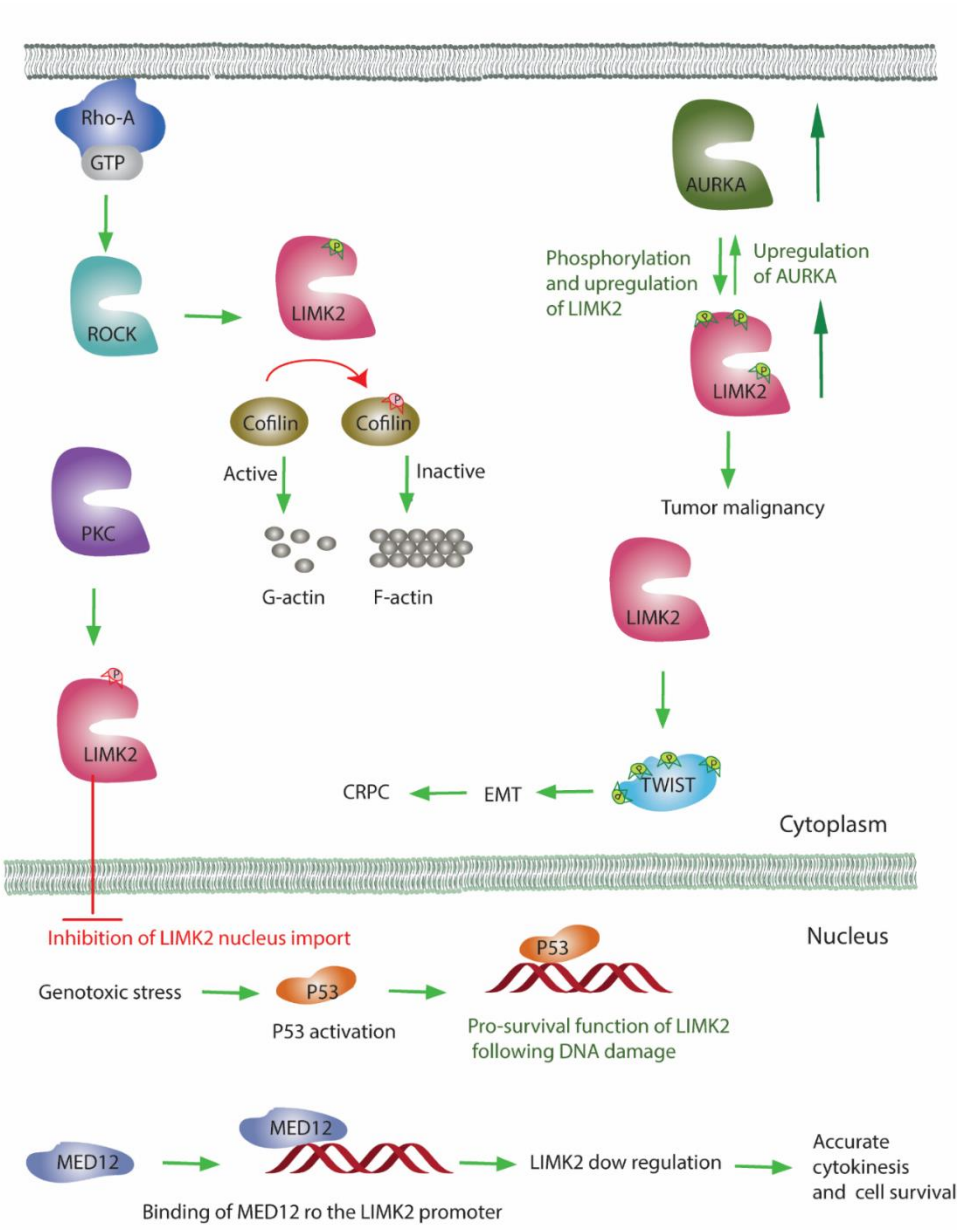

Figure 1-4. LIMK2 signaling

LIMK2 is activated by Rho-kinase at Thr505 (79). LIMK2 phosphorylates cofilin at Ser3 and results in cofilin inactivation (88, 89). Cofilin binds to G- and F-actin with a preference for ADP-bound actin subunits and decorates the filaments (86). Then, the filament is severed near boundaries between cofilin-decorated and bare regions (87). Aurora-A kinase phosphorylates LIMK2 and regulates LIMK2 in a positive feedback loop that leads to tumorigenesis (56). TWIST1 is phosphorylated by LIMK2. TWIST1-LIMK2 positive feedback loop promotes cancer aggressive phenotypes (93). P53 targets LIMK2b directly following genotoxic stress. The upregulation of LIMK2 by p53 promotes cancer cell survival and contributes to chemoresistance (71). MED12 downregulates LIMK2 and modulates tumorigenesis (54).

CHAPTER 2. MATERIAL AND METHOD

2.1 Cell lines and tissue culture

DMEM with 10% FBS was utilized to culture Phoenix and HEK-293T cells. RPMI with 10% FBS was used to culture C4-2 and 22Rv1 cells. All cell lines were incubated at 37 C, 5% C02. The cells were purchased from the American Type Culture Collection (ATCC).

2.2 Cloning and Site-Directed Mutagenesis

Full-length human NKX3.1 was N-terminally fused with Histidine cloned into a pTAT-HA and DH5α *E. Coli* cells. Bacterial competent cells were prepared using the Inoue method. NKX3.1 was cloned in p-TAT-HA vector at BamH1 and Xho1 sites and proteins were expressed in *Escherichia coli* BL21 (DE3) cells.

2.3 Transformation and production of DNA

Competent *E. coli* cells were mixed with DNA. The cell-DNA mixture was kept on ice for 30 minutes. The cells were placed at 42 ^{O}C for 45 seconds. Subsequently, the cells were put on ice for 120 seconds. Next, 1 mL LB broth was put into the cells and grown at 37 ^{O}C, 225 rpm for 1 hour to recover from heat shock. Following recovery, cells were spined at 1000 rpm for 5 minutes and plated on LB agar. Plates were kept for 16 hours at 37 ^{O}C. For DNA production, a 30 mL culture having 100 µg/mL carbenicillin was inoculated from the transformed plates and grown at 37 ^{O}C, 225 rpm for 10 hours. DNA was isolated from bacteria using standard mini-prep columns.

2.4 Protein production and purification

The DNA was transformed into *Escherichia coli* BL21 (DE3). A single colony from a transformed was inoculated in a 30 mL starter culture containing 100 µg/mL carbenicillin and incubated at 37 ^{O}C, 225 rpm for 10 hours. The culture was then centrifuged and washed with 20 mL of fresh media to remove any B-galactamase secreted by the bacteria into the culture media. Then the washes pellet was added to the flask having 600 ml LB broth. The cells were incubated at 37 ºC till an OD_{600} of 0.5-0.6. The protein was expressed by using 50 µM (isopropyl ß-D-1-

thiogalactopyranoside) IPTG for 8 hours at 22 ºC. Then the cells were collected by spinning at 6000 g. The cells were resuspended in a lysis buffer (50 mM Tris, pH 8.0, 10% glycerol, 500 mM NaCl, 1% NP-40, and 1 mM PMSF). Subsequently, the cells were lysed with the French press. The cells and medium separation were done using centrifugation at 10000 g for 20 min. During this step, 100 µL of Ni-NTA beads were washed with washing buffer (150 mM NaCl, 50 mM Tris, pH 8.0). Then, the soluble fraction and Nickel NTA agarose bead were incubated for 1 hour at 4 ºC. The beads were washed twice with low stringency wash buffer (150 mM NaCl, 50 mM Tris, pH 8.0), twice with medium stringency wash buffer (150 mM NaCl, 50 mM Tris, pH 8.0, 10 mM imidazole), and once with high stringency wash buffer (50 mM Tris, pH 8.0, 150 mM NaCl, 20 mM imidazole). After washing the beads, the protein was eluted using an elution buffer (250 mM imidazole, 50 mM Tris, pH 8.0).

2.5 *In vitro* kinase assay

The *in vitro* kinase assay for LIMK2 was performed as reported before (93). Briefly, LIMK2 was purified from Sf9 cells on Ni-NTA beads. LIMK2 was activated by 100 µM ATP in a buffer containing 50 mM Tris, and 10 mM $MgCl_2$ for 2 hours. The kinase activity of LIMK2 toward NKX3.1 was determined by incubating NKX3.1 (wild type or mutant protein) and 0.5 mCi [γ-^{32}P-ATP] at room temperature for half an hour. SDS-PAGE loading dye was used to stop the reaction. The SDS-PAGE gel was used to separate the proteins. The potential radioactivity was obtained by autoradiography.

2.6 DNA Transfection in Phoenix cells and retrovirus generation, cell infection and stable cell line generation

Constructs for the expression of S185A-NKX3.1 and S3A-NKX3.1 were created by overlapping PCR, subcloned into a puromycin-inducible retroviral expression vector VIP3.To generate retrovirus, Phoenix cells were transfected by NKX3.1-encoding plasmids using calcium phosphate. The media was changed after 8 hours. The supernatant containing the retrovirus was harvested 24 hours after the transfection. The virus was used to infect the prostate cancer cell lines (C4-2 and 22Rv1) using 8 mg/ml polybrene. 12 hours after infection a fresh medium was added.

Protein expression was analyzed by western blot 32-34 hours after infection. Puromycin was used to make a stable cell line.

2.7 Mammalian lentiviral shRNAs

The expression of the anti-NKX3.1 and anti-LIMK2 was accomplished by sub-cloning into PLKO.1 lentivirus vector (Addgene). HEK-293T cells were used to transfect them with either NKX3.1 shRNA or LIMK2 shRNA or AURKA shRNA constructs in combination with psPAX2 packaging and pMD2G envelope plasmids. The media was changed 8 hours after transfection and the supernatant containing-lentivirus was saved 24 hours posttransfection. Prostate cancer cell lines (C4-2 and 22Rv1) were infected with the lentivirus using 8 mg/ml polybrene. Thirty-two hours later, the cells were lysed for western blot analysis.

2.8 Isolation of cytosolic and nucleus fractions

C4-2 and 22Rv1 cells were washed with cold PBS, following resuspension in 10 mM Tris, pH 7.9 containing 10 mM KCl, 1.5 mM $MgCl_2$, 0.5 mM DTT, 0.05% NP40 and 1mM PMSF. The cells were kept on ice for 10 minutes. The lysates were centrifuged at 3000 rpm for 10 min at 4 °C. The nuclear fraction was isolated from the pellet using 5 mM Tris, pH 7.9 containing, 0.2 mM EDTA, 1.5 mM $MgCl_2$, 300 mM NaCl, 0. 26% glycerol (v/v), 0.5 mM DTT and 1 mM PMSF. Then it was homogenized by passing 10 times using a 27½ gauge needle. The lysates were kept on ice for 30 minutes. Finally, the nuclear fraction was isolated by spinning at 24000 g at 4 °C for 20 minutes. The cytosolic and nuclear extracts were further analyzed by western blot.

2.9 Immunofluorescence assays

Fibronectin-coated glass coverslips were seeded with C4-2 and 22Rv1. Then they were infected by NKX3.1 shRNA, LIMK2 shRNA, and AURKA shRNA. Slides were washed with PBS 32-34 hours postinfection. Subsequently, the slides were fixed by 4% paraformaldehyde for 15 min at room temperature. Permeabilization was done using 0.05% Triton X-100. Then the cells were treated with the primary antibody for 16 hrs at 4°C. Then again, the slides were washed with PBS. The slides were incubated with secondary antibody conjugated FITC for 4 hrs. Zeiss Laser Scanning Microscope was used to image the cells.

2.10 RNA isolation

RNA was extracted by TRIzol™ Reagent. To do so, the cells were lysed in 1000 µl of TRIzol™ Reagent. The cell lysate was cleared by spinning at 12000 g at 4 °C. 200 µl of chloroform was mixed with clear supernatant. After 3 minutes of incubation, the samples were again centrifuged and 500 µl of isopropanol was mixed with clear supernatant. RNA was isolated by sping the samples at 12000 g at 4°C. Then 1 mL of 75% ethanol was added to wash the precipitate. The supernatant was discarded after centrifugation. The RNA was resuspended in 20 µL of RNase-free water.

2.11 Synthesis of cDNA from total RNA and analysis of gene expression

3µg of RNA was mixed with Oligo(dT) at 65°C for 10 min. cDNA was synthesized using 0.1M DTT, dNTP, 1µl MLV Reverse Transcriptase, and 1µl of RNase inhibitor for 60 min at 37°C. Reverse Transcriptase was inactivated at 95°C for 2 minutes. The RT-PCR was performed using iScript™ Reverse Transcription Supermix. GAPDH was used as the control.

2.12 Cell viability assay

Cells were plated in triplicates in a 24-well plate at 1000 cells per well. After 12 hours the cells were infected with the virus. To detect cell viability, 24- and 48-hours post-infection, 25 µl of 3-(4,5-dimethylthiazol-2-yl)-2,5-diphenyl tetrazolium bromide (MTT) was added to each well. The final concentration of MTT is 0.5mg/ml. The cells were incubated with the MTT reagent for 4 hours at 37 °C. Then the media was removed and 500 µl DMSO was added to each well. A microplate reader (Tecan Spark multimode) was used to read cell viability at the absorbance of 570 nm.

2.13 Soft-agar colony formation

0.5% agar was made by mixing an equal amount of 1% of Noble agar and RPMI 1640 containing 20% of FBS. and seeded in a 24-well plate as a base. Then 1250 cells were mixed with 500 µl of 0.7% agarose in RPMI 1640 having 20% of FBS and added on top of solidified base agar. 500 µl of RPMI 1640 having 10% of FBS was added per well. The cells were supplied every

3 days with the medium. We incubated the cells at 37 °C for 3 weeks. We stained the colonies with 0.01% crystal violet and finally detected them by a light phase-contrast microscope.

2.14 Migration assay

For the migration assay, RPMI 1640 having FBS was added to the bottom of a Boyden chamber. The cells were starved in serum-free media for 12 hours and placed on top of the chamber. A polycarbonate filter membrane (Nuclepore Track-Etched Polycarbonate, Whatman) was used to separate RPMI 1640 with FBS and serum-free media. After 4 hours, the cells on the upper surface of the filter were cleaned by a cotton swab. Then, the membrane was placed on glass and counted under a microscope.

2.15 Ubiquitination assay

For the ubiquitination assay, Phoenix cells were transfected with 6-His Ubiquitin, NKX3.1, and LIMK2 separately. After 48 hours, target cells were coinfected with 6-His Ubiquitin and NKX3.1 (wild type or mutated plasmid) to detect LIMK2 ubiquitination. Similarly, target cells were coinfected with 6-His Ubiquitin and LIMK2 to detect NKX3.1 ubiquitination. To block the proteolytic activity of the 26S proteasome complex, cells were also treated with MG132 (Sigma) for12 hours. Then, the cells were lysed with 20 mM Tris, pH 7.4 having 0.25% Sodium deoxycholate, 150 mM NaCl, NP-40 1%, and 1 mM PMSF. Ubiquitination was analyzed by western blot analysis and the specific antibody against histidine.

2.16 C4-2 xenografts in nude mice

All mice were housed at the Purdue animal facility provided husbandry and clinical care. 106 cells were mixed with 50% matrigel and injected subcutaneously in nude mice. Tumor measurements were done every alternative day. Mice were sacrificed after 23 days of injection.

CHAPTER 3. LIMK2 AND NKX3.1 RELATIONSHIP

3.1 Hypothesis and specific aims

LIMK2 is a serine/threonine kinase that regulates cytoskeleton dynamics and is overexpressed in prostate cancer (93). The Shah lab's studies indicate that LIMK2 contributes to prostate cancer progression by phosphorylating PTEN (94), SPOP (95), and TWIST1 (93), all of which have a multitude of functions. Our studies indicated that LIMK2 is a promising target in castrate-resistant prostate cancer therapies, and its deletion reverts the tumorigenic phenotype (93). Although the role of LIMK2 in prostate cancer is well established, its mechanism of action remains unclear. Moreover, only a small number of LIMK2 substrates are currently known. Identification of additional LIMK2 substrates is a key step for discovering the role of LIMK2 in cancer progression. Here, we identified NKX3.1 as a new substrate for LIMK2 and unraveled the mechanism of LIMK2 and NKX3.1's crosstalk, which is involved in cancer progression. NKX3.1 is a gatekeeper suppressor and frequently deleted in prostate cancer. **We hypothesize that LIMK2 contributes to the tumorigenic phenotypes by phosphorylating NKX3.1 at specific sites. This phosphorylation then deregulates NKX3.1s expression.**

In this chapter, we plan to understand the role of LIMK2 in cancer progression by pursuing the following specific aims:

Aim1: We will examine how LIMK2 expression regulates NKX3.1 phosphorylation, expression, and localization.

Aim2: We will examine how NKX3.1 expression regulates LIMK2 expression and localization.

Aim3: We will identify the specific site in NKX3.1 that is phosphorylated by LIMK2. We will also examine the importance of the identified site in the aggressive oncogenic phenotypes.

3.2 Results

3.2.1 Aim1

In this aim, we will examine how LIMK2 expression regulates NKX3.1 phosphorylation, expression, and localization.

NKX3.1 is a substrate of LIMK2

Our primary screen proposed NKX3.1 as the potential substrate of LIMK2. To explore this, *in vitro* kinase assay has been performed using [γ-^{32}P] ATP. We purified NKX3.1 from bacteria and LIMK2 from Sf9 and then we performed the kinase assay. As shown in **figure 3-1**, LIMK2 phosphorylates NKX3.1 directly.

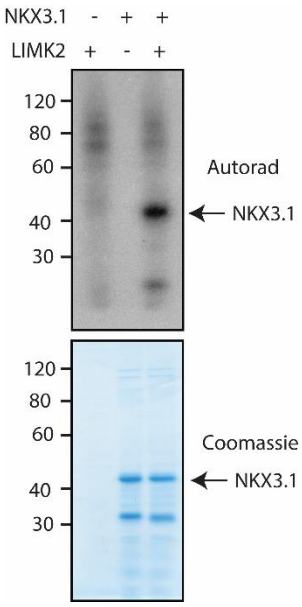

Figure 3-1. LIMK2 phosphorylates NKX3.1 directly.

LIMK2 and NKX3.1 were incubated with [γ-^{32}P] ATP. The mixtures were separated by SDS-PAGE. NKX3.1 phosphorylation was detected by autoradiography. The gel was stained with Coomassie Brilliant Blue. The upper panel shows an autoradiograph. The lower panel shows a gel stained with Coomassie blue. In lane1, LIMK2 was incubated with radiolabeled ATP and without NKX3.1. In lane 2, NKX3.1 was incubated with radiolabeled ATP and without LIMK2. In lane 3, NKX3.1 was incubated with radiolabeled ATP and LIMK2. *In vitro* kinase assay was repeated three times.

NKX3.1 promotes LIMK2 nuclear localization

Because LIMK2 phosphorylates NKX3.1, we next asked whether NKX3.1 and LIMK2 change the subcellular localization of one another.

To do so, the cells were treated with LIMK2 lentivirus for 32-34 hours. Then, NKX3.1 localization was checked with immunofluorescence analysis using NKX3.1 specific antibody. Immunofluorescence analysis indicates that the treatment of cells with LIMK2 lentivirus did not affect NKX3.1 localization in C4-2 cells **(figure 3-2 A)**. Consistent with immunostaining results, knockdown of LIMK2 lacked an effect on NKX3.1 localization using fractionation analysis in C4-2 cells **(figure 3-2B)**. We verified our data using 22Rv1 cells. In agreement with C4-2 cells, knockdown of LIMK2 did not affect NKX3.1 localization **(figure 3-2C, 3-2D)**.

We also treated the cells with NKX3.1 lentivirus. Then we checked LIMK2 localization using immunofluorescence and western blot analysis. Immunostaining data indicated that treatment of C4-2 cells with NKX3.1 lentivirus caused the distribution of LIMK2 from the cytosol to the nucleus **(figure 3-3A, 3-3B)**. To confirm our immunostaining study, we performed a subcellular fractionation analysis. As indicated in **figure 3-3C**, knockdown of NKX3.1 causes diffusely localized LIMK2 throughout the cell. We confirmed our data by using 22Rv1 cells. Consistent with data from C4-2 cells, the knockdown of NKX3.1 leads to the LIMK2 distribution throughout the cell **(figure 3-3D-F)**.

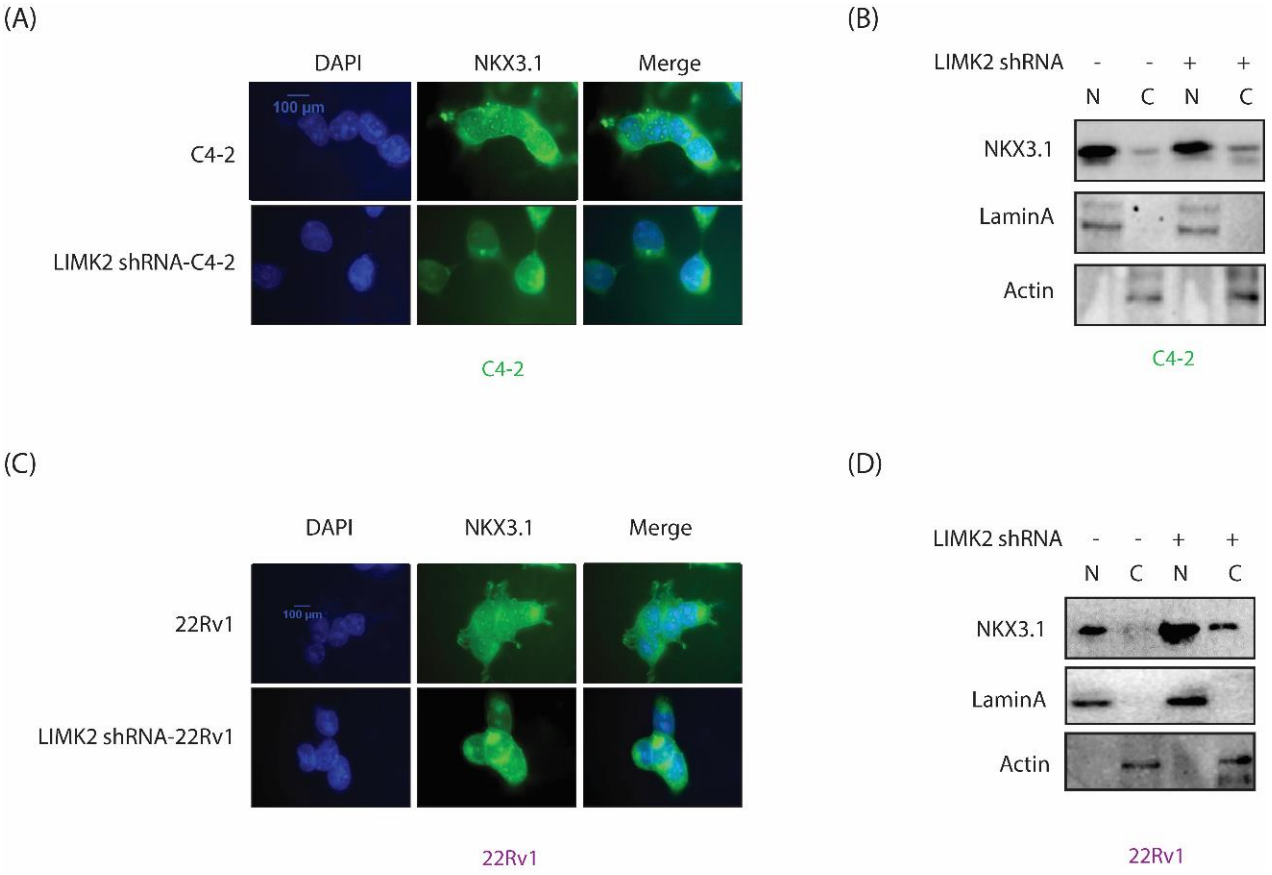

Figure 3-2. Subcellular localization of NKX3.1 in response to LIMK2.

(A) Treatment of C4-2 cells with LIMK2 lentivirus did not change NKX3.1 localization. Subcellular localization of NKX3.1 in C4-2 cells infected by LIMK2 lentivirus using immunofluorescence is shown in A. NKX3.1 (green) and nucleus (blue). C4-2 cells were stained with an anti-NKX3.1 monoclonal antibody. We used a FITC-conjugated antibody as the secondary antibody. Nuclei were stained with DAPI. Scale bar equals 100 µM. 100 cells were counted. The experiment is performed three times. **(B)** Subcellular fractionation of NKX3.1 in C4-2 cells in response to knockdown of LIMK2 is shown B. C4-2 cells were treated with LIMK2 lentivirus, and NKX3.1 location was checked by western blot analysis. Actin and lamin were used as the control. The experiment is performed three times. **(C)**Treatment of 22Rv1 cells with LIMK2 lentivirus did not change NKX3.1 localization. Subcellular localization of NKX3.1 in 22Rv1 cells infected by LIMK2 shRNA using immunofluorescence is shown in C. NKX3.1 (green) and nucleus (blue). 22Rv1 cells were stained with an anti-NKX3.1 monoclonal antibody. We used a FITC-conjugated antibody as the secondary antibody. Nuclei were stained with DAPI. Scale bar equals 100 µM. 100 cells were counted. The experiment is performed three times. **(D)** Subcellular fractionation of NKX3.1 in 22Rv1 cells in response to knockdown of LIMK2 is shown D. 22Rv1 cells were treated with LIMK2 lentivirus, and NKX3.1 location was checked by western blot analysis. Actin and lamin were used as the control. The experiment is performed three times.

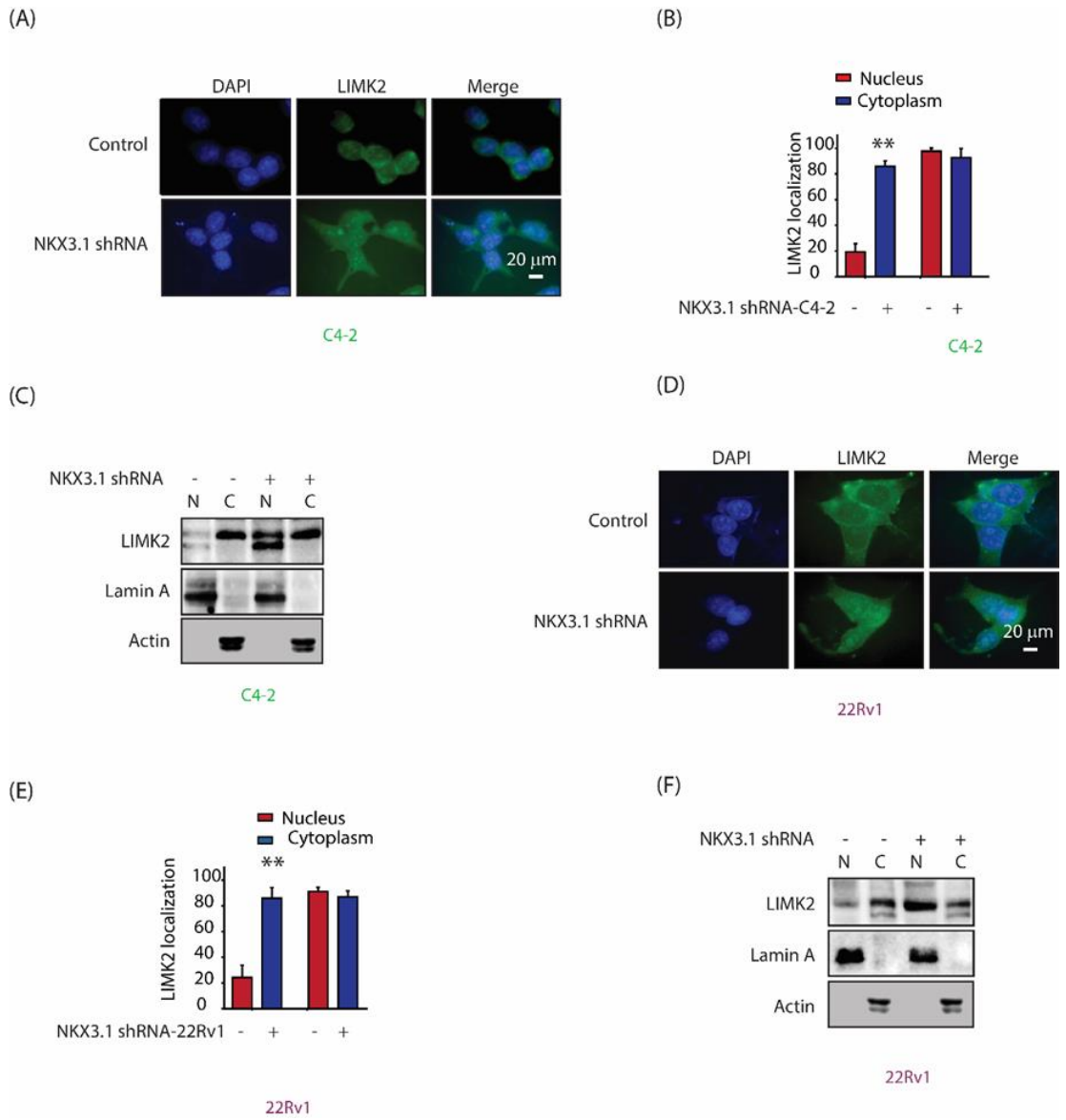

Figure 3-3. Subcellular localization of LIMK2 in response to NKX3.1.

(A) Treatment of C4-2 cells with NKX3.1 lentivirus caused the distribution of LIMK2 from the cytosol to the nucleus. Subcellular localization of LIMK2 in C4-2 cells infected by NKX3.1 shRNA using immunofluorescence is shown in A. LIMK2 (green) and nucleus (blue). C4-2 cells were stained with an anti-LIMK2 monoclonal antibody. The secondary antibody was the FITC-conjugated antibody. Nuclei were stained with DAPI. Scale bar equals 100 µM. 100 cells were counted. The experiment is performed three times. **(B)** Quantification of LIMK2 localization in response to the NKX3.1 lentivirus in C4-2 cells is shown in B. Bar graph shows the mean number of counted cells. The data are shown as the number of cells ± SD. The experiment was performed three times. ** $P < 0.01$ **(C)** Subcellular fractionation of LIMK2 in C4-2 cells in response to knockdown of NKX3.1 is shown C. C4-2 cells were treated with NKX3.1 lentivirus and LIMK2 location was checked by western blot analysis. Actin and lamin were used as the control. The experiment is performed three times. **(D**) Subcellular localization of LIMK2 in 22Rv1 cells infected by NKX3.1 shRNA using immunofluorescence is shown D. LIMK2 (green) and nucleus (blue). 22Rv1 cells were stained with an anti-LIMK2 monoclonal antibody. The secondary antibody was conjugated to FITC. Nuclei were stained with DAPI. Scale bar equals 100 µM. The counted cells were 100. The experiment was performed three times. **(E)** Quantification of LIMK2 localization in response to the NKX3.1 lentivirus in 22Rv1 cells is presented in E. The experiment is performed three times.** $P < 0.01$. **(F)** Subcellular fractionation of LIMK2 in 22Rv1 cells in response to the NKX3.1 knockdown as ascertained by western blot analysis**.** The experiment was performed three times.

LIMK2 negatively regulates NXX3.1 protein levels

We suspected that LIMK2 expression might regulate NKX3.1 expression because LIMK2 phosphorylates NKX3.1. To check this hypothesis, we infected C4-2 cells with LIMK2 retrovirus. Then we check the NKX3.1 protein level by western blot analysis. This analysis revealed that the upregulation of LIMK2 results in the downregulation of NKX3.1 **(figure 3-4A)**. We have quantified the western blot results to analyze our data statistically. The histogram presents the quantitative analyses of the data **(figure 3-4B)**. Consistent with this finding, overexpression of LIMK2 inhibits the expression of NKX3.1 in 22Rv1 cells **(figure 3-4C, 3-4D)**. Besides, suppression of LIMK2 by shRNA in the C4-2 enhanced the NKX3.1 level, as detected by western blot analysis **(figure 3-4E)**. The histogram shows the statistical analysis of the western blot **(figure 3-4F).** Similarly, in 22Rv1cells, the knockdown of LIMK2 increased the NKX3.1 protein levels **(figure 3-4G, 3-4H)**. Thus, we conclude that LIMK2 regulates NKX3.1 at the protein level.

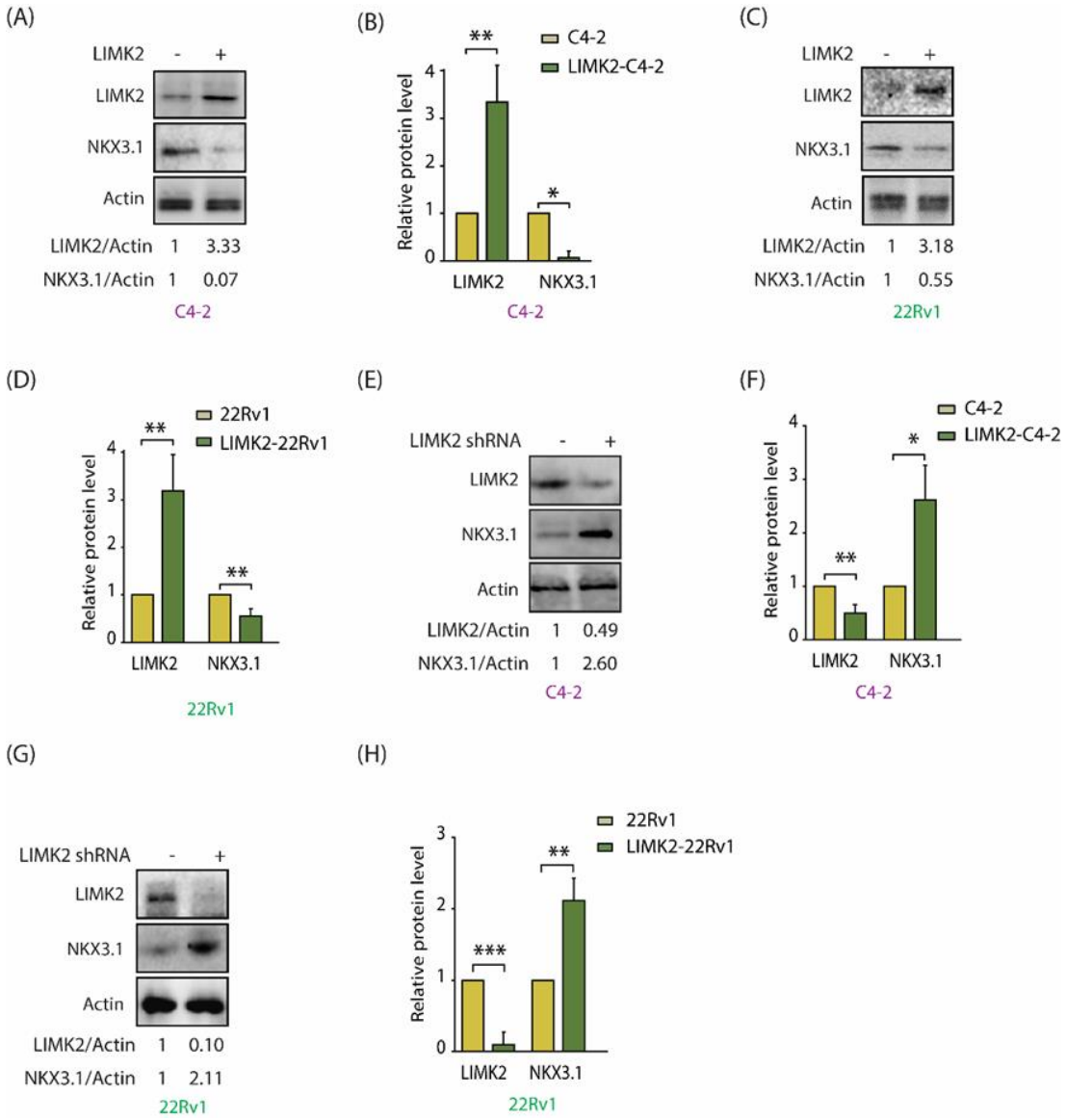

Figure 3-4 LIMK2 negatively regulates NXX3.1 protein levels.

(A) Overexpression of LIMK2 decreases NKX3.1 protein level. C4-2 cells were infected with LIMK2 retrovirus. Cells were harvested after thirty-three hours. Then the cells were lysed and analyzed by western blot. Actin was used as a control. (B) Quantitative analysis of detected LIMK2 and NKX3.1 protein levels is presented in B. The data obtained from three independent experiments and normalized to the actin. * $P < 0.05$, ** $P < 0.01$. (C) Overexpression of LIMK2 decreases NKX3.1 protein level. 22Rv1 cells were infected with LIMK2 retrovirus. Thirty-three hours later, the cells were collected and lysed by western blot. We used actin as a control. (D) Quantitative analysis of protein levels is presented in D. The data were analyzed from three independent experiments. Signals obtained from western blot are normalized to the actin. ** $P < 0.01$. (E) Downregulation of LIMK2 increases NKX3.1 protein level. C4-2 cells were infected with LIMK2 lentivirus. Thirty-three hours after infection, we collected the cells and analyzed them by western blot. Actin was used as a control. (F) Quantitative analysis of detected LIMK2 and NKX3.1 protein levels is presented in F. The data obtained from three independent experiments and normalized to the actin. * $P < 0.05$, ** $P < 0.01$. (G) Downregulation of LIMK2 increases NKX3.1 protein level. 22Rv1 cells were infected with LIMK2 lentivirus. Thirty-three hours later, the cells were collected and lysed by western blot. We used actin as a control. (H) Quantitative analysis of detected LIMK2 and NKX3.1 protein levels is presented in H. The data obtained from three independent experiments. Signals obtained from western blot are normalized to the actin. ** $P < 0.01$, *** $P < 0.001$.

LIMK2 negatively regulates NKX3.1 mRNA level

Since our protein expression analysis showed that LIMK2 regulates NKX3.1 negatively at the protein level, we reasoned that LIMK2 might regulate NKX3.1 at the mRNA level. To test this hypothesis, we examined the effect of LIMK2 expression on NKX3.1 mRNA level. We treated target cells (C4-2 and 22Rv1) with LIMK2 retrovirus or lentivirus. Thirty hours later, RNA was extracted and cDNA was prepared using MLV Reverse Transcriptase and random hexamer. mRNA abundance was measured by quantitative PCR (qPCR) using SYBR Green PCR mix and specific primers for LIMK2, NKX3.1, GAPDH, and RAMP1. The signals were then normalized to GAPDH and presented as a histogram. Receptor activity–modifying protein 1 (RAMP1) is a target of NKX3.1 that is upregulated in prostate cancer. Thereby we used it as an internal control. When LIMK2 was overexpressed, the mRNA level of NKX3.1 was decreased in both C4-2 **(figure 3-5A)**.and 22Rv1 cells **(figure 3-5B)**. The shRNA-mediated knockdown of LIMK2 increased NKX3.1 at the mRNA level in both C4-2 **(figure 3-5C)** and 22Rv1 cells **(figure 3-5D)**. These data suggest that LIMK2 modulates the expression of NKX3.1 at mRNA levels.

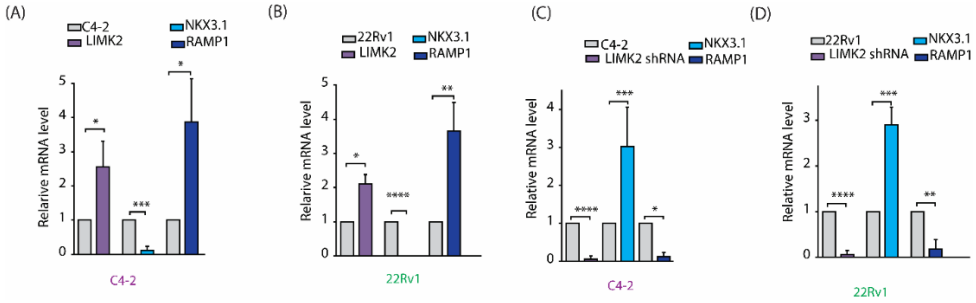

Figure 3-5 LIMK2 expression negatively regulates NXX3.1 mRNA level.

(A) LIMK2 overexpression reduced the mRNA levels of NKX3.1 in C4-2 and **(B)** 22Rv1 cells. The target cells were treated with LIMK2 retrovirus. Total RNA was isolated and mRNA levels were measured by qRT–PCR. The data are from three independent experiments. * $P < 0.05$, ** $P < 0.01$, *** $P < 0.001$ and **** $P < 0.0001$. **(C)** shRNA-mediated knockdown of LIMK2 increased NKX3.1 mRNA level in C4-2 cells and **(D)** 22Rv1 cells. Data were obtained from three independent experiments. * $P < 0.05$, ** $P < 0.01$, *** $P < 0.001$ and **** $P < 0.0001$. The signal was normalized to the GAPDH.

LIMK2 decreases NKX3.1 stability

Since we had demonstrated that LIMK2 regulates the NKX3.1 level, we next investigated whether LIMK2 regulates NKX3.1 turnover. To answer this question, we knocked down LIMK2 in C4-2 cells using LIMK2 lentivirus. Then we treated the cells with cycloheximide (CHX) for

two and four hours. Cycloheximide is a protein synthesis inhibitor. Thus, we can estimate the protein's half-life. The cells were collected, lysed, and evaluated by Western blotting after cycloheximide treatment. Our results indicate that the suppression of LIMK2 promotes NKX3.1 stability and increases its half-life **(figure 3-6A)**. The graph presents the statistical analysis of the CHX experiment **(figure 3-6B)**. Consistent with the C4-2 cell line finding, LIMK2 knockdown 22Rv1cells increases NKX3.1' half-life (**figure 3-6C)**. The graph presents the statistical analysis of the CHX experiment (**figure 3-6D)**.

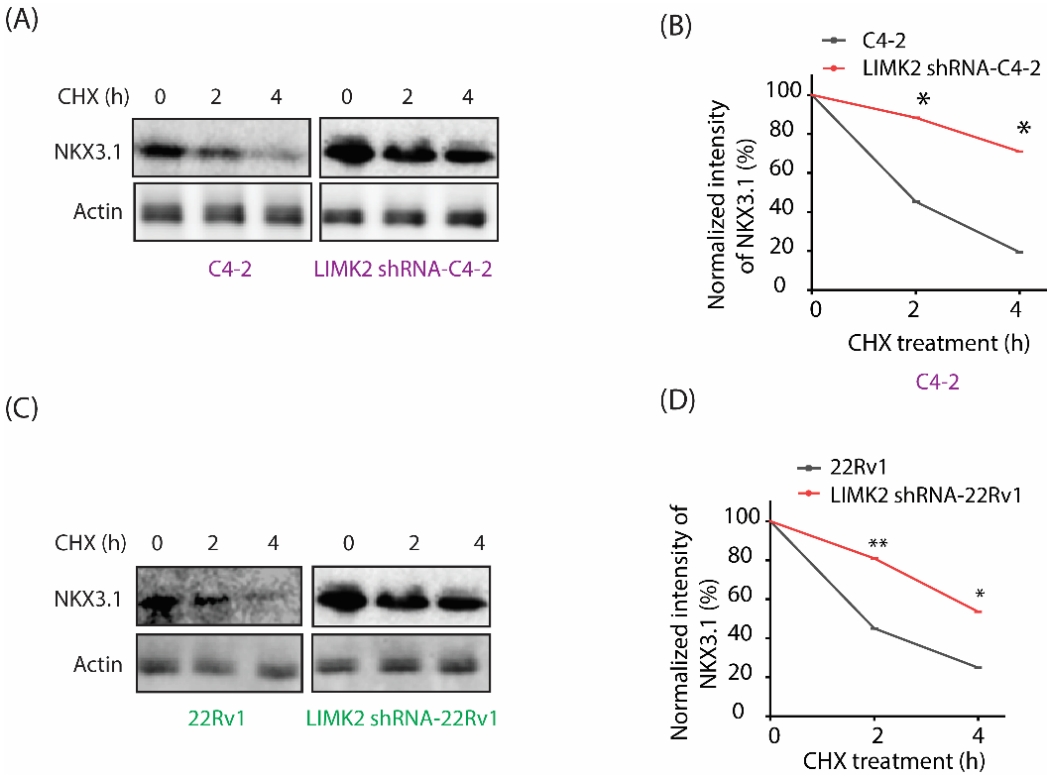

Figure 3-6 LIMK2 reduces NKX3.1 protein stability.

(A) NKX3.1 degradation in C4-2 cells treated with LIMK2 shRNA and CHX. We treated C4-2 cells with LIMK2 lentivirus to knock down LIMK2 for thirty-three hours. We then treated the cells with CHX (20 µg/ml) for 2 and 4 hours. Next, we collected the cells and analyzed the level of NKX3.1 by western blot. **(B)** NKX3.1 protein level was normalized to actin, and the graph is presented in B. * $P < 0.05$. **(C)** NKX3.1 degradation in 22Rv1 cells treated with LIMK2 lentivirus and CHX. 22Rv1 cells were treated by LIMK2 lentivirus for thirty-three hours. Next, we treated the cells with CHX (20 µg/ml) for 2 and 4 hours. Then, we collected the cells and analyzed the level of NKX3.1 by western blot. **(D)** The graph represents the statistical analysis of three independent experiments. * $P < 0.05$, ** $P < 0.01$.

LIMK2 promotes NKX3.1 degradation via phosphorylation

To determine how LIMK2 overexpression reduces the NKX3.1 protein levels, we asked whether LIMK2 overexpression leads to NKX3.1 degradation through ubiquitylation. To do so, C4-2 cells were co-infected by 6x-His-ubiquitin and LIMK2 retrovirus. We added MG132 after 24 hours of infection. MG132 (carbobenzoxy-Leu-Leu-leucinal) is a peptide aldehyde that inhibits the proteolytic activity of the 26S proteasome complex. After 12 hours, NKX3.1 was pulled down using the NKX3.1 antibody. Then NKX3.1 ubiquitylation was evaluated by western blot using histidine antibody. Our data indicated that NKX3.1 phosphorylation by LIMK2 resulted in proteasomal degradation of NKX3.1, thus decreasing the protein level of NKX3.1 **(figure 3-7A)**. We also tested NKX3.1 degradation by ubiquitination in 22Rv1 cells. Briefly, 22Rv1 cells were infected with 6x-His-ubiquitin and LIMK2 and treated with MG132. NKX3.1 was pulled down, and its degradation was evaluated by western blot analysis. In agreement with the results obtained in C4-2 cells, we detected NKX3.1 ubiquitination in response to the LIMK2 upregulation **(figure 3-7B)**.

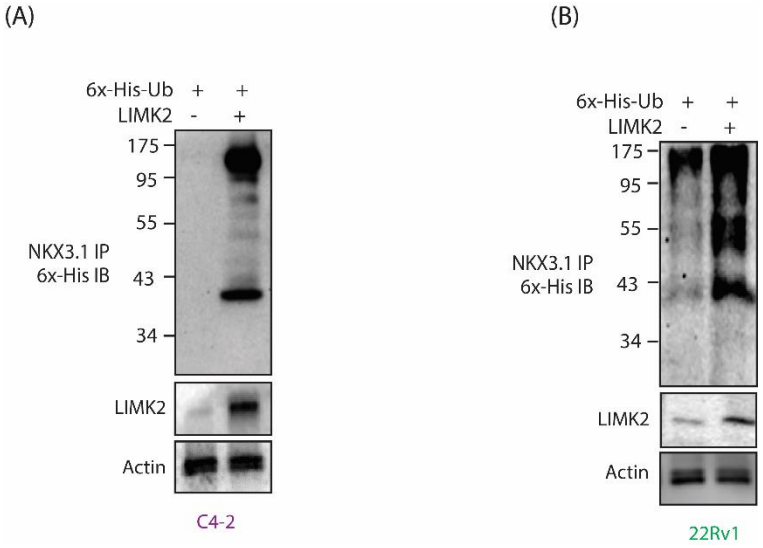

Figure 3-7 The ubiquitination of LIMK2 is promoted by NKX3.1.

(A) Western blots analysis NKX3.1 ubiquitination upon LIMK2 protein upregulation. C4-2 cells overexpressing LIMK2 were infected with 6x-His-Ubiquitin retrovirus. Then MG132 was added to the cells for 10 hours. Next, IgG or NKX3.1 was immunoprecipitated from the cells, and ubiquitination was checked using a 6x-His antibody. **(B)** Western blots of 6x-His Ubiquitin after control IgG or NKX3.1 immunoprecipitation from 22Rv1 cells infected with LIMK2 and 6x-His-Ubiquitin retrovirus. Protein degradation was checked using a 6x-His antibody.

3.2.2 Aim2

In this aim, we will examine how NKX3.1 expression regulates LIMK2 expression and localization.

NKX3.1 negatively regulates LIMK2 protein levels

Our lab has identified TWIST1 (93), PTEN (94), and SPOP (95) as LIMK2 substrates that regulate LIMK2 expression. Thus, we reasoned that NKX3.1 might also regulate the LIMK2 levels in the cells. To unravel the effect of NKX3.1 on the LIMK2 protein level, the C4-2 cell line was infected with NKX3.1 retrovirus. We then tested the protein level by western blot analysis using NKX3.1 and LIMK2 antibodies. Our data showed that upregulation of NKX3.1 resulted in a reduction of LIMK2 levels **(figure 3-8A)**. We analyzed our data statistically and presented them in a histogram (**figure 3-8B)**. We then tested the LIMK2 protein level in response to NKX3.1 upregulation in 22Rv1 cells. Like the data from C4-2 cells, our results showed that an enhanced level of NKX3.1 leads to downregulation of LIMK2 protein level **(figure 3-8C, 3-8D)**. We have also tested the effect of NKX3.1 downregulation on the LIMK2 protein level. Thus, we infected the C4-2 cells with NKX3.1 lentivirus, and after thirty-two hours, we checked LIMK2 protein level using western blot analysis. Our data indicated that knockdown of NKX3.1 results in the overexpression of LIMK2 **(figure 3-8E, 3-8-F).** We have confirmed our knockdown experiment using the 22Rv1 cells. Infection of 22Rv1 cell with NKX3.1 lentivirus results in an enhanced level of LIMK2 **(figure 3-8G)**. We analyzed our data statistically and presented them in a histogram (**figure 3-8H).**

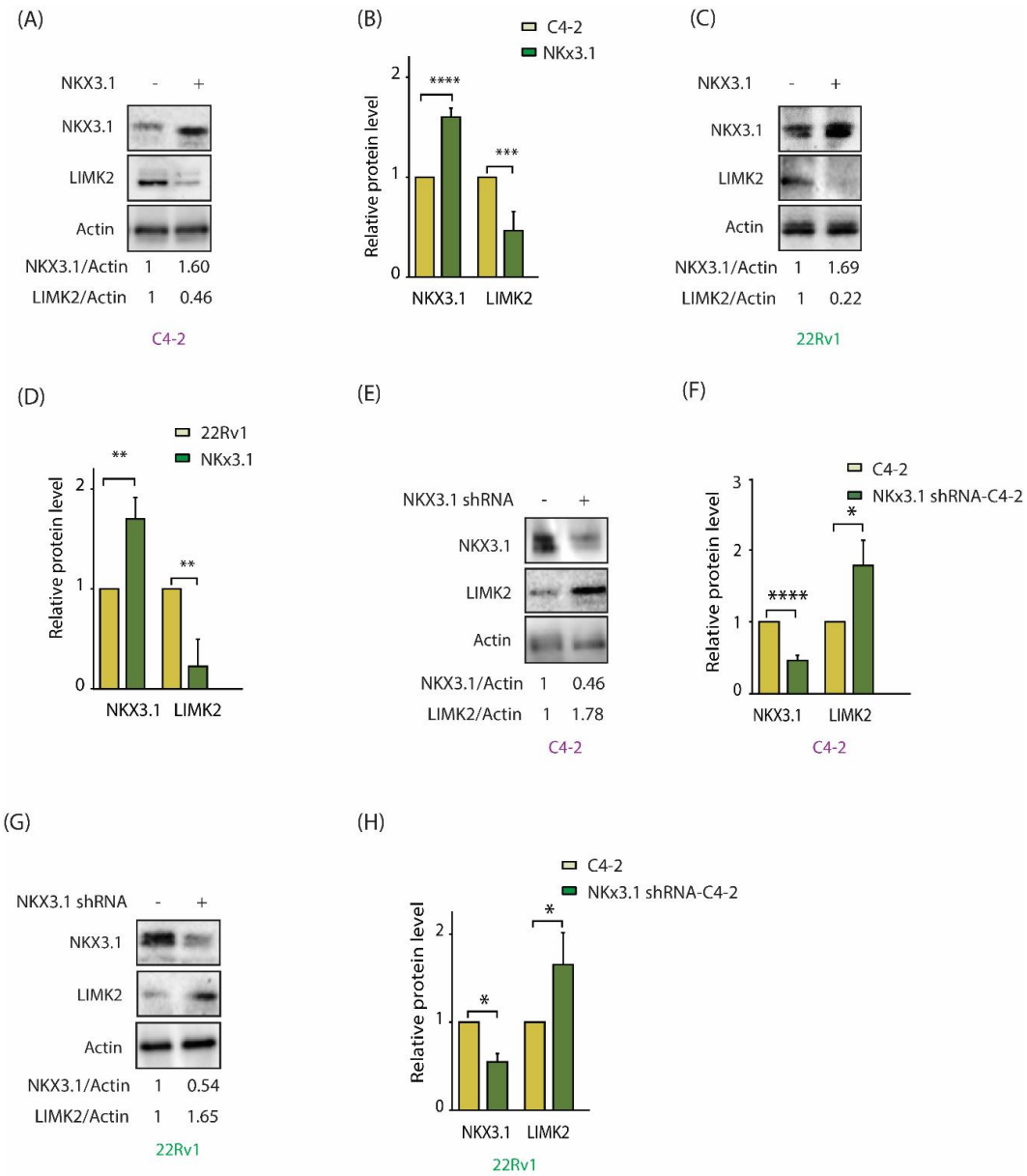

Figure 3-8 NKX3.1 negatively regulates LIMK2 protein level.

(A) NKX3.1 overexpression results in LIMK2 protein level downregulation. C4-2 cells were harvested after thirty-three hours of infection. Then the cells were analyzed by western blot. We used actin as a control. **(B)** The graph in B presents quantitative analysis of protein levels for n=3. The protein levels are normalized to the actin. *** $P < 0.001$ and **** $P < 0.0001$. **(C)** NKX3.1 upregulation results in LIMK2 protein level downregulation. 22Rv1 cells were infected with NKX3.1 retrovirus for thirty-three hours. Then we collected the cells and assessed the protein levels by western blot. We used actin as a control. **(D)** The graph in D is the quantitative analysis of protein levels for n=3. The protein levels are normalized to the actin. ** $P < 0.01$. **(E)** Downregulation of NKX3.1 increases LIMK2 protein level. C4-2 cells were infected with NKX3.1 lentivirus for thirty-three hours. We then collected the cells and analyzed them by western blot using actin as a control. **(F)** The histogram in F is the quantitative analysis of protein levels for n=3. The protein levels are normalized to the actin. * $P < 0.05$, **** $P < 0.0001$. **(G)** Downregulation of NKX3.1 increases LIMK2 protein level. 22Rv1 cells were infected with NKX3.1 lentivirus. The cells were lysed after thirty-three hours. We assessed the protein levels by western blot. Actin was used as a control. **(H)** Quantitative analysis of detected protein levels is presented in H. The data obtained from three independent experiments. Signals obtained from western blot are normalized to the actin. * $P < 0.05$.

NKX3.1 negatively regulates LIMK2 mRNA level

To get more understanding into the regulation of LIMK2 by NKX3.1, first, we have tested the LIMK2 mRNA level in the cells overexpressing NKX3.1. There was a marked decrease in LIMK2 mRNA in the cells overexpressing wild-type NKX3.1 in C4-2 and 22Rv1 cell lines **(figure3-9A, 3-9B)**. Because of the control of LIMK2 mRNA levels by NKX3.1, we next wanted to confirm the effect of NKX3.1 on the LIMK2 mRNA level. Thus, we knockdown NKX3.1 using shRNA, and we measured mRNA level. Our data have shown that NKX3.1 downregulation resulted in upregulation of LIMK2 mRNA level **(figure3-9C, C-9D)**.

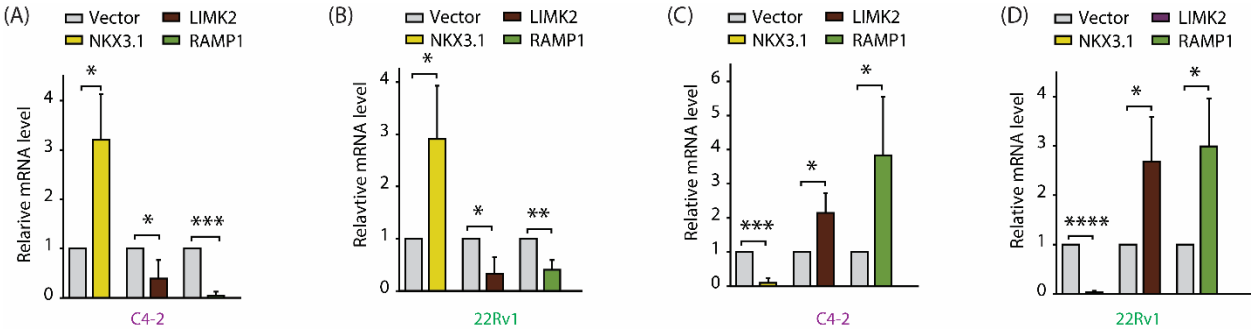

Figure 3-9 LIMK2 expression is regulated at the mRNA level by NKX3.1.

(A) An enhancement in NKX3.1 mRNA level results in the reduction of LIMK2 mRNA level in C4-2 and **(B)** 22Rv1 cells. The target cells were infected with NKX3.1 retrovirus. Total RNA was extracted, and mRNA levels were quantified by qRT–PCR from n=3. * P < 0.05, ** P < 0.01, and *** P < 0.001. **(C)** Depletion of NKX3.1 results in an enhanced level of LIMK2 mRNA level in C4-2 cells and **(D)** 22Rv1 cells. Data were obtained from three independent experiments. * P < 0.05, *** P < 0.001 and **** P < 0.0001. The signal was normalized to the GAPDH.

NKX3.1 modulates LIMK2 stability

To get a better understanding of LIMK2 regulation by NKX3.1, we test the effect of cycloheximide (CHX) on the LIMK2 half-life in the target cells. To do so, we infected C4-2 cells with NKX3.1 lentivirus. Then we added cycloheximide for 2 and 4 hours. After the mentioned time points, we harvested the cells and performed western blot analysis to check LIMK2 stability. We found the knockdown of NKX3.1 prolongs LIMK2 half-life in C4-2 cells**(figure3-10A)**. We analyzed our data statistically and presented them in a histogram (**figure 3-10B).** We further validate this finding in 22Rv1 cells. To do so, we knock down NKX3.1 in 22Rv1 cells, and then we inhibit protein synthesis with cycloheximide. Our data have suggested that a decreased level

of NKX3.1 increases LIMK2 stability **(figure3-10C, 3-10D)**. Collectively, these data have shown that NKX3.1 regulates LIMK2 steady-state.

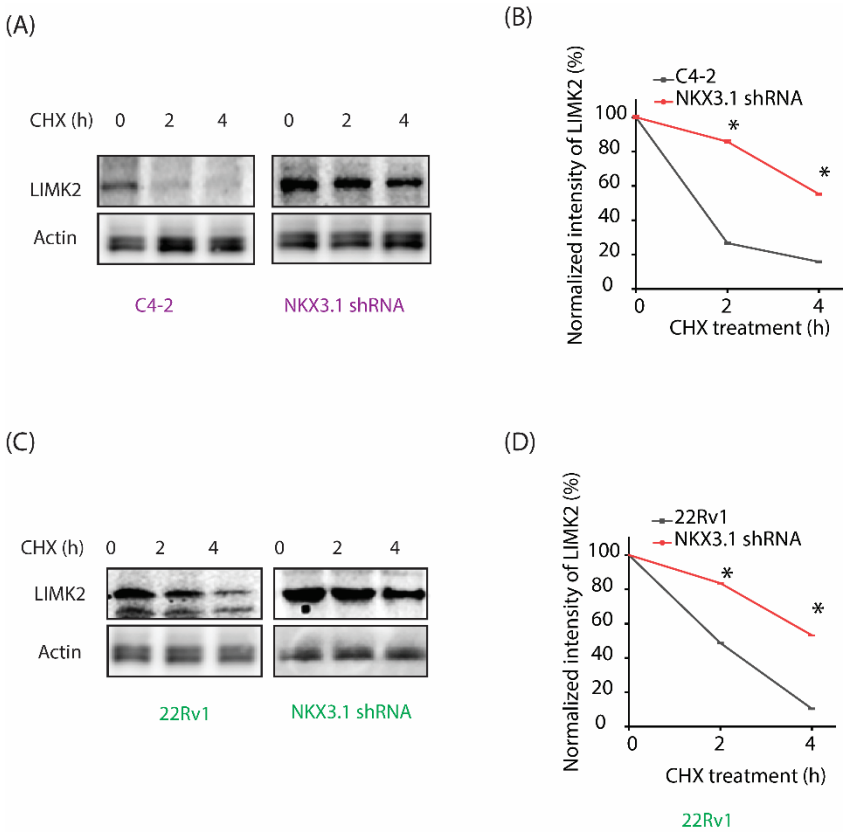

Figure 3-10 NKX3.1 modulates LIMK2 protein stability.

(A) LIMK2 degradation in C4-2 cells treated with NKX3.1 lentivirus and CHX (20 µg/ml). C4-2 cells were treated by NKX3.1 lentivirus. Thirty-three hours postinfection, the cells were treated with CHX (20 µg/ml) for 2 and 4 hours. Subsequently, the cells were lysed, and the LIMK2 protein level was analyzed by western blot. (B) The graph represents the statistical analysis of three independent experiments. * $P < 0.05$. (C) LIMK2 degradation in 22Rv1 cells treated with NKX3.1 lentivirus and CHX (20 µg/ml) is shown in C. (D) The graph represents the statistical analysis from n=3. * $P < 0.05$.

NKX3.1 promotes LIMK2 degradation via phosphorylation

Because NKX3.1 downregulates LIMK2 expression, we sought to understand if NKX3.1 targets LIMK2 for degradation through the ubiquitin-dependent proteolytic pathway. Thus, we carried out a ubiquitination assay. The target cells were co-infected with NKX3.1 and 6x His-tag-ubiquitin for 48 h. 12 h before harvesting the cells, a proteasome inhibitor, MG132, was added to the cells. Then we pulled down LIMK2 with LIMK2 antibody. We tested LIMK2 ubiquitination

with histidine antibody using western blot. As shown in **figure 3-11**, we observed more ubiquitinated LIMK2 in the cells overexpressing NKX3.1 compared to the control.

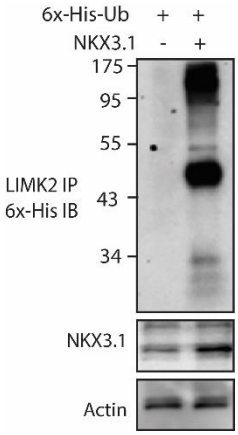

Figure 3-11 NKX3.1 overexpression increases LIMK2 ubiquitination.

NKX3.1 overexpression increases LIMK2 ubiquitination in C4-2 cells. Target cells stably expressing NKX3.1 were infected by 6x-His Ubiquitin retrovirus. Cells were treated with MG132 for 10 hours. Then ubiquitination of LIMK2 was analyzed by western blot with 6x-His antibody. We detected more ubiquitinated LIMK2 in the cells overexpressing NKX3.1.

LIMK2 phosphorylates NKX3.1 at S185

We aimed to identify the specific phosphorylation site of LIMK2 on NKX3.1. To do so, we predicted the phosphorylation sites of LIMK2 on NKX3.1. The predicted motif contains Ser followed by either an alanine, serine, or glycine is a target sequence of LIMK2. Based on this analysis, we proposed S185 as a possible LIMK2 phosphorylation site. To confirm our hypothesis, we mutated S185 to alanine. Then we performed a kinase assay using radioactive ATP. Our results indicated a marked decrease in NKX3.1 phosphorylation when S185 was changed to alanine. This data suggested that LIMK2 phosphorylates NKX3.1 at the S185 position **(figure 3-12).**

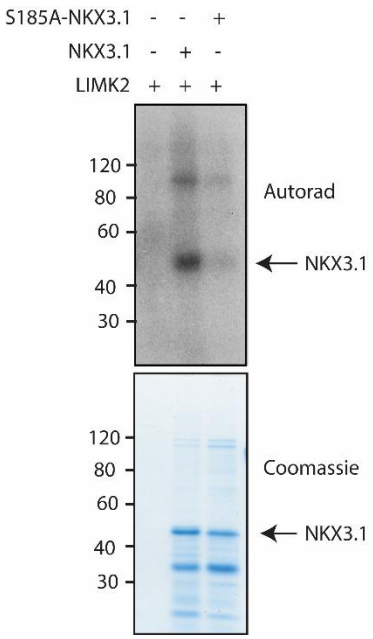

Figure 3-12 Mutation of LIMK2 phosphorylation sites of NKX3.1 at positions S185.

In vitro phosphorylation assay was performed using LIMK1, NKX3.1 wild type, and S185A-NKX3.1. LIMK2 phosphorylates wild-type NKX3.1, but it does not phosphorylate S185A mutant. In vitro phosphorylation assay was performed using LIMK1, NKX3.1 wild type, and S185A-NKX3.1. NKX3.1 phosphorylation was detected by autoradiography. The gel was stained with Coomassie Brilliant Blue. The Top panel represents an autoradiograph. The bottom panel shows a gel stained with Coomassie blue. In lane1, LIMK2 was incubated with radiolabeled ATP and without NKX3.1. In lane 2, NKX3.1 was incubated with radiolabeled ATP and LIMK2. In lane 3, S185A-NKX3.1 was incubated with radiolabeled ATP and LIMK2. In vitro kinase assay was repeated three times.

Mutation of S185 to alanine increases its expression

Since our results indicated that LIMK2 phosphorylates NKX3.1, we investigated whether this phosphorylation might affect NKX3.1 stability. Thus C4-2 and 22Rv1 cells were infected with NKX3.1 will and S185-NKX3.1. Our results suggested that mutation of S185 to alanine increases NKX3.1 expression that, in turn, decreases LIMK2 level. More specifically, the protein levels of NKX3.1 and LIMK2 were quantified in the target cells (C4-2 and 22Rv1). The effect of the mutation on NKX3.1 protein level could be detected in the target cells. As shown in **figure 3-13,** higher levels of NKX3.1 expression were detected in western blot analysis in the cells overexpressing S185A-NKX3.1. Furthermore, the LIMK2 protein level is reduced by NKX3.1 S185A, and the downregulation was more than when the target cells were infected with NKX3.1. Serine phosphorylation is known to modulate NKX3.1 stability. Consistent with the previous report, these data show that the phosphorylation of Ser185 plays a significant role in NKX3.1 stability and thus regulates the LIMK2 protein level **(figure 3-13)**.

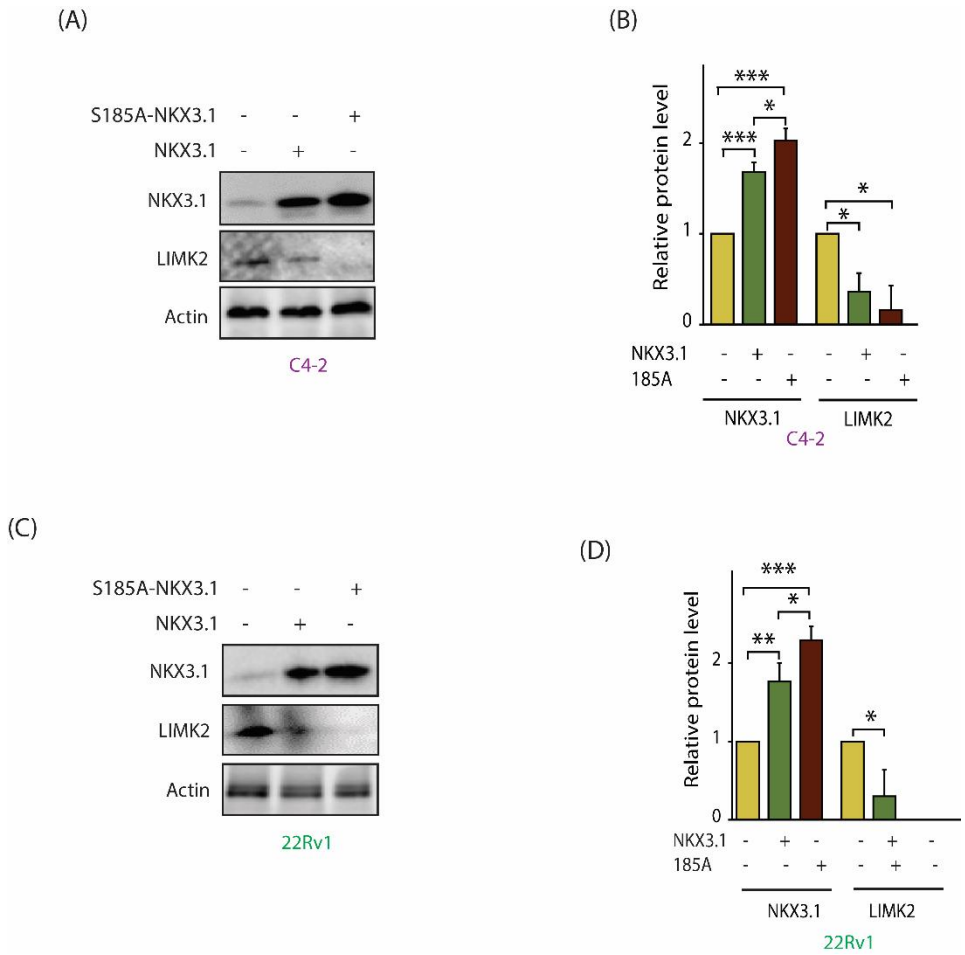

Figure 3-13 The effect of S185 phosphorylation on NKX3.1 and LIMK2 protein levels.

(A) S185A-NKX3.1 is expressed at a higher level compared to wild-type. C4-2 cells infected with NKX3.1 and S185A-NKX3.1 retrovirus for thirty-three hours. Cell lysates were analyzed were by western blot to detect NKX3.1 and LIMK2 protein levels. (B) Quantification of western blot analysis normalized to the actin is shown B. The data are from three independent experiments. * $P < 0.05$, *** $P < 0.001$ and **** $P < 0.0001$. (C) S185A-NKX3.1 is expressed at a lower level compared to wild-type in 22Rv1 cells. (D) Quantification of western blot analysis normalized to the actin is shown in D. The data are from three independent experiments. * $P < 0.05$, ** $P < 0.01$, *** $P < 0.001$.

NKX3.1 phosphorylation by LIMK2 decrease its stability

Since our result has shown that changing the serine 185 to alanine results in higher expression of NKX3.1 compared to the wild type, we checked the effect of S185A on NKX3.1 stability. Thus, we performed a cycloheximide (CHX) experiment. C4-2 cells were infected with NKX3.1 and S185A-NKX3.1 retrovirus. Next, the cells were treated with cycloheximide for 2 and 4 hours. Subsequently, we did a western blot experiment using the NKX3.1 antibody. Our results indicated that mutation of S185A increases NKX3.1 stability compared to the wild-type **(figure 3-**

14A). We have also analyzed our data statistically and presented them in **figure 3-14B**. We confirmed our results by using 22Rv1 cells **(figure 3-14C)**, and we showed statistical analysis in **figure 3-14D**. Collectively, our data suggest that S185A increases NKX3.1 stability.

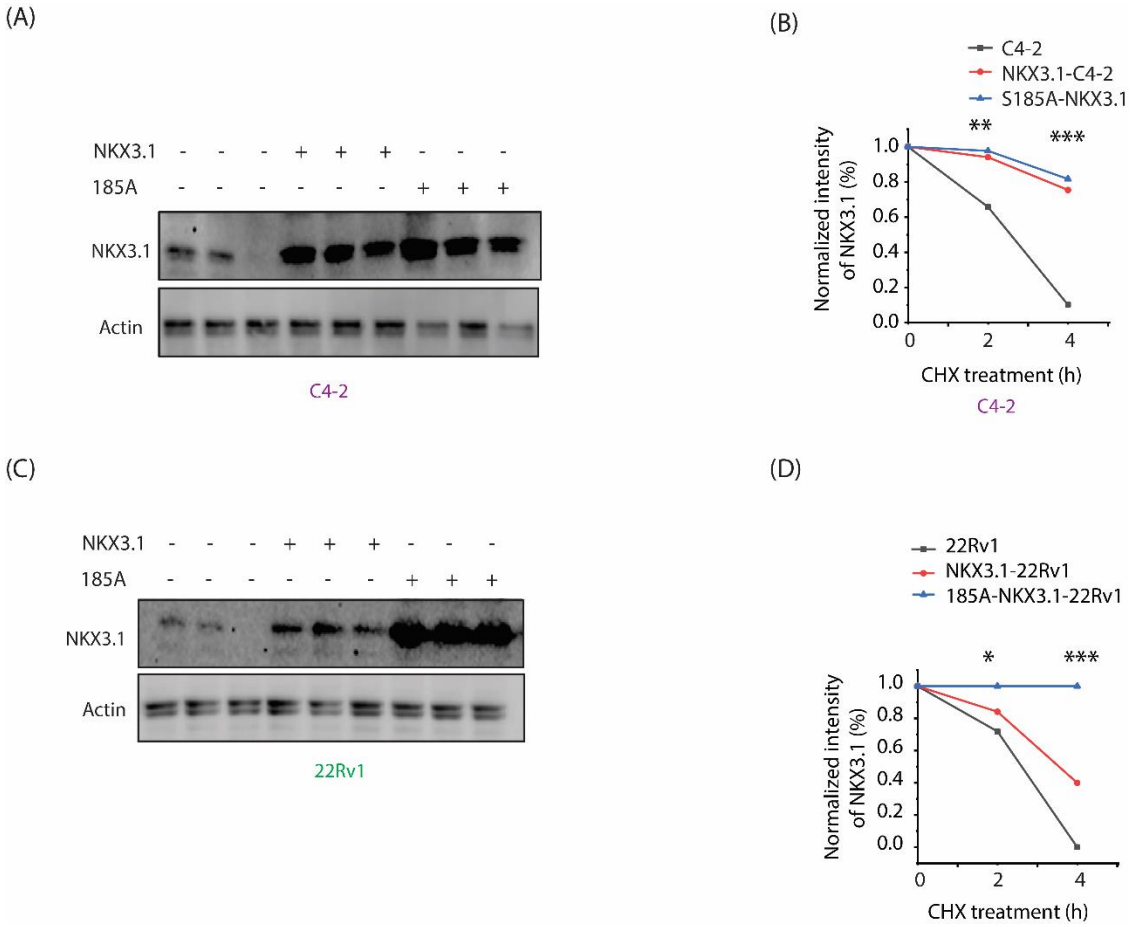

Figure 3-14 Stabilization of NKX3.1 correlates with S185.

(A) The stability of S185A-NKX3.1 is increased due to the mutation of serine to the alanine. NKX3.1 degradation in C4-2 cells was tested using CHX. C4-2 cells were treated with NKX3.1 and S185A-NKX3.1 for thirty-three hours. Then the cells were treated with CHX (20 µg/ml) for the indicated times. Subsequently, protein levels were analyzed by western blot. **(B)** Quantification of western blot analysis normalized to the actin is shown in B for n=3. ** P < 0.01, and *** P < 0.001 (C) Stability of NKX3.1-S185A due to the mutation of serine to the alanine in 22rRv1 cells. 22Rv1 cells were treated with NKX3.1 and S185A-NKX3.1, and CHX (20 µg/ml). Next, we assessed NKX3.1 stability by western blot. (D) Quantification of western blot analysis normalized to the actin is shown in D. Data are from three independent experiments. * P < 0.05, and *** P < 0.001.

S185A-NKX3.1 promotes LIMK2 degradation more significantly

Since our data have shown that S185A increased NKX3.1 stability, we next investigated whether enhanced degradation of LIMK2 was a result of NKX3.1 mediated ubiquitination. Thus we infected the target cells (C4-2 and 22Rv1 cells) with NKX3.1 wild-type and S185A-NKX3.1 along with 6x-His-ubiquitin. Then we immunoprecipitated LIMK2 and performed western blot analysis. We used histidine antibody to check ubiquitination. Our results indicated that the improvement in the stability of NKX3.1 increases LIMK2 degradation by enhancing its ubiquitination. This means we detected more ubiquitinated-LIMK2 in the cells overexpressing S185A-NKX3.1 compared to the cells overexpressing wild-type NKX3.1 **(figure 3-15A, 3-15C)**.

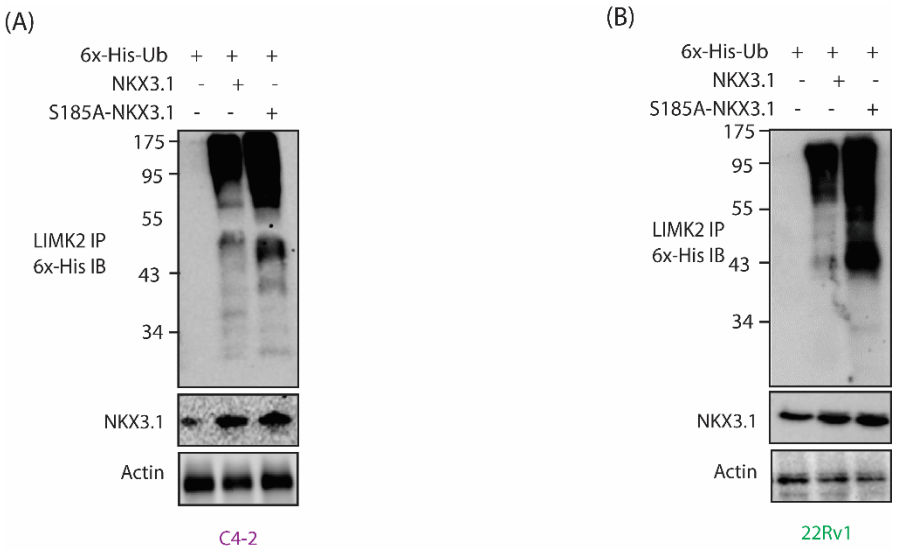

Figure 3-15 NKX3.1 regulates ubiquitination of LIMK2.

(A) C4-2 and **(B)** 22Rv1 cells overexpressing NKX3.1 and S185A-NKX3.1 were infected with 6x-His-ubiquitin retrovirus following MG132 treatment. Then we lysed the cells and the lysate was subjected to immunoprecipitation by the anti-LIMK2 antibody. Ubiquitination was detected by western blot using a 6x-Histidine antibody. NKX3.1 regulates the ubiquitination of LIMK2. The assay is repeated three times.

3.2.3 Aim3

In this aim, we will identify the specific site which is phosphorylated by LIMK2. We will also examine the importance of identified sites in aggressive oncogenic phenotypes.

NKX3.1 inhibits cell proliferation

NKX3.1 serves as a tumor suppressor and inhibits cell proliferation. S185A increases NKX3.1 stability raised the possibility that S185A enhanced the inhibitory effect of NKX3.1 on cell proliferation. To test this assumption, we measured the effect of S185A-NKX3.1 on cell viability. Thus, we plated the cells (C4-2 and 22Rv1) and after 12 hours, we added the retrovirus (NKX3.1 and S185A-NKX3.1). Then we measured cell viability at different time points (18 and 36 hours). As expected, NKX3.1 inhibited cell proliferation significantly compared to the control **(figure 3-16A, 3-16B)**. Besides, we observed that S185A increases the inhibitory effect of NKX3.1 on cell proliferation. These data suggest that S185A has a key role in NKX3.1 stability, and its mutation represses cell proliferation. We have also tested the effect of NKX3.1 and S185A on the stable cell line expressing LIMK2. We have seen that the infected cells with NKX3.1 and S185A grow slowly as compared to control. We have also noticed that S185A-NKX3.1 dampens cell proliferation more significantly compared to NKX3.1 **(figure 3-16C)**.

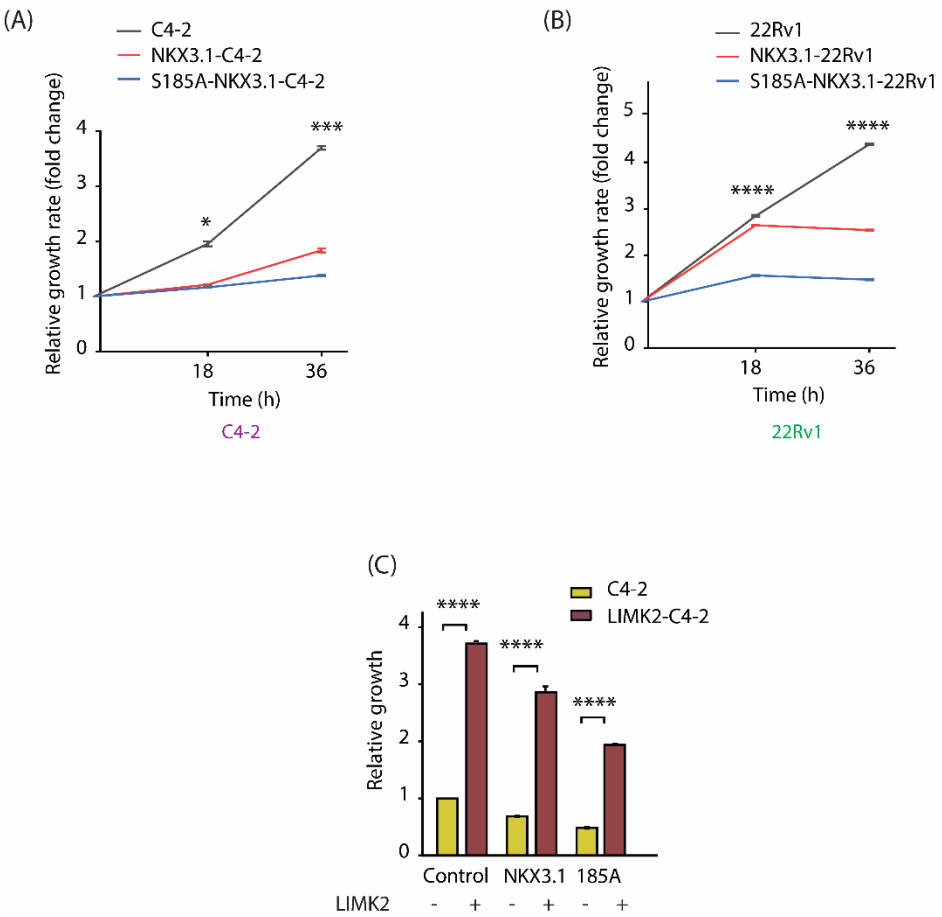

Figure 3-16 NKX3-1 inhibited prostate cancer cell proliferation.

(A) NKX3-1 inhibited prostate cancer cell proliferation in C4-2 and **(B)** 22Rv1 cells. Target cells were seeded in a 24-well plate and infected by NKX3.1 and S185A-NKX3.1 retrovirus for 18 and 36 hours. Proliferative activity was measured by MTT assay. The absorbance was measured at 570 nm. All data are from three independent experiments. * $P < 0.05$. **(C)** C4-2 cells stably expressed NKX3.1, S185A-NKX3.1 were infected by LIMK2 retrovirus. Proliferative activity was measured by MTT assay. The absorbance was read at 570 nm. All data are from three independent experiments. **** $P < 0.0001$.

NKX3.1 inhibits cell invasion

Next, we studied the effect of NKX3.1 expression on C4-2 cell migration and invasion. Thus the cells overexpressing NKX3.1 and S185A-NKX3.1 were treated with the serum-free media for 12 hours. Then we used the Boyden chamber to perform the migration assay. The results of *in vitro* migration assay showed that NKX3.1 reduced the migration of the C4-2 cells. The data showed that LIMK2 increased cell migration **(figure 3-17A)**. This result is consistent with the published data. We then explore if S185A-NKX3.1 suppresses cell migration and invasion. Our migration data suggested that S185A dampens cell migration **(figure 3-17A)**. We have analyzed

our data statistically and presented them in **figure 3-17B**. Collectively, the migration assay data confirmed that S185 phosphorylation is important for the NKX3.1 function. Subsequently, we verified our results using 22Rv1 cells. Our data from 22Rv1 is in agreement with our results from C4-2 cells **(figure 3-17C, 3-17D)**. These results confirm S185 plays a key role in NKX3.1 activity.

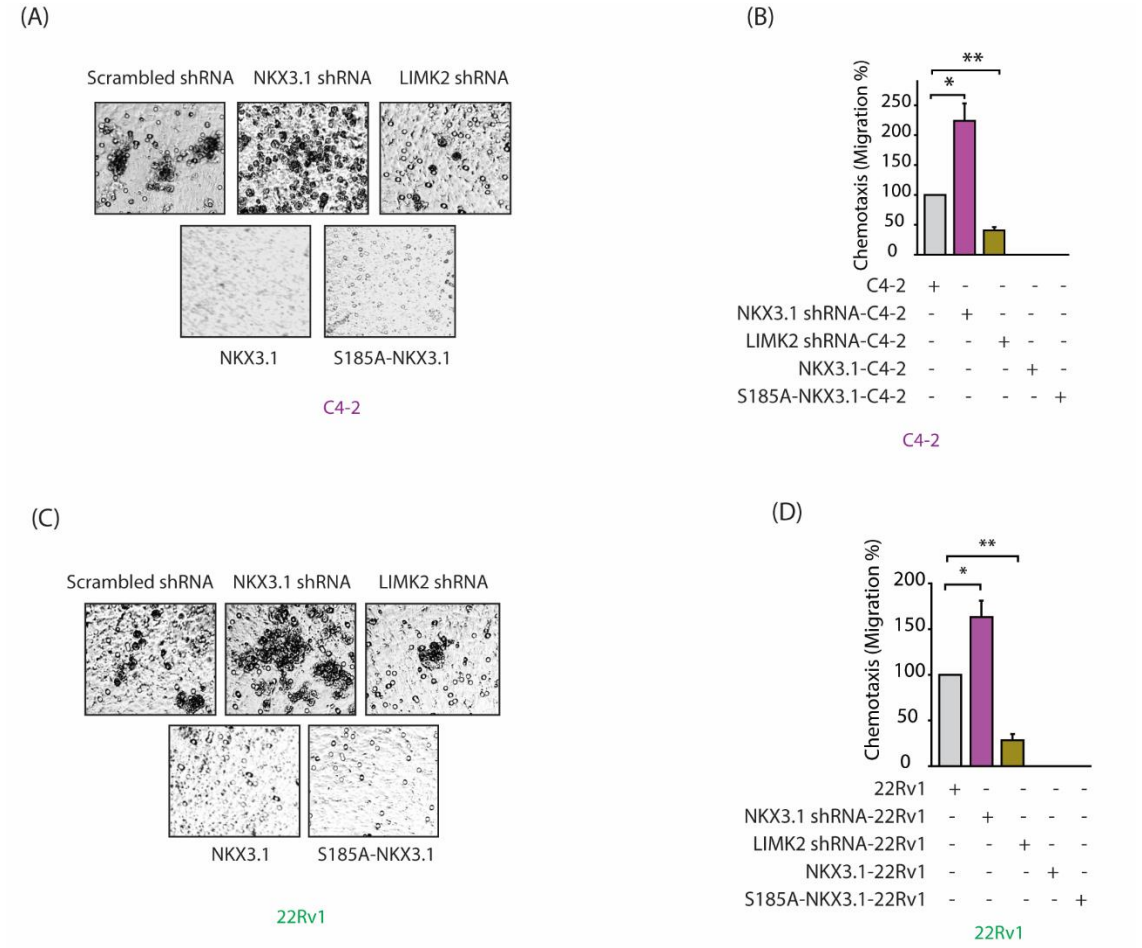

Figure 3-17 NKX3.1 suppressed cell migration *in vitro*.

(A) NKX3.1 suppressed cell migration in C4-2 cells. Target cells infected by NKX3.1 lentivirus, LIMK2 lentivirus, NKX3.1 retrovirus, and S185A-NKX3.1 retrovirus. The cells were starved in serum-free media for 12 hours and migration assay was performed using Boyden chambers. **(B)** The results are plotted as the means ± SD of three independent experiments. * $P < 0.05$, ** $P < 0.01$. **(C)** NKX3.1 suppressed cell migration in 22Rv1 cells. **(D) T**he results are plotted as the means ± SD of three independent experiments. * $P < 0.05$, ** $P < 0.01$.

To verify that S185 plays an important role in NKX3.1 stability and suppression of tumor growth, colony formation assays were performed in the C4-2 prostate cancer cell line. VIP3-NKX3.1, VIP3-NKX3.1-185, were transfected into Phoenix cells. A control transfection has been performed as a negative control. Puromycin has been used for selection, and colonies were visualized using 0.01% crystal violet. We have seen mock-infected cells forming colonies. However, NKX3.1, S185A-NKX3.1 infected cells failed to form colonies. These data suggested that phosphorylation of S185 is an important mechanism by which regulates NKX3.1 stabilization and function **(figure 3-18).**

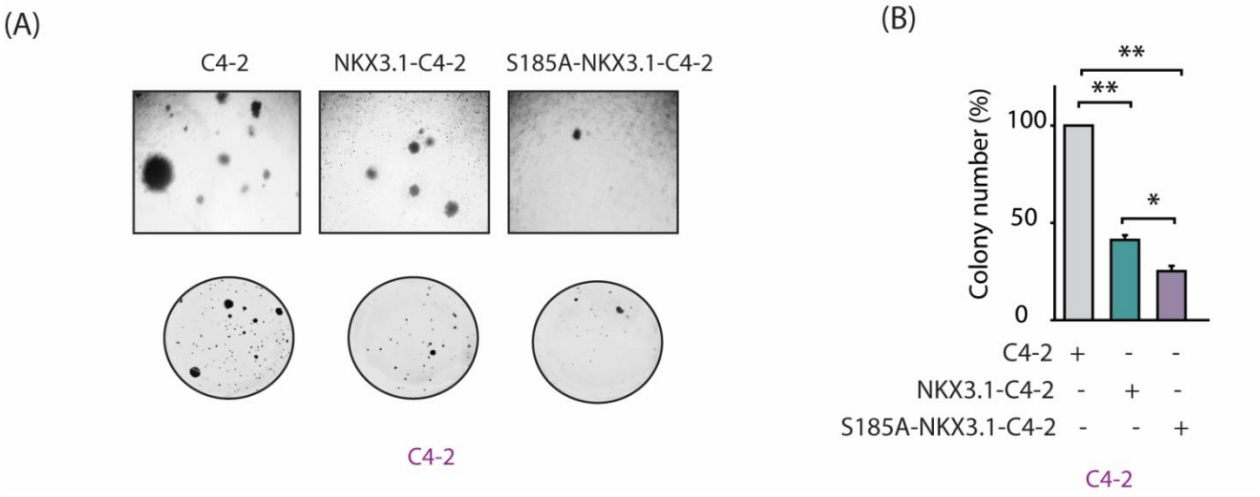

Figure 3-18 NKX3.1 inhibits colony formation of C4-2 cells in soft agar.

(A) Colony formation assay showed that NKX3.1 and S185A-NKX3.1 inhibit the proliferation ability of C4-2 cells in a soft-agar experiment. (B) Quantitative data analysis of the soft agar experiment is shown in B. All data were from n=3. *, P<0.05; **, P<0.01.

NKX3.1 phosphorylation at S185 decreases its expression

Our data have shown that LIMK2 directly phosphorylates NKX3.1 at S185. Our cell experiment data have revealed that mutation of S185 to the alanine increase NKX3.1 stability and thus results in a significant reduction of LIMK2. We also noted that S185A increases the antitumorigenic properties of NKX3.1. Therefore, in the next step, we change S185 to aspartic acid (D) to explore how enhanced phosphorylation modulates NKX31 and LIMK2 expression in the cells. Aspartic acid is a phosphomimetic residue, thereby increasing NKX3.1 phosphorylation. Thus, we infected C4-2 cells with NKX3.1 wild type and NKX3.1-185D retrovirus, and after 32

hours, we measured NKX3.1 and LIMK2 protein levels using western blot analysis. As shown in **figure 3-19**A, the NKX3.1-185D expression was markedly less than the NKX3.1 wild type, suggesting that phosphorylation of NKX3.1 at S185 sites lowers the NKX3.1 expression level. The statistical analysis of the experiment is shown in **figure 3-19B**. In turns, we detected an enhanced level of LIMK2 in the cells treated with S185D-NKX3.1 **(figure 3-19C, figure3-19D)**. We verified our results in 22Rv1 cells.

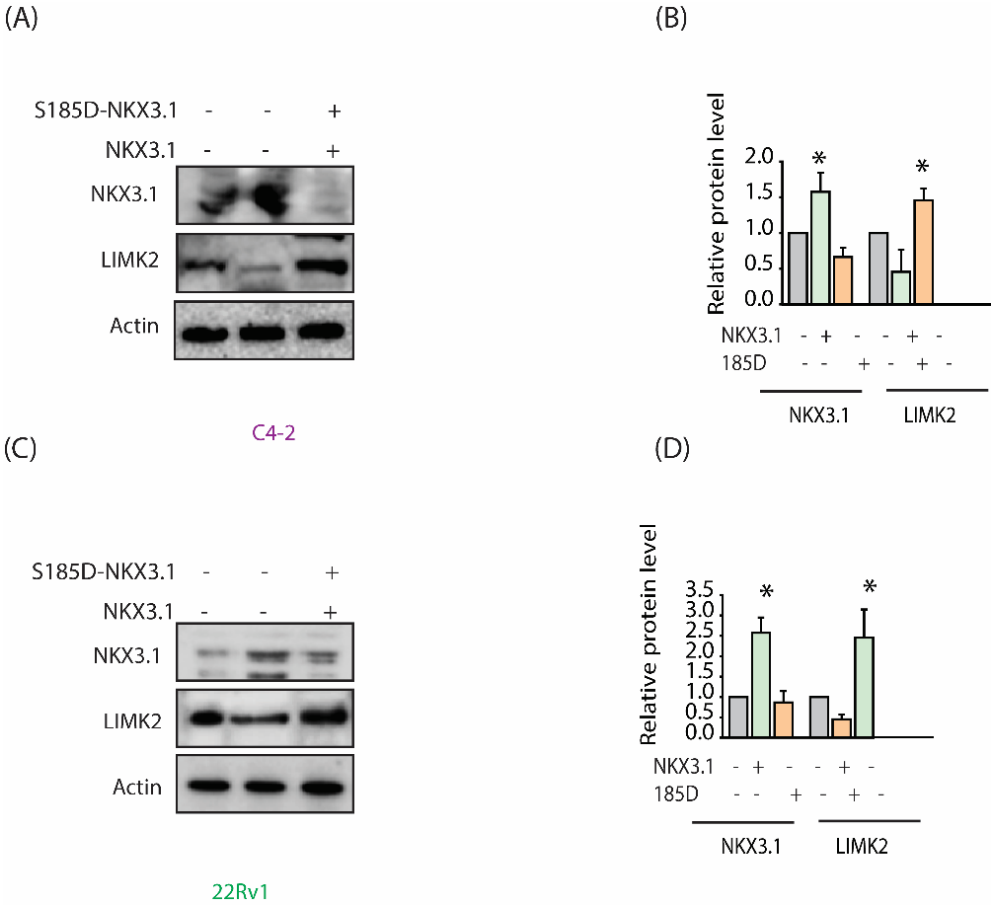

Figure 3-19 The effect of S185D phosphorylation on NKX3.1 and LIMK2 protein levels.

(A) S185D-NKX3.1 is expressed at a lower level compared to wild-type. C4-2 cells infected with NKX3.1 and S185D-NKX3.1 retrovirus for thirty-three hours. Cell lysates were analyzed were by western blot to detect NKX3.1 and LIMK2 protein levels. **(B)** Quantification of western blot analysis normalized to the actin is shown B. The data are from three independent experiments. * $P < 0.05$. **(C)** S185D-NKX3.1 is expressed at a higher level compared to wild-type in 22Rv1 cells. **(D)** Quantification of western blot analysis normalized to the actin is shown in D. The data are from three independent experiments. * $P < 0.05$.

LIMK2 regulates NKX3.1 protein stability

To uncover the possible mechanisms for the observed relationship between LIMK2 and NKX3.1, we assessed the half-life of NKX3.1 using the protein synthesis inhibitor cycloheximide. We treated C4-2 cells with NKX3.1 and S185D-NKX3.1. Then we inhibited protein synthesis using cycloheximide for 2 and 4 hours. Subsequently, we tested LIMK2 half-life using western blot analysis. Our result indicated that increased phosphorylation of NKX3.1 in the cells treated with S185D-NKX3.1 increases LIMK2 half-life in C4-2 **(figure 3-20A)**. The statistical analysis of immunoblotting is shown in **figure 3-20B**. We confirmed our data in 22Rv1 cells **(figure 3-20C, 3-20D)**.

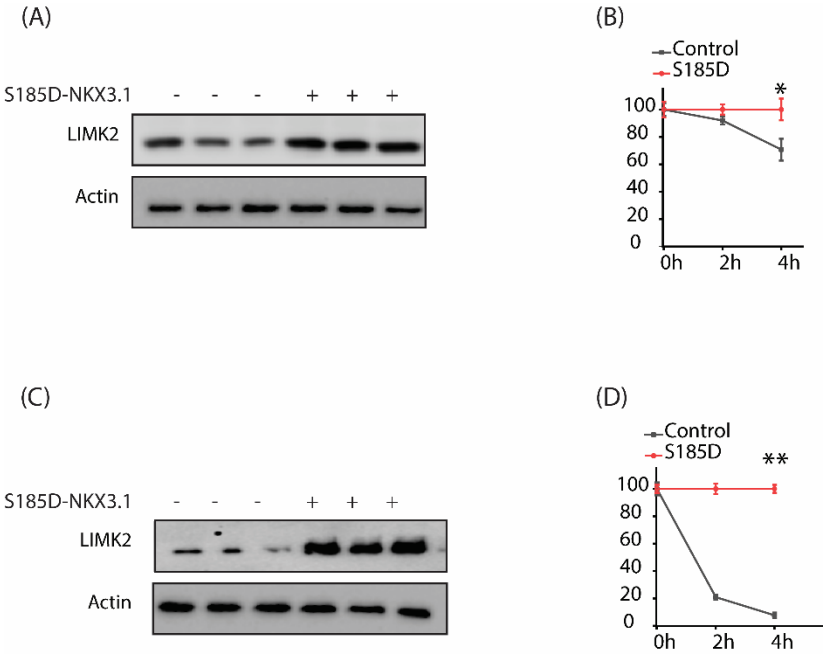

Figure 3-20 Stabilization of NKX3.1 correlates with S185.

(A) The stability of LIMK2 protein is increased due to the mutation of serine to the aspartic acid of NKX3.1. LIMK2 degradation in C4-2 cells was tested using CHX. C4-2 cells were treated with NKX3.1 and S185D-NKX3.1 retrovirus for thirty-three hours. Then the cells were treated with CHX (20 µg/ml) for the indicated times. Subsequently, protein levels were analyzed by western blot. (B) Quantification of western blot analysis normalized to the actin is shown in B for n=3. * $P < 0.05$. (C) Stability of LIMK2 due to the mutation of serine to the aspartic acid in 22Rv1 cells. 22Rv1 cells were treated with NKX3.1 and S185D-NKX3.1, and CHX (20 µg/ml). Next, we assessed LIMK2 stability by western blot. (D) Quantification of western blot analysis normalized to the actin is shown in D. Data are from three independent experiments. ** $P < 0.01$.

NKX3.1 inhibits cell migration

Substantial evidence indicates that NKX3.1 shows tumor suppressor properties in cell culture and *nude* mice (117-119). To understand whether phosphorylation of NKX3.1 by LIMK2 regulates its antitumorigenic properties, we performed a cell migration assay. C4-2 and 22Rv1 cells were infected by NKX3.1 wild type and S185D-NKX3.1. Then we performed a migration assay. Our results revealed that cells overexpressing S185D-NKX3. migrate significantly more than the vector-treated control. Overall, the data have shown that NKX3.1 phosphorylation by LIMK2, which subsequently regulates NKX3.1 function as a tumor suppressor, regulates NKX3.1 stability. Thereby, the phosphomimetic version of NKX3.1 decreases its anti-tumorigenic function and increases cell migration (**figure 3-21**).

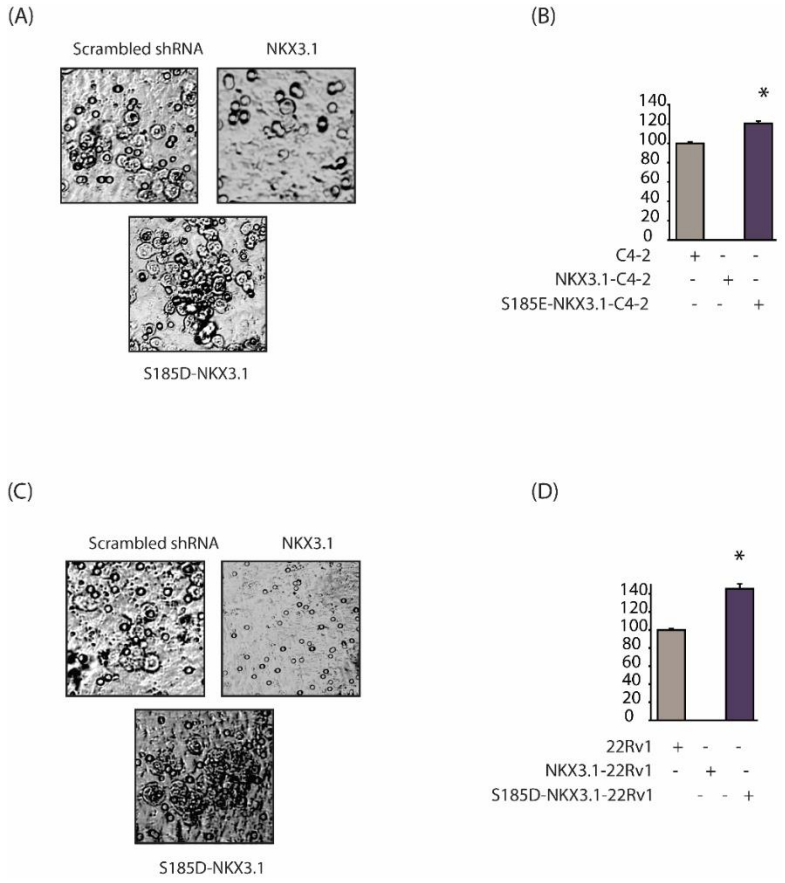

Figure 3-21 NKX3.1 suppressed cell migration *in vitro*.

(A) NKX3.1 suppressed cell migration in C4-2 cells. Target cells were infected by NKX3.1, and S185D-NKX3.1 retrovirus. The cells were starved in serum-free media for 12 hours and migration assay was performed using Boyden chambers. **(B)** The results are plotted as the means ± SD of three independent experiments. * $P < 0.05$. **(C)** NKX3.1 suppressed cell migration in 22Rv1 cells. **(D)** The results are plotted as the means ± SD of three independent experiments. * $P < 0.05$.

NKX3.1 suppresses tumor growth in vivo

Our results indicated that NKX3.1 suppresses aggressive phenotypes *in vitro*. Next, we wanted to test the role of NKX3.1 in tumor growth *in vivo*. Thus, we assess the potential of NKX3.1 *in vivo* in tumor suppression. Thereby, 10^6 cells were injected subcutaneously into immunocompromised mice to establish tumor xenograft. We measured tumor size every alternative day. As expected, animals receiving C4-2 developed tumors. By contrast, noticed that tumors do not arise in animals that received NKX3.1 and S185A-NKX3.1 after 23 days of injection **(figure 3-22).** This provided further evidence of the tumor-suppressor properties of NKX 3.1 and its phosphoresistant mutant.

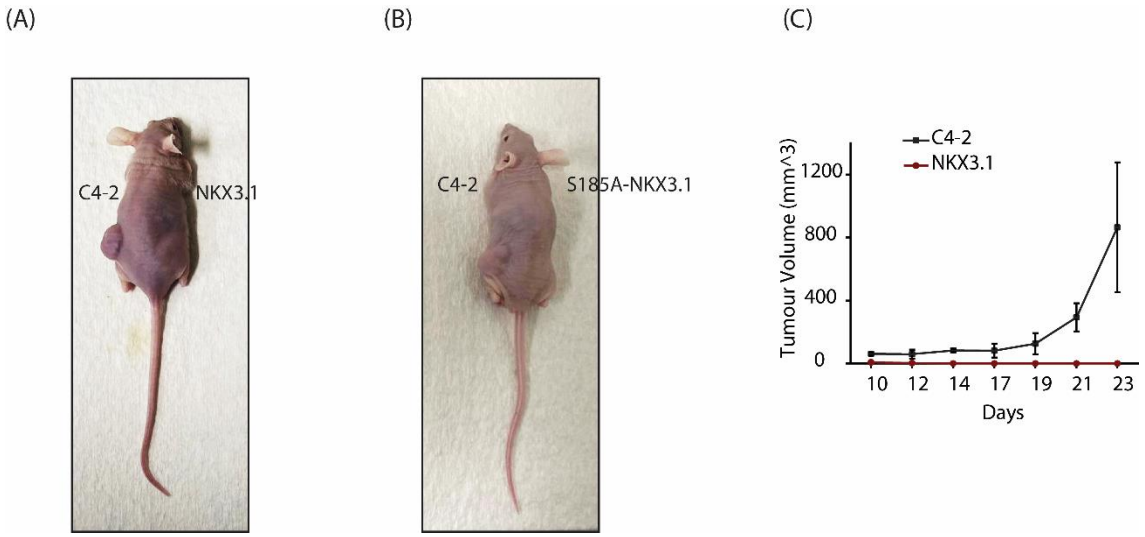

Figure 3-22 NKX3.1 inhibits tumor growth *in vivo*

(A) Representative xenografts 23 days after subcutaneous injection with NKX3.1 and **(B)** S185A-NKX3.1. **(C)** Tumor volumes measured 23 days after subcutaneous transplantation of wild-type and S185A-NKX3.1

3.3 Discussion

By analyzing NKX3.1 expression and phosphorylation status, we showed a new mechanism that NKX3.1 downregulation results in prostates cancer. We showed that NKX3.1 and S185A-NKX3.1 overexpressing cell lines decreased LIMK2 Levels and revealed anti-tumorogenic properties. These factors are cell growth, cell migration, and anchorage-independent growth. Thus, it appears that post-translational modification of NKX3.1 affects its stability and its function as a tumor suppressor. Although NKX3.1 overexpressed cells displayed suppression of growth migration and anchorage-independent growth, S185A-NKX3.1 showed more anti-tumorigenic properties. A key step in the mechanism in which S185A-NKX3.1 has more antitumorigenic characteristics is due to lack of phosphorylation by LIMK2.

It was shown that NKX3.1 phosphorylation controls its stability. For example, single phosphorylation of NKX3.1 at S185 by PIM1 kinase and DYRK (128) destabilizes NKX3.1 and promotes NKX3.1 turnover. It also has shown that PTEN affects S185 phosphorylation and loss of PTEN increases NKX3.1 half-life (94). These data implied that NKX3.1 phosphorylation at S185 decreases NKX3.1 half-life and results in cancer development. High levels of LIMK2 are associated with tumor progression in prostate cancer. Our results show that LIMK2 promotes cancer progression by affecting NKX3.1 steady-state. Therefore, we propose that an accumulation of LIMK2 in cells, following phosphorylation and downregulation of NKX3.1, can promote cellular transformation **(figure 3-23).**

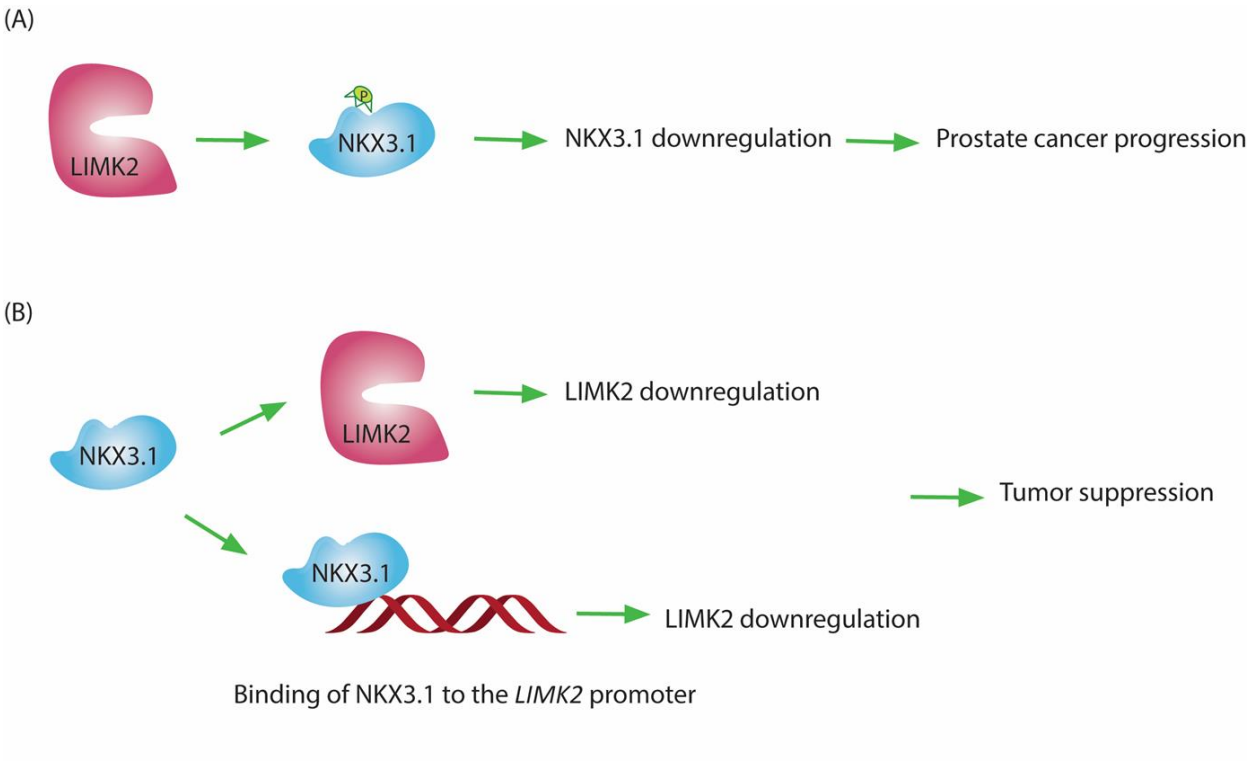

Figure 3-23 Proposed model of LIMK2 and NKX3.1 regulation

(A) LIMK2 phosphorylates NKX3.1 and results in its downregulation. NKX3.1 downregulation leads to prostate cancer progression. **(B)** NKX3.1 functions as a tumor suppressor and downregulates LIMK2 at mRNA and protein levels.

CHAPTER 4. AURKA AND NKX3.1 REALSHIOSHIP

4.1 Hypothesis and specific aims

Prostate cancer (PCa) is the second leading cause of cancer in men worldwide (120). Although local therapies such as surgery and radiotherapy are effective in most patients, some patients may develop a metastatic disease such as castration-resistant prostate cancer (121). Additionally, androgen deprivation therapy (ADT), which targets androgen, can result in castration-resistant prostate cancer (CRPC) in some patients (122). CRPC is characterized by an adenocarcinoma phenotype and dependence on androgen receptor (AR) signaling (123). Non-AR–driven prostate cancer is a clinical concern. Thus, the identification of non-AR-target genes may provide alternatives to treat CRPC (124). In this context, there is evidence that AURKA is upregulated in prostate tumors (125). AURKA is a serine-threonine kinase that contributes to mitotic spindle formation, chromosome segregation, and G2- M transition during the cell cycle (15). Furthermore, AURKA upregulation has been detected in several human cancers. Targeting AURKA is currently being explored as a possible treatment for cancer. However, the clinical trials of AURKA inhibitors have not been successful. Moreover, the underlying mechanism of this failure is currently unknown (126). Thus, it is essential to map the kinase-substrate network to facilitate drug development. Using an innovative chemical-genetic approach, our lab has identified NKX3.1 as the direct target of AURKA. NKX3.1 is a transcription factor that functions in cell proliferation and differentiation. Findings have revealed that *NKX3.1* is the most frequently deleted gene in prostate cancer. In ∼50% of primary prostate tumors and 80% of metastatic tumors, NKX3.1 is either absent or significantly reduced (127). Phosphorylation regulates the steady-state of NKX3.1 protein levels. One regulator of NKX3.1 is the dual-specificity tyrosine-regulated kinase (DYRK). DYRK's phosphorylation of NKX3.1 results in NKX3.1's polyubiquitination and proteasomal degradation (128). **We hypothesize that AURKA phosphorylates NKX3.1 at specific sites. This phosphorylation regulates NKX3.1's expression and contributes to the tumorigenic phenotype.**

In this chapter, we aim to learn the function of AURKA in cancer progression by pursuing the following aims:

Aim 1: We will examine how AURKA expression regulates NKX3.1 phosphorylation, expression, and localization.

Aim 2: We will examine how NKX3.1 expression regulates AURKA expression and localization.

Aim 3: We will identify the specific sites on NKX3.1 that are phosphorylated by AURKA. Moreover, we will examine the importance of these identified sites in aggressive oncogenic phenotypes.

4.2 Results

4.2.1 Aim 1

The investigation of how AURKA expression regulates NKX3.1 phosphorylation, expression, and localization.

Aurora kinase A phosphorylates NKX3.1

We examined the phosphorylating capability of Aurora kinase A on NKX3.1 by *in vitro* kinase assay. To do so, we expressed histidine-tagged NKX3.1 in *E. coli* BL21(DE3) and AURKA in insect cells. The purified proteins and γ^{32}P ATP were incubated together for 30 minutes. We used SDS-PAGE to separate the proteins. Phosphorylation has been detected by autoradiography. As indicated **in figure 4-1**, Aurora kinase A phosphorylated NKX3.1**.**

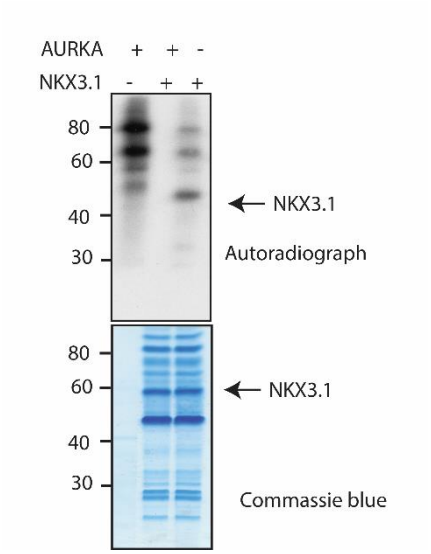

Figure 4-1 NKX3.1 is phosphorylated by AURKA.

(A) NKX3.1 was incubated with AURKA for 30 minutes. The reaction was stopped and proteins were separated by SDS-PAGE. Phosphorylation of NKX3.1 was detected by autoradiography. The upper panel shows an image of an autoradiograph of NKX3.1 phosphorylation. The lower panel shows an image of the Coomassie blue stain of NKX3.1. In vitro kinase assay was repeated three times. In lane1, AURKA was incubated with radiolabeled ATP and without NKX3.1. In lane 2, NKX3.1 was incubated with radiolabeled ATP and without AURKA. In lane 3, NKX3.1 was incubated with radiolabeled ATP and AURKA. *In vitro* kinase assay was repeated three times.

NKX3.1 associates with AURKA

To understand the mechanistic basis by which AURKA phosphorylated NKX3.1, we sought to understand whether NKX3.1 interacts with AURKA. We first immunoprecipitated NKX3.1 from C4-2 cells. Our results indicated that immunoprecipitation of NKX3.1 copurified AURKA. We also performed a reverse assay in which we immunoprecipitated AURKA from C4-2 cells. Our results showed that immunoprecipitation of AURKA copurified NKX3.1, confirming that AURKA interacts with NKX3.1 **(figure 4-2)**.

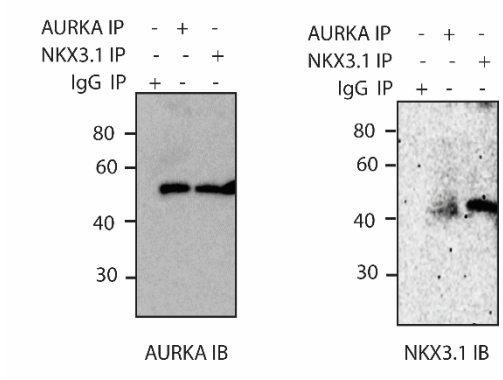

Figure 4-2 Co-immunoprecipitation assays reveal NKX3.1 and AURKA association.

(A) NKX3.1 was immunoprecipitated with an NKX3.1-specific antibody (IP: NKX3.1). The association was analyzed by western blot analyses using the AURKA antibody. **(B)** AURKA was immunoprecipitated with an AURKA-specific antibody (IP: AURKA). The association was analyzed by western blot analyses using the NKX3.1 antibody. The assay was repeated three times.

AURKA and NKX3.1 do not regulate each other localization

Since AURKA interacts with NKX3.1 and phosphorylates it, we sought to test if AURKA and NKX3.1 regulate each other localization. Thus, we have performed an immunofluorescence experiment along with fractionation analysis using C4-2 cells. Experiment with immunofluorescence experiment has revealed that in the untreated cells, NKX3.1 is in the nucleus, and treating cells with AURKA shRNA lentivirus does not change NKX3.1 localization **(figure 4-3A)**. To confirm immunofluorescence staining, we have performed subcellular fractionation following western blot analysis. C4-2 cells were transiently infected with AURKA shRNA lentivirus. Consistent with the immunofluorescence experiment NKX3.1, was mainly detected in the nucleus **(figure 4-3B)**. We verified or results using 22Rv1 cells **(figure 4-3C, figure 4-3D).**

We next investigated the subcellular distribution AURKA in response to the NKX3.1 level by performing fluorescence microscopy and fractionation. Fluorescence microscopy has indicated that AURKA is mainly localized in the cytosol in the untreated cells, and treatment of cells with NKX3.1 lentivirus has not changed AURKA localization significantly **(figure 4-4A)**. In agreement with our fluorescence experiment, NKX3.1 knockdown did not change AURKA localization using fractionation experiment **(figure 4-4B)**. We confirmed AURKA localization in 22Rv1 cells **(figure 4-4C, figure 4-4D)**. Overall, our results suggested that NKX3.1 and AURKA do not regulate each other localization.

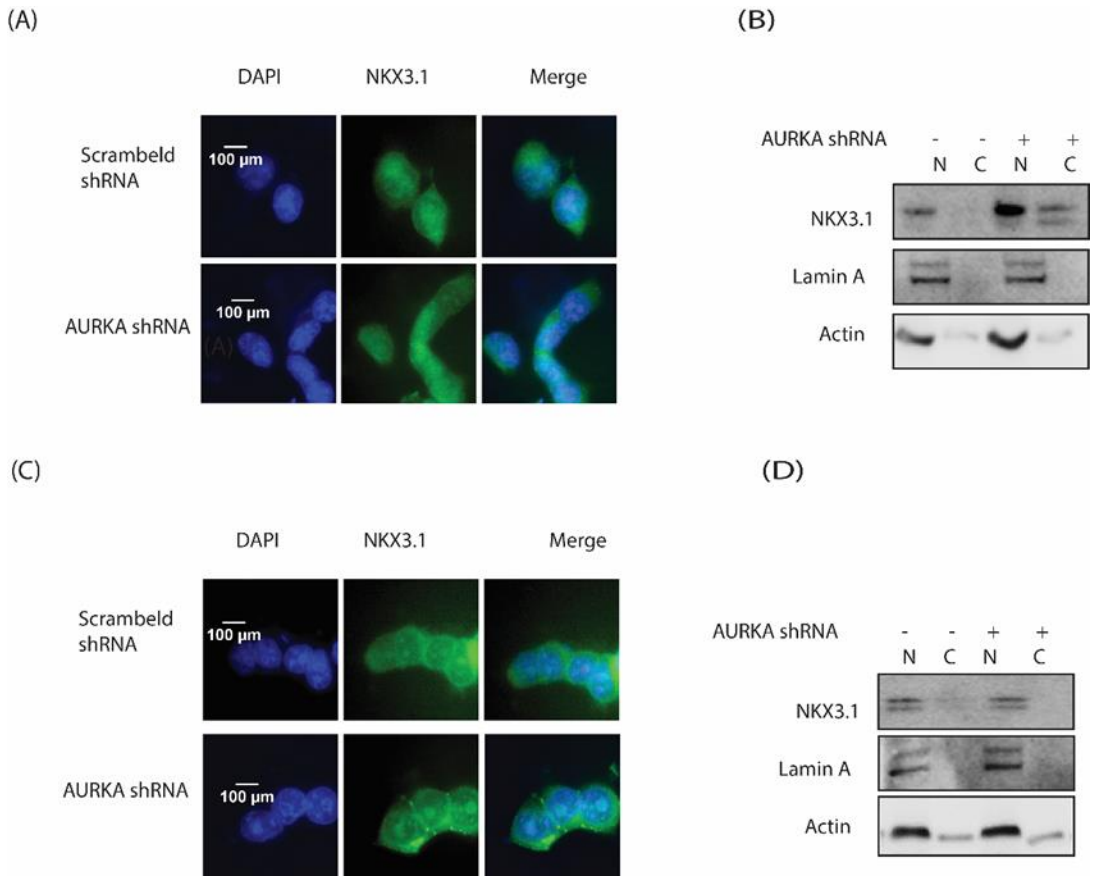

Figure 4-3 Localization of NKX3.1 and AURKA in C4-2 and 22Rv1 cells.

(A) Treatment of C4-2 cells with AURKA lentivirus did not change NKX3.1 localization. Subcellular localization of NKX3.1 in C4-2 cells infected by AURKA shRNA using immunofluorescence is shown in A. NKX3.1 (green) and nucleus (blue). C4-2 cells were stained with an anti-NKX3.1 monoclonal antibody and FITC-conjugated secondary antibody. Nuclei were stained with DAPI. Scale bar equals 100 µM. 100 cells were counted. The experiment is performed three times. **(B)** Subcellular fractionation of NKX3.1 in C4-2 cells in response to knockdown of AURKA is shown B. C4-2 cells were treated with AURKA lentivirus, and NKX3.1 location was checked by western blot analysis. Actin and lamin were used as the control. The experiment is performed three times. **(C)** Treatment of 22Rv1 cells with AURKA lentivirus did not change NKX3.1 localization. Subcellular localization of NKX3.1 in 22Rv1 cells infected by AURKA shRNA using immunofluorescence is shown in C. NKX3.1 (green) and nucleus (blue). 22Rv1 cells were stained with an anti-NKX3.1 monoclonal antibody and FITC-conjugated secondary antibody. Nuclei were stained with DAPI. Scale bar equals 100 µM. 100 cells were counted. The experiment is performed three times. **(D)** Subcellular fractionation of NKX3.1 in 22Rv1 cells in response to knockdown of AURKA is shown D. 22Rv1 cells were treated with AURKA lentivirus, and NKX3.1 location was checked by western blot analysis. Actin and lamin were used as the control. The experiment was performed three times.

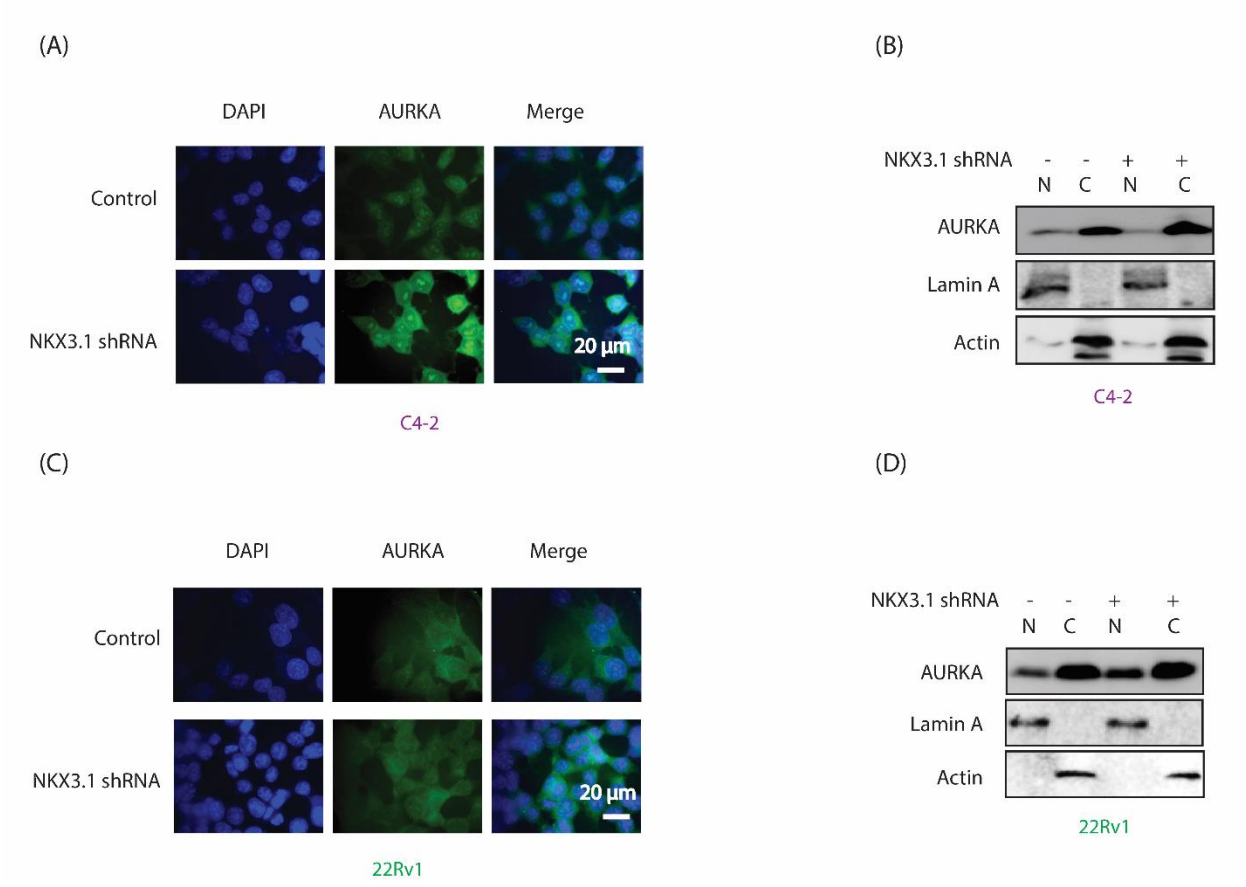

Figure 4-4 Immunofluorescent localization of AURKA.

(A) Treatment of C4-2 cells with NKX3.1 lentivirus did not change AURKA localization. Subcellular localization of AURKA in C4-2 cells infected by NKX3.1 shRNA using immunofluorescence is shown in A. AURKA (green) and nucleus (blue). C4-2 cells were stained with an anti-AURKA monoclonal antibody and FITC-conjugated secondary antibody. Nuclei were stained with DAPI. Scale bar equals 100 µM. 100 cells were counted. The experiment is performed three times. **(B)** Subcellular fractionation of AURKA in C4-2 cells in response to knockdown of NKX3.1 is shown B. C4-2 cells were treated with NKX3.1 lentivirus, and AURKA location was checked by western blot analysis. Actin and lamin were used as the control. The experiment is performed three times. **(C)** Treatment of 22Rv1 cells with NKX3.1 lentivirus did not change AURKA localization. Subcellular localization of AURKA in 22Rv1 cells infected by NKX3.1 shRNA using immunofluorescence is shown in C. AURKA (green) and nucleus (blue). 22Rv1 cells were stained with an anti-AURKA monoclonal antibody and FITC-conjugated secondary antibody. Nuclei were stained with DAPI. Scale bar equals 100 µM. 100 cells were counted. The experiment is performed three times. **(D)** Subcellular fractionation of AURKA in 22Rv1 cells in response to knockdown of NKX3.1 is shown D. 22Rv1 cells were treated with NKX3.1 lentivirus, and AURKA location was checked by western blot analysis. Actin and lamin were used as the control. The experiment was performed three times.

AURKA regulates NKX3.1 protein level

We next considered the possibility that AURKA regulates the protein expression of NKX3.1. To test the effect of the increased expression of AURKA on NKX3.1 protein level, we infected C4-2 cells with AURKA retrovirus. We collected the cell lysates after 33 hours and

determine the protein levels using western blot analysis. As shown in **figure 4-5A** expression of AURKA in cells resulted in a decreased level of NKX3.1 in the cells. The graph in **figure 4-5B** shows statistical analysis. We confirmed our results in 22Rv1 cells **(figure 4-5C, 4-5D)**.

We also investigate the impact of AURKA knockdown on the NKX3.1 protein level. Thus, we infected C4-2 with AURKA lentivirus. Then, the cells were collected after 33 hours and we determine the protein levels by western blot analysis. As indicated in **Figures 4-5E** cells infected by shRNA targeting AURKA had significantly elevated NKX3.1 protein levels. The histogram in **figure 4-5F** shows statistical analysis from n=3. We validated our results in 22Rv1 cells **(figure 4-5G, 4-5H)**. To this end, we conclude that AURKA regulates the NKX3.1 protein level negatively.

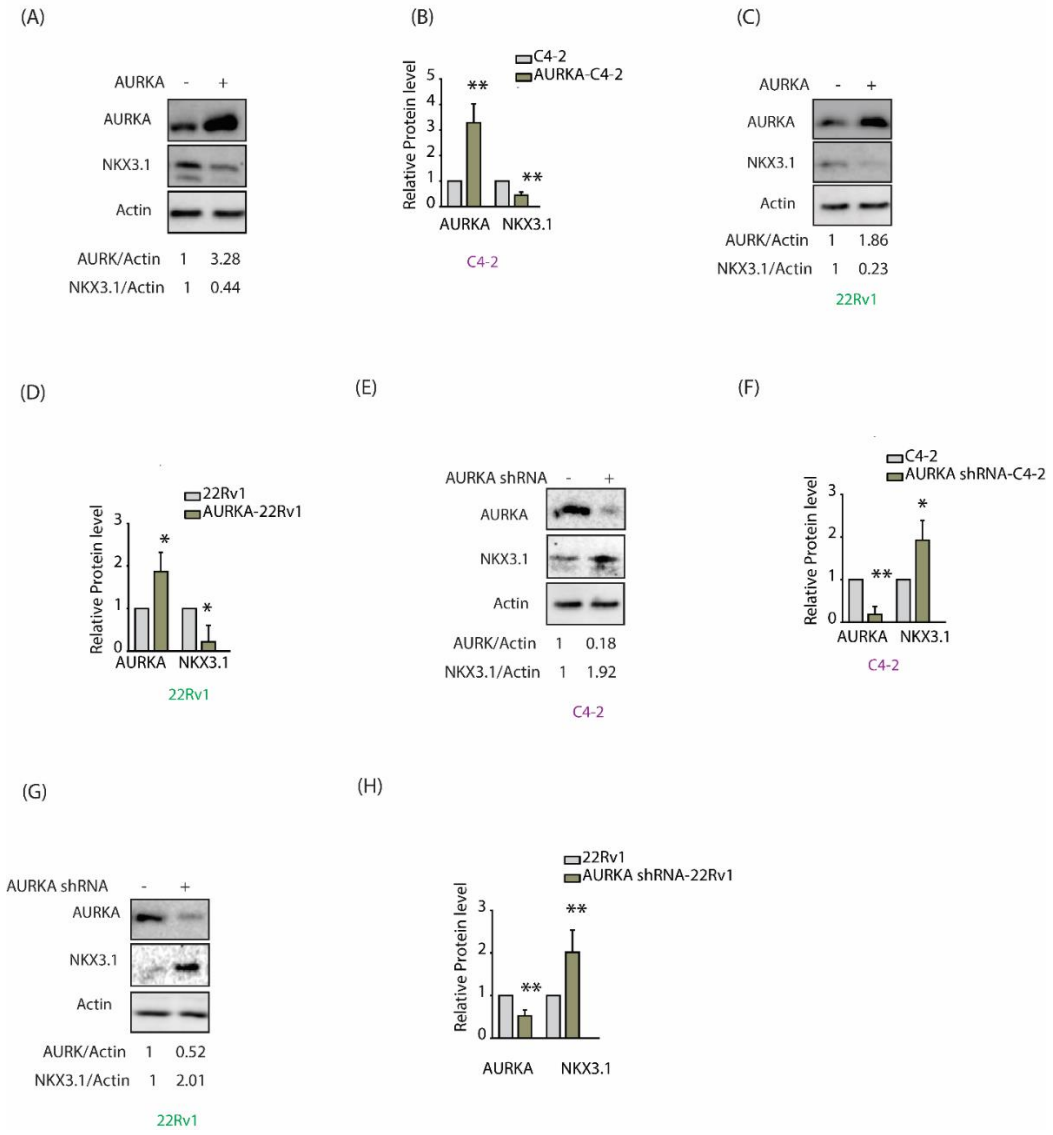

Figure 4-5 Expression of NKX3.1 was regulated by AURKA.

(A) Overexpression of AURKA decreases NKX3.1 protein level. C4-2 cells were infected with AURKA retrovirus. Cells were harvested after thirty-three hours. Then the cells were lysed and analyzed by western blot. Actin was used as a control. **(B)** Quantitative analysis of detected AURKA and NKX3.1 protein levels is presented in B. The data obtained from three independent experiments and normalized to the actin. ** $P < 0.01$. **(C)** Overexpression of AURKA decreases NKX3.1 protein level. 22Rv1 cells were infected with AURKA retrovirus. Thirty-three hours later, the cells were collected and lysed by western blot. We used actin as a control. **(D)** Quantitative analysis of protein levels is presented in D. The data were analyzed from three independent experiments. Signals obtained from western blot are normalized to the actin. * $P < 0.05$. **(E)** Downregulation of AURKA increases NKX3.1 protein level. C4-2 cells were infected with AURKA lentivirus. Thirty-three hours after infection, we collected the cells and analyzed them by western blot. Actin was used as a control. **(F)** Quantitative analysis of detected AURKA and NKX3.1 protein levels are presented in F. The data obtained from three independent experiments and normalized to the actin. * $P < 0.05$, ** $P < 0.01$. **(G)** Downregulation of AURKA increases NKX3.1 protein level. 22Rv1 cells were infected with AURKA lentivirus. Thirty-three hours later, the cells were collected and lysed by western blot. We used actin as a control. **(H)** Quantitative analysis of detected AURKA and NKX3.1 protein levels is presented in H. The data obtained from three independent experiments. Signals obtained from western blot are normalized to the actin. ** $P < 0.01$.

AURKA regulates NKX3.1 protein stability

To understand the possible mechanisms for the observed relationship between AURKA and NKX3.1 we assessed the half-life of NKX3.1. Therefore, C4-2 cells were infected with AURKA shRNA lentivirus for 33 hours. Then cycloheximide (CHX), a protein synthesis inhibitor was added to get protein half-life. After 2 and 4 hours of treatment, the cells were collected and evaluated by western blot analysis. As indicated in **figure 4-6A** NKX3.1 protein level in the cells infected with AURKA shRNA decreased much more slowly than that of untreated cells. **Figure 4-6B** indicates data analysis from three different experiments. The results have been validated in 22Rv1 cells **(figure 4-6C, figure 4-6D)**.

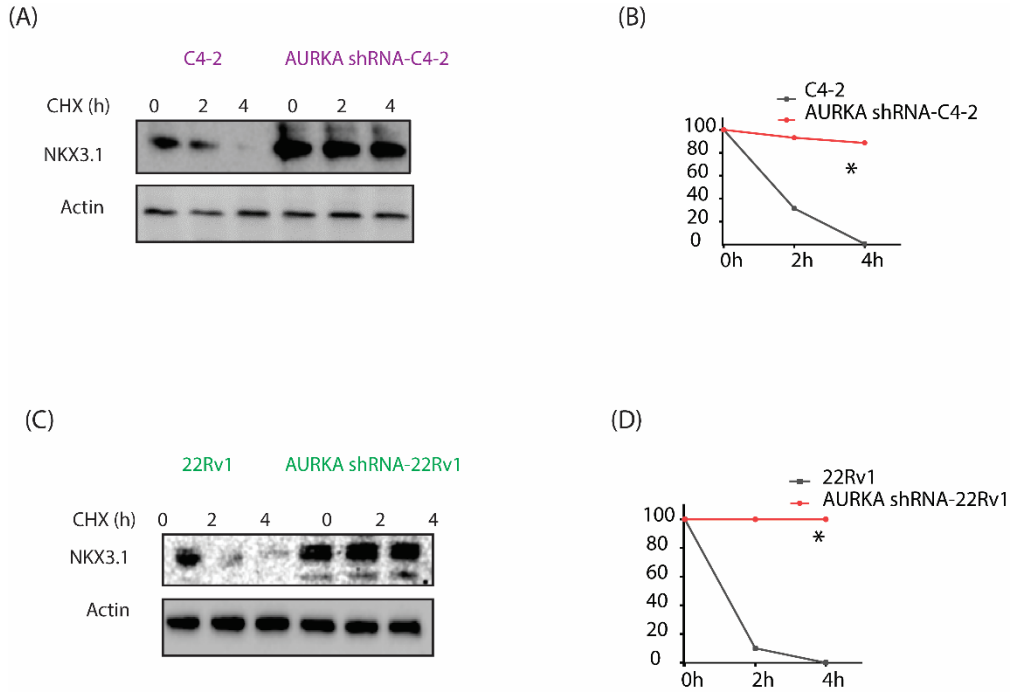

Figure 4-6 AURKA decreases NKX3.1 protein stability.

(A) NKX3.1 degradation in C4-2 cells treated with AURKA shRNA and CHX. We treated C4-2 cells with AURKA lentivirus to knockdown AURKA for thirty-three hours. We then treated the cells with CHX (20 µg/ml) for 2 and 4 hours. Next, we collected the cells and analyzed the level of NKX3.1 by western blot. **(B)** NKX3.1 protein level was normalized to actin, and the graph is presented in B. * $P < 0.05$. **(C)** NKX3.1 degradation in 22Rv1 cells treated with AURKA lentivirus and CHX. 22Rv1 cells were treated by AURKA lentivirus for thirty-three hours. Next, we treated the cells with CHX (20 µg/ml) for 2 and 4 hours. Then, we collected the cells and analyzed the level of NKX3.1 by western blot. **(D)** The graph represents the statistical analysis of three independent experiments. * $P < 0.05$.

AURKA mediates NKX3.1 ubiquitination

To investigate the mechanism by which AURKA regulates NKX3.1 expression, we wanted to study the impact of overexpression of AURKA on NKX3.1 ubiquitination. To do so, ubiquitination analyses were performed in C4-2 cells infected with AURKA and ubiquitin retrovirus. Ubiquitinated NKX3.1 was pulled down using NKX3.1 antibody and ubiquitination was checked by western blot using 6x-Histidine antibody. When AURKA was overexpressed NKX3.1 ubiquitination was observed suggesting that attenuation of NKX3.1 protein level go through proteasomal degradation **(figure 4-7).**

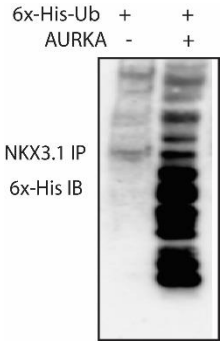

Figure 4-7 Ubiquitination of NKX3.1 when AURKA was overexpressed.

Ectopic expression of AURKA results in NKX3.1 ubiquitination. Cells were infected with AURKA and 6x-His-Ub and then treated with MG132. NKX3.1 was purified, and ubiquitination was detected by western blot analysis and 6x-His antibody. The assay is repeated three times.

4.2.2 Aim2

We will examine how NKX3.1 expression regulates AURKA expression.

NKX3.1 regulates AURKA protein level

AURKA is upregulated in prostate cancer cells. On the other hand, reduced expression of NKX3.1 plays a role in prostate cancer initiation. Thus, we examined the effect of NKX3.1 on AURKA protein level. To do so, C4-2 cells were treated with NKX3.1 retrovirus. The cells were harvested after thirty-three hours and analyzed by western blot. We observed a decreased level of AURKA in the cells overexpressing NKX3.1 **(figure 4-8A)**. The graph in **figure 4-85B** shows statistical analysis. We confirmed our results in 22Rv1 cells **(figure 4-8C, 4-8D)**.To test whether NKX3.1 can suppress AURKA protein levels; we downregulate NKX3.1 expression in C4-2 and

22Rv1 cells by shRNA. Then we tested AURKA protein levels by western blot analysis. AURKA protein levels were increased in C4-2 and 22Rv1 cells upon NKX3.1 shRNA infection compared to the control, suggesting the contribution of NKX3.1 to the AURKA protein level regulation. Collectively, these findings suggest that AURKA and NKX3.1 regulate each other in a negative feedback loop **(figure 4-8 E-H)**.

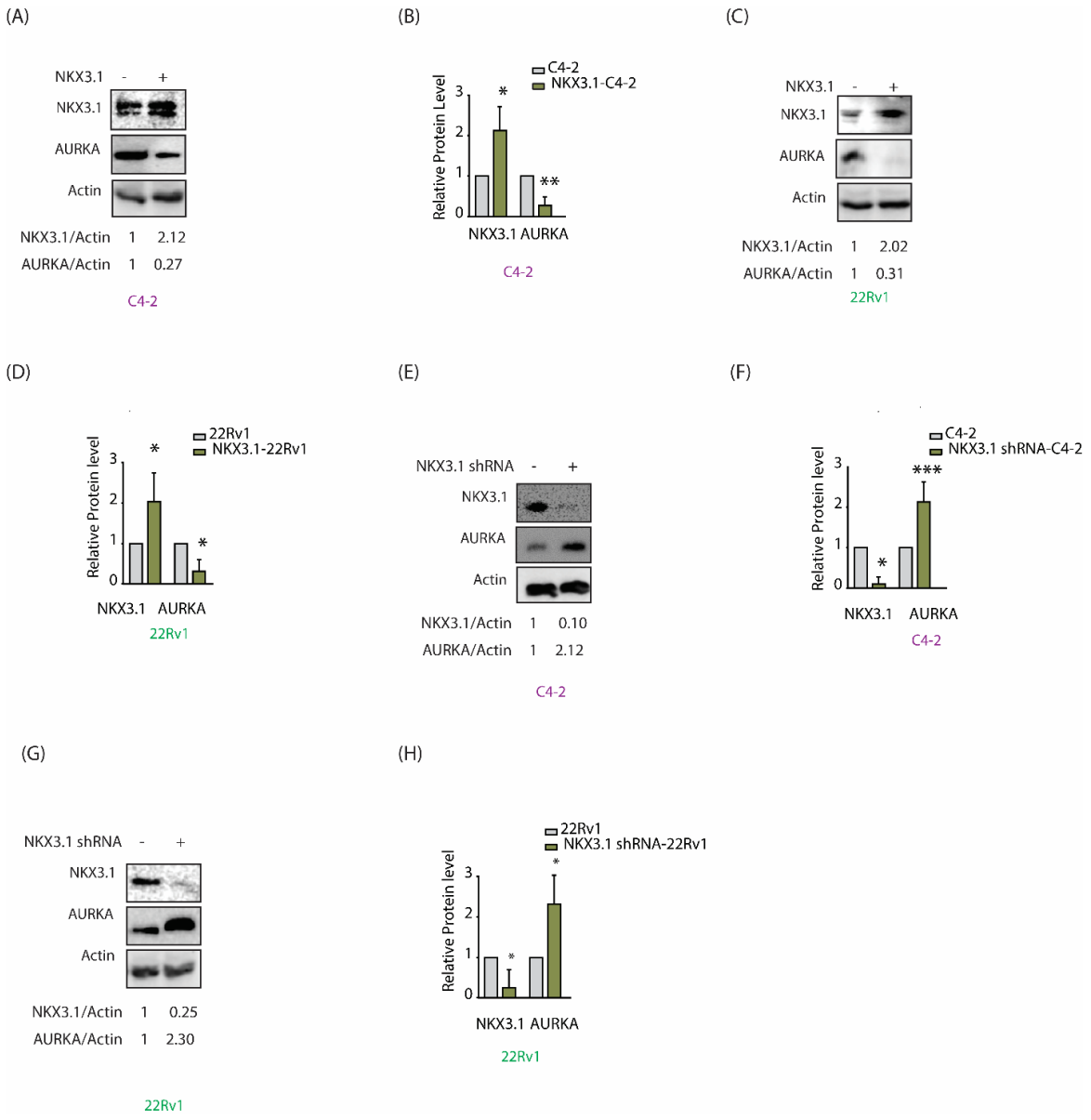

Figure 4-8 Expression of NKX3.1 was regulated by AURKA.

(A) NKX3.1 overexpression results in AURKA protein level downregulation. C4-2 cells were harvested after thirty-three hours of infection. Then the cells were analyzed by western blot. We used actin as a control. **(B)** The graph in B presents quantitative analysis of protein levels for n=3. The protein levels are normalized to the actin. * $P < 0.05$ and . ** $P < 0.01$.. **(C)** NKX3.1 upregulation results in AURKA protein level downregulation. 22Rv1 cells were infected with NKX3.1 retrovirus for thirty-three hours. Then we collected the cells and assessed the protein levels by western blot. We used actin as a control. **(D)** The graph in D is the quantitative analysis of protein levels for n=3. The protein levels are normalized to the actin. * $P < 0.05$. **(E)** Downregulation of NKX3.1 increases AURKA protein level. C4-2 cells were infected with NKX3.1 lentivirus for thirty-three hours. We then collected the cells and analyzed them by western blot using actin as a control. **(F)** The histogram in F is the quantitative analysis of protein levels for n=3. The protein levels are normalized to the actin. * $P < 0.05$ and *** $P < 0.001$. **(G)** Downregulation of NKX3.1 increases AURKA protein level. 22Rv1 cells were infected with NKX3.1 lentivirus. The cells were lysed after thirty-three hours. We assessed the protein levels by western blot. Actin was used as a control. **(H)** Quantitative analysis of detected protein levels is presented in H. The data obtained from three independent experiments. Signals obtained from western blot are normalized to the actin. * $P < 0.05$.

1 regulates AURKA protein stability

Having demonstrated that NKX3.1 regulates AURKA protein level, we explore the mechanisms by which NKX3.1 decreased AURKA protein level. abundance. Thus, we next examine whether NKX3.1 regulates AURKA turnover using cycloheximide. To do so, C4-2 cells were infected with NKX3.1 lentivirus for thirty-two hours. Then, the cells were then incubated with cycloheximide for 2 and 4 h. Cell lysates were resolved by SDS-PAGE and analyzed by western blot with anti-AURKA **(figure4-9A)**. We noted that the reduced expression of NKX3.1 increases AURKA's half-life and stability **(figure4-9B)**. We validated our results in 22rv1 cells **figure4-9C, 4-9D)**. Together, these results suggest that NKX3.1 controls AURKA expression.

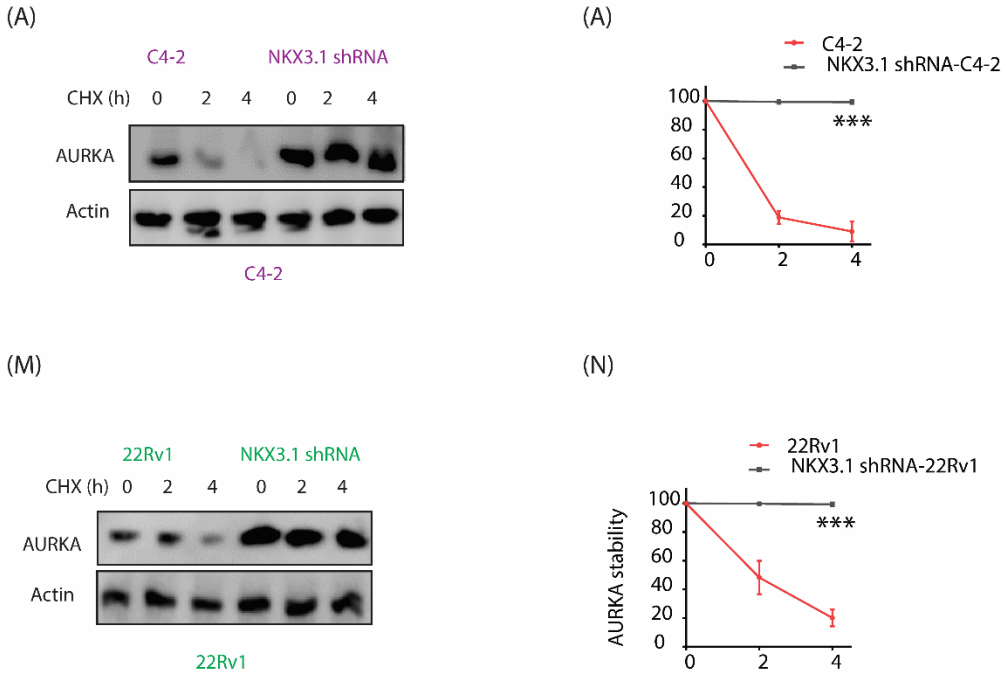

Figure 4-9 NKX3.1 mediated AURKA protein stability.

(A) AURKA degradation in C4-2 cells treated with NKX3.1 lentivirus and CHX (20 µg/ml). C4-2 cells were treated by NKX3.1 lentivirus. Thirty-three hours postinfection, the cells were treated with CHX (20 µg/ml) for 2 and 4 hours. Subsequently, the cells were lysed, and the AURKA protein level was analyzed by western blot. **(B)** The graph represents the statistical analysis of three independent experiments. * $P < 0.05$. **(C)** AURKA degradation in 22Rv1 cells treated with NKX3.1 lentivirus and CHX (20 µg/ml) is shown in C. **(D)** The graph represents the statistical analysis from n=3. * $P < 0.05$.

NKX3.1 mediates AURKA ubiquitination

To understand the mechanism of how NKX3.1 promotes AUKKA downregulation, we examined ubiquitin-mediated AURKA degradation. To do so, ubiquitinated AUTKA levels were measured by western blot analysis. We infected C4-2 cells with NKX3.1 and ubiquitin retrovirus. Then, AURKA was immunoprecipitated using an anti-AURKA antibody. We tested and AURKA ubiquitination by western blotting using anti histidine antibody. Our results showed an increase in the level of ubiquitination in the cells overexpressing NKX3.1 **(figure4-10)**.

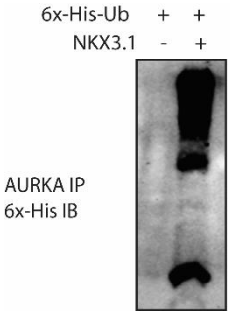

Figure 4-10 Ubiquitination of NKX3.1 when AURKA was overexpressed.

NKX3.1 overexpression increases AURKA ubiquitination in C4-2 cells. Target cells expressing NKX3.1 were infected by 6x-His Ubiquitin retrovirus. Cells were treated with MG132 for 10 hours. Then ubiquitination of AURKA was analyzed by western blot with 6x-His antibody. We detected more ubiquitinated AURKA in the cells overexpressing NKX3.1. The assay is repeated three times.

4.2.3 Aim 3

In this aim, we will identify the specific sites on NKX3.1, which are phosphorylated by AURKA. We will further examine the importance of these identified sites in aggressive oncogenic phenotype.

Aurora-A phosphorylates NKX3.1 at serine 28, 102 and 209

Since AURKA phosphorates NKX3.1 and regulates its expression, we next identify the potential phosphorylation sites of AURKA on NKX3.1. Based on prior knowledge of the AURKA consensus phosphoacceptor motif, we know that it recognizes R/K/N-R-X-S/ T-B, where B denotes any hydrophobic residue except for proline. Therefore, we predict serin 28,101, and 209 as the phosphorylation targets. We mutagenized each of these serines to alanines to abolish

phosphorylation. Then, the proteins were incubated with [γ-^{32}P]ATP and AURKA. Then, the proteins were separated by SDS-PAGE, and phosphorylation was examined by autoradiography. We observed that mutated proteins showed a significant decrease in phosphorylation compared to the wild type **(figure 4-11A)**. After identification of the specific phosphorylation sites, we mutated all tree targets to alanine and performed *in vitro* kinase assay. As shown in **figure 4-11B** we observed that mutation of these three positions abolished phosphorylation completely.

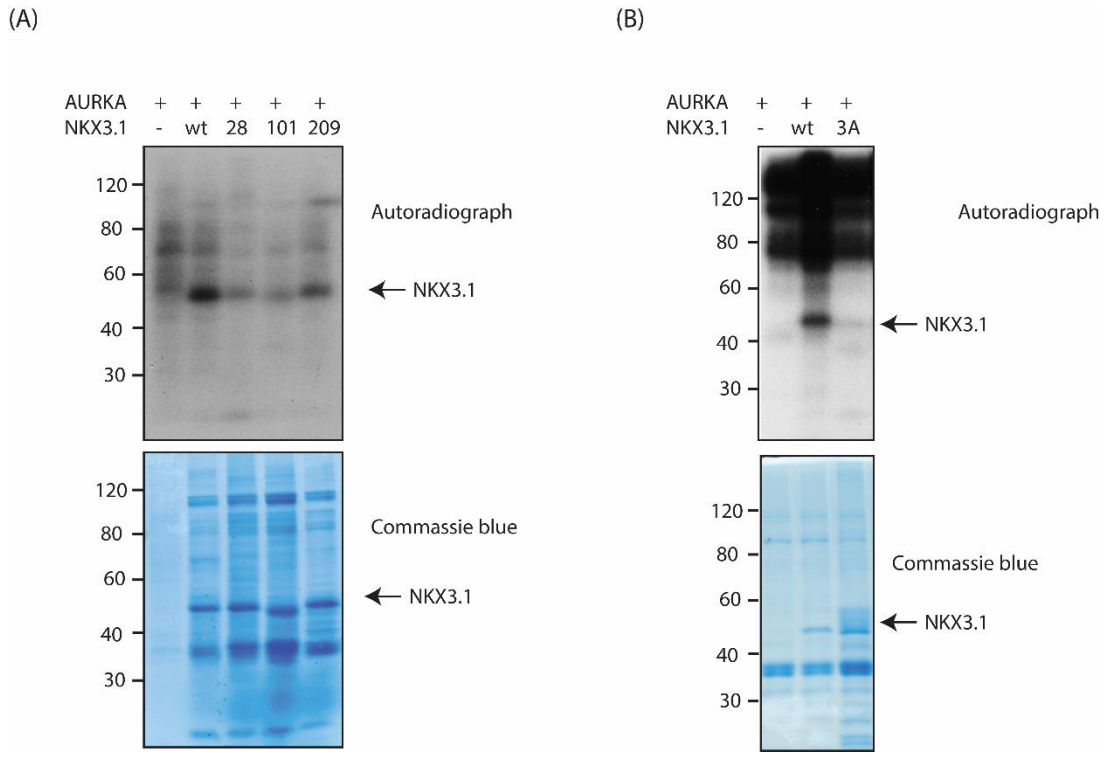

Figure 4-11 AURKA phosphorylates NKX3.1 at S28, 101, and 209 positions.

(A) *In vitro* phosphorylation assay indicated that S28, 101, and 209 are the potential AURKA phosphorylation sites on NKX3.1. **(B)** *In vitro* phosphorylation assay indicated that AURKA phosphorylates wild-type NKX3.1 but it does not phosphorylate 3A mutant. NKX3.1 phosphorylation was detected by autoradiography. The gel was stained with Coomassie Brilliant Blue. The Top panel represents an autoradiograph. The bottom panel shows a gel stained with Coomassie blue. The assay is repeated three times.

AURKA decreases NKX3.1 stability via phosphorylation at S28, S101, and S209

Since AURKA directly phosphorylates NKX3.1 at three positions, we, therefore, examined whether the phosphorylation of NKX3.1 at the identified sites (S28, S101, and S209) regulates its stability. We infected C4-2cells with NKX3.1 wild type and S3A-NKX3.1 retrovirus and after 32 hours, we treated them with cycloheximide for indicated periods (2 and 4 hours). Then we

measured the turnover of NKX3.1 using western blot analysis. As shown in **figure 4-12A** the NKX3.1-3A stability was markedly higher than the NKX3.1 wild type, suggesting that phosphorylation of NKX3.1 at S28, S101, and S209 sites lowers NKX3.1 stability. **Figure 4-12B** represents the statistical analysis. We validated our results in 22Rv1 cells **(figure 4-12C, 4-13D)**.

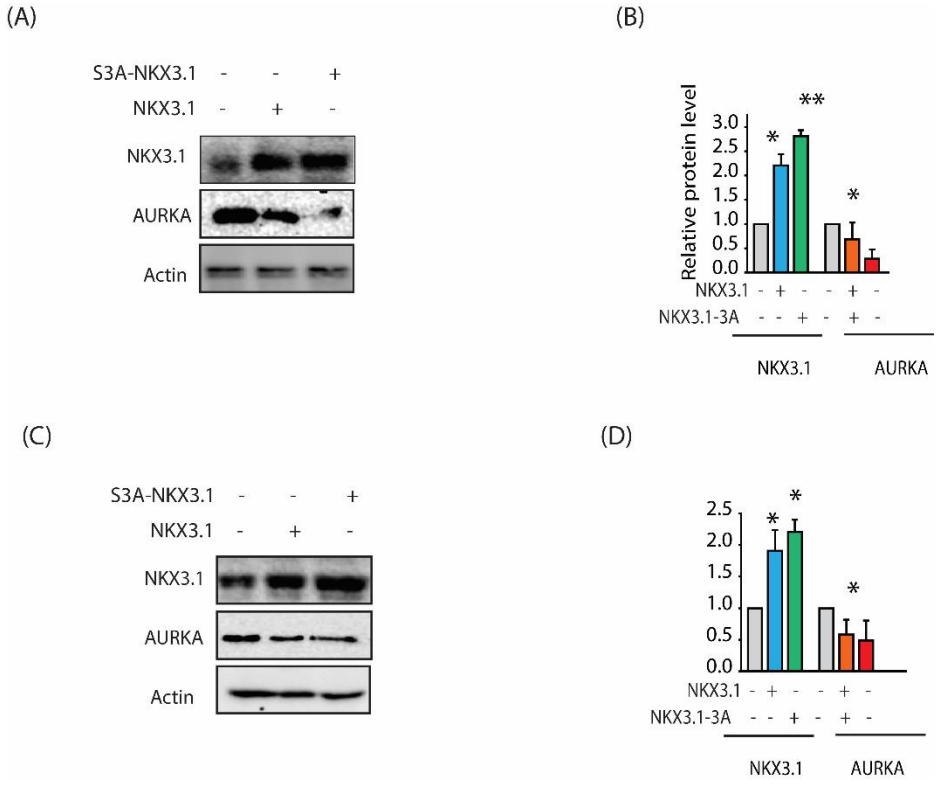

Figure 4-12 Effect S3A phosphorylation on the protein level of NKX3.1 and AURKA.

(A) S3A-NKX3.1 is expressed at a higher level compared to wild-type. C4-2 cells infected with NKX3.1 and S13A-NKX3.1 retrovirus for thirty-three hours. Cell lysates were analyzed were by western blot to detect NKX3.1 and AURKA protein levels. **(B)** Quantification of western blot analysis normalized to the actin is shown B. The data are from three independent experiments. * $P < 0.05$ and ** $P < 0.01$. **(C)** S3A-NKX3.1 is expressed at a higher level compared to wild-type in 22Rv1 cells. **(D)** Quantification of western blot analysis normalized to the actin is shown in D. The data are from three independent experiments. * $P < 0.05$.

To determine the significance of phosphorylation at Ser 28, 101, and 209 on NKX3.1 stability, we performed a cycloheximide experiment using NKX3.1 and S3A-NKX3.1. We observed an increase in protein stability of S3A-NKX3.1. This provides further evidence for the importance of NKX3.1 phosphorylation by AURKA on its stability **(figure4-13)**.

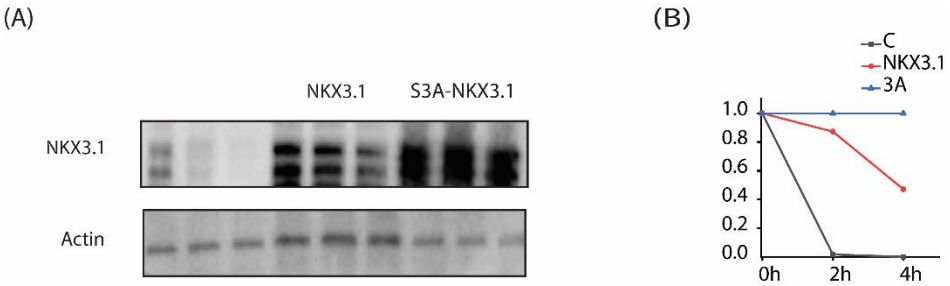

Figure 4-13 NKX3.1 phosphorylation decreases NKX3.1 protein stability.

(A) Immunoblot analysis of cell lysates from C4-2 cells ectopically expressing NKX3.1 and S3A-NKX3.1 treating with CHX. C4-2 cells were treated with NKX3.1 and S3A-NKX3.1 for thirty-three hours. Then the cells were treated with CHX (20 µg/ml) for the indicated times. Subsequently, protein levels were analyzed by western blot **(B)** Normalized fold changes of NKX3.1 are presented in B. The data show the analysis of three independent experiments. * $P < 0.05$, ** $P < 0.01$, *** $P < 0.001$ and **** $P < 0.0001$.

NKX3.1 phosphorylation regulates AURKA stability via ubiquitination

To assess the effect of NKX3.1 phosphorylation on AURKA degradation by ubiquitination, we infected cells overexpressing wild-type NKX 3.1 and S3A-NKX3.1 with 6x-His-ubiquitin and detect the ubiquitination pattern using western blot analysis. As shown in **figure 4-14A** S3A-NKX3.1 enhanced AURKA ubiquitination compared to the wild-type NKX 3.1. These data suggest that phosphorylation of NKX3.1 at the three identified sites (S28, S101, and S209) would decrease NKX3.1 stability and result in attenuating degradation of AURKA. We validated our results in 22Rv1 cells **(figure 4-14B)**.

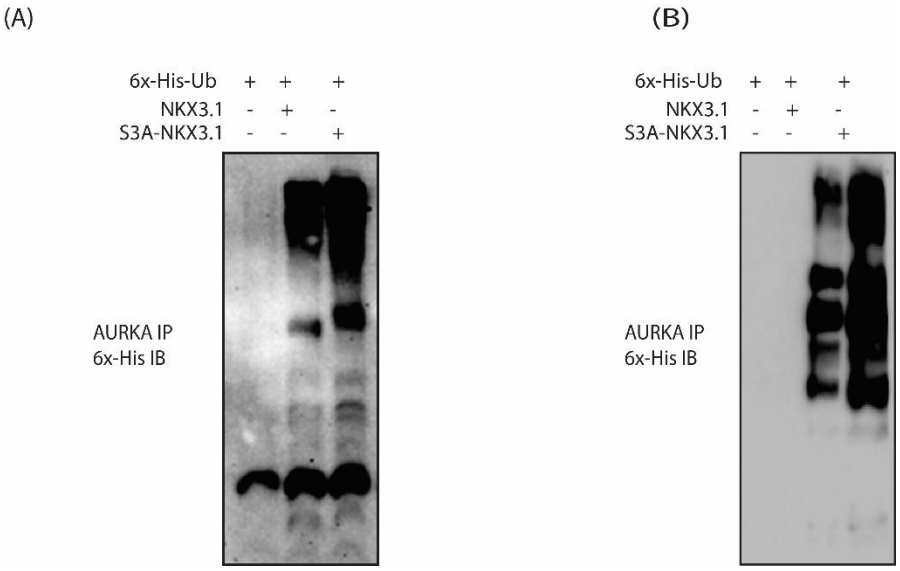

Figure 4-14 Ubiquitination of AURKA is promoted by S3A-NKX3.1

(A) AURKA immunoprecipitated with AURKA antibody and analyzed with western blot. We detected an increased level of AURKA degradation when C4-2 cells were treated with S3A-NKX3.1. The cells were infected with 6x-His-ubiquitin retrovirus following MG132 treatment. Then we lysed the cells and the lysate was subjected to immunoprecipitation by the anti-AURKA antibody. Ubiquitination was detected by western blot using a 6x-Histidine antibody. NKX3.1 regulates the ubiquitination of AURKA. **(B)** AURKA immunoprecipitated with AURKA antibody and analyzed with western blot. We detected an increased level of ubiquitination when 22Rv1 cells were treated with S3A-NKX3.1.

NKX3.1 inhibits cell proliferation growth of cancer cell lines

NKX3.1 is a transcription factor that plays an important role in normal prostate development. Moreover, loss-of-function of NKX3.1 has been reported in prostate cancer (127). Thus, we examined the effect of NKX3.1 and S3A-NKX3.1 on cell proliferation using MTT assay. Briefly, cells were transiently infected with NKX3.1 and S3A-NKX3.1. At the indicated times (18 and 36 h).MTT reagent was added to the cells the absorbance value was measured at 570 nm. Consistent with previous findings, ectopic expression of NKX3.1 reduce cell growth in C4-2 and 22Rv1 cells **(figure4-15A, figure 4-15B)**. Our results also indicated that S3A-NKX3.1 inhibited cell growth more effectively. Cell proliferation was further analyzed by infecting NKX3.1 and S3A-NKX3.1 stable cell lines with AURKA retrovirus. Expression of AURKA increased cell viability of stable cell lines **(figure4-15C)**. Together, these results indicate that NKX3.1 inhibits the proliferation of human prostate cells. Also, the mutation of AURKA phosphorylation sites on NKX3.1 enhances the anti-tumorigenic properties of NKX3.1 on cell proliferation at the analyzed time points.

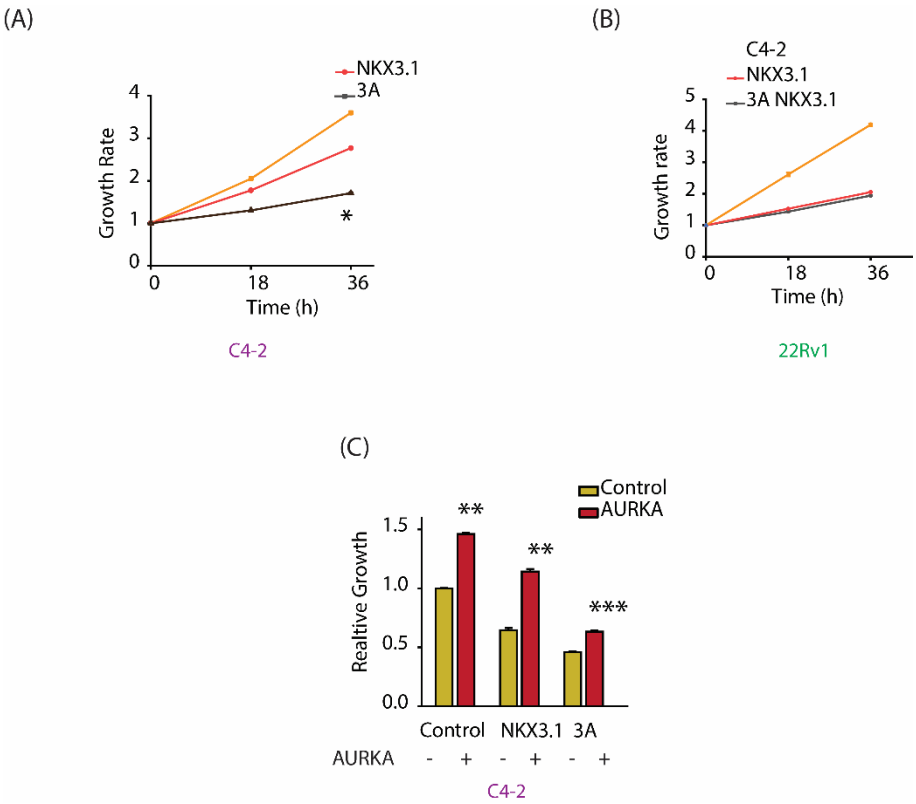

Figure 4-15 NKX3.1 inhibits aggressive cancer phenotype in prostate cancer cells.

(A) Cell proliferation measurement after indicated time in the C4-2 and (B) 22 Rv1 cells treated with NKX3.1 and S3A-NKX3.1. Target cells were seeded in a 24-well plate and infected by NKX3.1 and S3A-NKX3.1 retrovirus for 18 and 36 hours. Proliferative activity was measured by MTT assay. The absorbance was measured at 570 nm. All data are from three independent experiments. * $P < 0.05$. (C) C4-2 cells stably expressed NKX3.1, S3A-NKX3.1 were infected by AURKA retrovirus. Proliferative activity was measured by MTT assay. The absorbance was read at 570 nm. All data are from three independent experiments. , ** $P < 0.01$, and *** $P < 0.001$.

NKX3.1 inhibits cell migration and cell proliferation growth of cancer cell lines in soft agar assay

Next, we determined the effect of NKX3.1 protein level on cell migration. The results of the migration assay indicated that NKX3.1 and S3A-NKX3.1 overexpression inhibited C4-2 and 22Rv1 cell migration compared to the control **(figure4-16A-D)**. In addition to C4-2 and 22Rv1 cells, we also tested the effect of AURKA protein level on cell migration in the NKX3.1. S3A-NKX3.1 cell lines. We observed S3A-NKX3.1 expression decrease the number of migrated cells compared with NKX3.1 **(figure4-16F)**. These results further showed that phosphorylation of NKX3.1 by AURKA decreases its tumor suppressor ability. We next determine the role of NKX3.1 in cloning-forming ability. We detected a decrease in colony formation upon NKX3.1 and S3A-NKX3.1 expression. Our results showed a decrease in the level of colonies when the cells have

been treated by S3A-NKX3.1 **(figure4-16G-H).** The results validate the conclusions drawn by the role of NKX3.1 as a tumor suppressor. Additionally, our results confirmed that AURKA regulates NKX3.1 stability by phosphorylation as reflected in cell migration cell proliferation growth in soft agar assay.

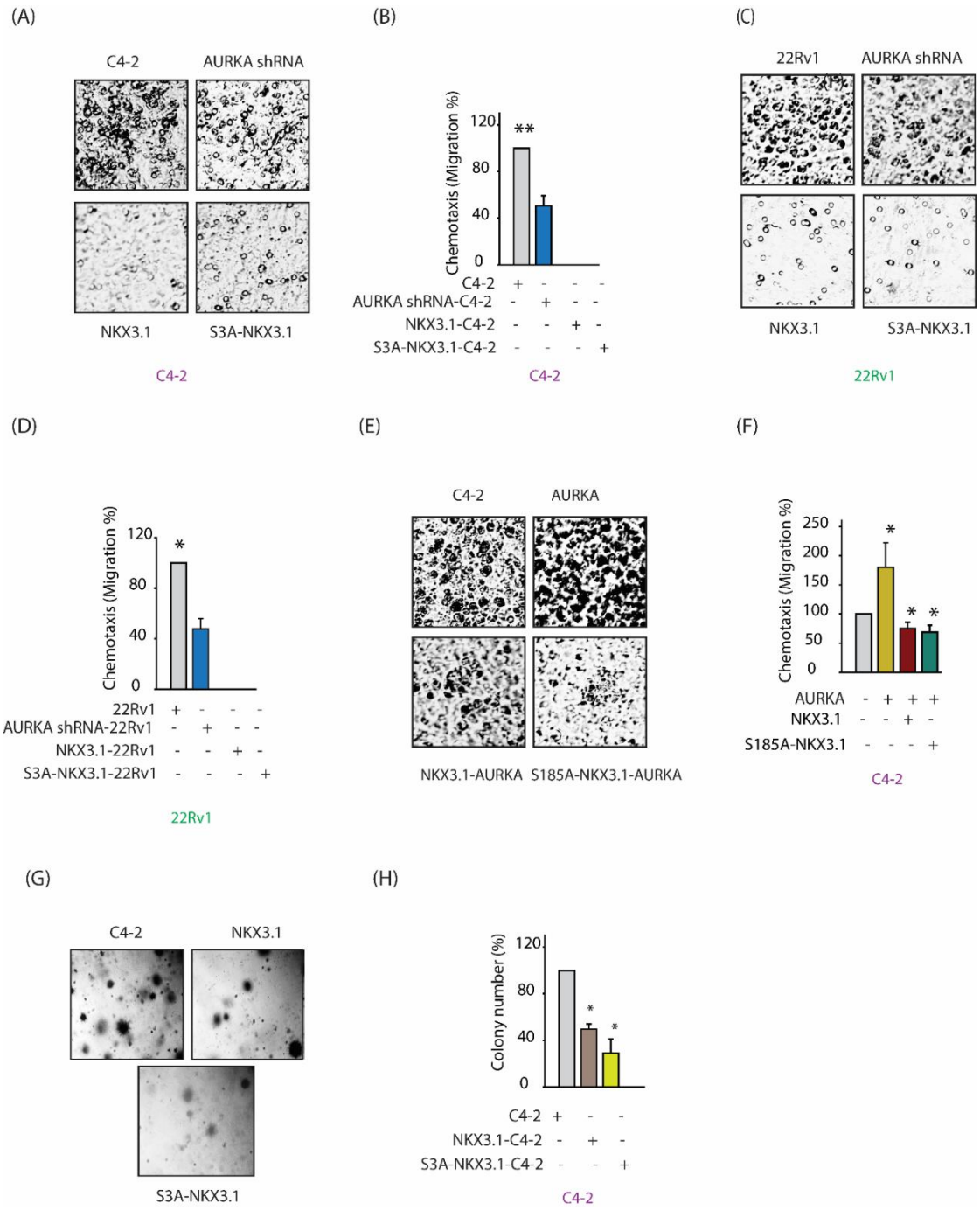

Figure 4-16 NKX3.1 inhibits aggressive phenotypes.

(A) NKX3.1 suppressed cell migration in C4-2 cells. Migration assay of C4-2 cell infected with AURKA shRNA, NKX3.1, and S3A-NKX3.1 is shown in A. The cells were starved in serum-free media for 12 hours and migration assay was performed using Boyden chambers. **(B)** The results are plotted as the means ± SD of three independent experiments. ** $P < 0.01$. **(C)** Migration assay of 22Rv1 cell infected with AURKA shRNA, NKX3.1, and S3A-NKX3.1 is shown in C. **(D)** The results are plotted as the means ± SD of three independent experiments. * $P < 0.05$. **(E)** Migration assay of NKX3.1 and S3A cell lines infected with AURKA **(F))** The results are plotted as the means ± SD of three independent experiments. * $P < 0.05$. **(G)** Colony formation assay showed that NKX3.1 and S3A-NKX3.1 inhibit the proliferation ability of C4-2 cells in a soft-agar experiment. **(H)** Quantitative data analysis of the soft agar experiment is shown in B. All data were from n=3. *. $P<0.05$.

4.3 Discussion

NKX3.1 is a tumor suppressor that plays a prominent role in normal prostate development. The NKX3.1 protein level is underexpressed in the early stage of prostate cancer (129). NKX3.1 is downregulated in 65% to 78% of metastatic prostate cancers (130). AURKA is a serine/threonine kinase that is upregulated in prostate cancer cells (131). In the current study, we identified NKX3.1 as the direct substrate of AURKA. Our results have shown that AURKA phosphorylates NKX3.1 at three positions and downregulates its expression. Knockout of AURKA results in stabilization and increased levels of NKX3.1. Our results indicate that NKX3.1 also regulates AURKA protein expression. In specific, NKX3.1 induces ubiquitin-mediated degradation of AURKA and reduces AURKA protein levels. We also investigate the consequences of NKX3.1 phosphorylation by AURKA in the oncogenic phenotype. We demonstrate that overexpression of NKX3.1 inhibited cell proliferation and migration. NKX3.1 phosphorylation by AURKA decreases NKX3.1 stability and promotes the oncogenic phenotype. Together, our results indicated that AURKA and NKX3.1 regulate each other in a negative feedback loop and result in prostate cancer progression **(figure4-17)**.

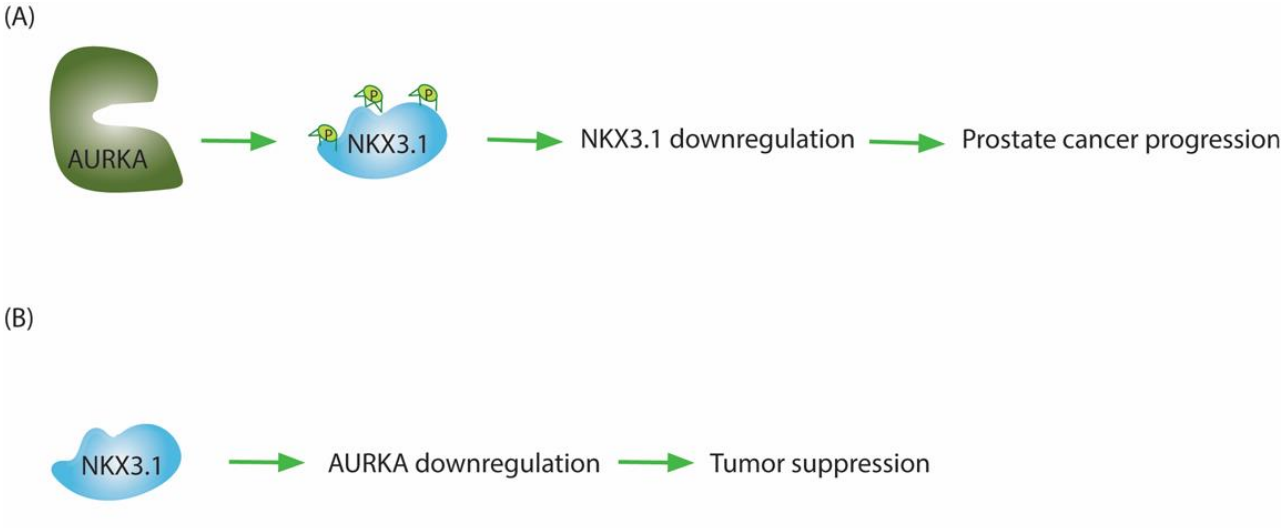

Figure 4-17 Proposed model of NKX3.1 and AURKA regulation.

(A) AURKA phosphorylates NKX3.1 and results in its downregulation. NKX3.1 downregulation leads to prostate cancer progression. **(B)** NKX3.1 functions as a tumor suppressor and downregulates AURKA at protein levels.

CHAPTER 5. FUTURE DIRECTION

AURKA is a serine-threonine kinase that regulates the cell cycle. AURKA overexpression drives several human cancers; however, AURKA inhibitors in clinical trials are not successful due to their toxicity. Our lab has shown that AURKA and LIMK2 regulate each other in a positive feedback loop. Moreover, unlike AURKA, LIMK2 is a non-toxic target.

LIMK2 is a serine-threonine kinase that regulates cytoskeleton dynamics. Its overexpression is detected in prostate cancer yet, the detailed mechanism by which LIMK2 promotes prostate cancer is not well established. Currently, there are only 5 known substrates of LIMK2.

This thesis provides valuable information on how LIMK2 and AURKA contribute to prostate cancer progression. First, we identified NKX3.1 as a direct substrate of LIMK2. Our results also indicated that AURKA phosphorylates NKX3.1. Then we uncovered the nature of the feedback loop that regulates NKX3.1-LIMK2 and NKX3.1-AURKA expression. In this chapter, we discuss several ideas that come from this thesis.

Does NKX3.1 phosphorylation regulate NKX3.1-mediated gene expression?

NKX3.1 functions as a transcription factor and its stability is regulated by phosphorylation. However, whether phosphorylation regulates NKX3.1 activity is currently unknown. In order to investigate this, we can measure NKX3.1 transactivation using NKX3.1 response element–driven luciferase. Moreover, to uncover the gene expression program modulated by NKX3.1 phosphorylation, we can compare gene expression profiles of the cells overexpressing wild-type with dominant-negative NKX3.1 using RNA sequencing.

How many more LIMK2 substrates remain to be discovered?

The number of known LIMK2 substrates is likely a small fraction of LIMK2's total substrates. Developing high-accuracy mass spectrometry techniques could help determine LIMK2 phospho-signaling profiles. After the initial screening, we can analyze the phospho-signaling profile to find potential LIMK2 substrates. A combination of proteomics and *in-vivo* models can investigate LIMK2 signaling networks and cancer progression.

What determines how cells respond to the LIMK2?

Signaling pathways respond to the extracellular stimuli and determine cell fate. Accurate regulation of biological networks can assist cells in maintaining homeostasis. Inappropriate activation of the signaling network leads to a variety of diseases.

LIMK2 is upregulated in CRPC but downregulated in colorectal cancer. This phenomenon indicates that not all cell types have the same response to LIMK2 expression. Understanding the context in which LIMK2 level results in cancer progression would have therapeutic application. A multitude of factors could lead to the heterogeneity of LIMK2 signaling. For example, multiple transcription factors can contribute to the LIMK2 expression level and its behavior. Additional experiments are required to identify the transcription factors regulating LIMK2 expression.

Potential future exploration for therapy of ADT-resistant cancer

It is also possible to explore the role of S185A-NKX3.1 as a method to overcome androgen resistance. Since NKX3.1 has been directly linked to AR-associated signaling events (116), it would be worthwhile to study the effect of the phospho-resistant mutant in overcoming androgen resistance in prostate cancer. For example, cell viability and oncogenic phenotypes can be assessed upon reinstatement of S185A-NKX3.1 and treatment with ADT drugs like enzalutamide. Any enhancement in chemoresistance will be indicative of successful therapy. The study can then be taken up in clinical specimens using biopsy samples from ADT resistant.

REFERENCES

1. Kiel C, Yus E, Serrano L. Engineering signal transduction pathways. Cell. 2010;140(1):33-47.
2. Sever R, Brugge JS. Signal transduction in cancer. Cold Spring Harb Perspect Med. 2015;5(4).
3. Ardito F, Giuliani M, Perrone D, Troiano G, Lo Muzio L. The crucial role of protein phosphorylation in cell signaling and its use as targeted therapy (Review). Int J Mol Med. 2017;40(2):271-80.
4. Schenk PW, Snaar-Jagalska BE. Signal perception and transduction: the role of protein kinases. Biochim Biophys Acta. 1999;1449(1):1-24.
5. Gavriilidis P, Giakoustidis A, Giakoustidis D. Aurora Kinases and Potential Medical Applications of Aurora Kinase Inhibitors: A Review. J Clin Med Res. 2015;7(10):742-51.
6. Cicenas J, Zalyte E, Bairoch A, Gaudet P. Kinases and Cancer. Cancers (Basel). 2018;10(3).
7. Sansregret L, Swanton C. The Role of Aneuploidy in Cancer Evolution. Cold Spring Harb Perspect Med. 2017;7(1).
8. Glover DM, Leibowitz MH, McLean DA, Parry H. Mutations in aurora prevent centrosome separation leading to the formation of monopolar spindles. Cell. 1995;81(1):95-105.
9. Carvajal RD, Tse A, Schwartz GK. Aurora kinases: New targets for cancer therapy. Clin Cancer Res. 2006;12(23):6869-75.
10. Glover DM. Mitosis in Drosophila. J Cell Sci. 1989;92 (Pt 2):137-46.
11. Hoar K, Chakravarty A, Rabino C, Wysong D, Bowman D, Roy N, et al. MLN8054, a small-molecule inhibitor of Aurora A, causes spindle pole and chromosome congression defects leading to aneuploidy. Mol Cell Biol. 2007;27(12):4513-25.
12. Qi G, Ogawa I, Kudo Y, Miyauchi M, Siriwardena BS, Shimamoto F, et al. Aurora-B expression and its correlation with cell proliferation and metastasis in oral cancer. Virchows Arch. 2007;450(3):297-302.
13. Tsou JH, Chang KC, Chang-Liao PY, Yang ST, Lee CT, Chen YP, et al. Aberrantly expressed AURKC enhances the transformation and tumourigenicity of epithelial cells. J Pathol. 2011;225(2):243-54.

14. Ke YW, Dou Z, Zhang J, Yao XB. Function and regulation of Aurora/Ipl1p kinase family in cell division. Cell Res. 2003;13(2):69-81.
15. Willems E, Dedobbeleer M, Digregorio M, Lombard A, Lumapat PN, Rogister B. The functional diversity of Aurora kinases: a comprehensive review. Cell Div. 2018;13:7.
16. Quartuccio SM, Schindler K. Functions of Aurora kinase C in meiosis and cancer. Front Cell Dev Biol. 2015;3:50.
17. Goldenson B, Crispino JD. The aurora kinases in cell cycle and leukemia. Oncogene. 2015;34(5):537-45.
18. Rannou Y, Troadec MB, Petretti C, Hans F, Dutertre S, Dimitrov S, et al. Localization of aurora A and aurora B kinases during interphase: role of the N-terminal domain. Cell Cycle. 2008;7(19):3012-20.
19. Cheetham GMT, Knegtel RMA, Coll JT, Renwick SB, Swenson L, Weber P, et al. Crystal structure of aurora-2, an oncogenic serine/threonine kinase. J Biol Chem. 2002;277(45):42419-22.
20. Bayliss R, Sardon T, Vernos I, Conti E. Structural basis of Aurora-A activation by TPX2 at the mitotic spindle. Mol Cell. 2003;12(4):851-62.
21. Fu JY, Bian ML, Jiang Q, Zhang CM. Roles of aurora kinases in mitosis and tumorigenesis. Mol Cancer Res. 2007;5(1):1-10.
22. Bayliss R, Burgess SG, McIntyre PJ. Switching Aurora-A kinase on and off at an allosteric site. Febs J. 2017;284(18):2947-54.
23. Castro A, Vigneron S, Bernis C, Labbe JC, Prigent C, Lorca T. The D-Box-activating domain (DAD) is a new proteolysis signal that stimulates the silent D-Box sequence of Aurora-A. Embo Rep. 2002;3(12):1209-14.
24. Honda K, Mihara H, Kato Y, Yamaguchi A, Tanaka H, Yasuda H, et al. Degradation of human Aurora2 protein kinase by the anaphase-promoting complex-ubiquitin-proteasome pathway. Oncogene. 2000;19(24):2812-9.
25. Littlepage LE, Ruderman JV. Identification of a new APC/C recognition domain, the A box, which is required for the Cdh1-dependent destruction of the kinase Aurora-A during mitotic exit. Gene Dev. 2002;16(17):2274-85.
26. Min M, Mayor U, Lindon C. Ubiquitination site preferences in anaphase promoting complex/cyclosome (APC/C) substrates. Open Biol. 2013;3(9):130097.

27. Yan M, Wang C, He B, Yang M, Tong M, Long Z, et al. Aurora-A Kinase: A Potent Oncogene and Target for Cancer Therapy. Med Res Rev. 2016;36(6):1036-79.
28. Bayliss R, Burgess SG, McIntyre PJ. Switching Aurora-A kinase on and off at an allosteric site. Febs J. 2017;284(18):2947-54.
29. Marumoto T, Hirota T, Morisaki T, Kunitoku N, Zhang DW, Ichikawa Y, et al. Roles of aurora-A kinase in mitotic entry and G2 checkpoint in mammalian cells. Genes Cells. 2002;7(11):1173-82.
30. Rivera-Rivera Y, Saavedra HI. Centrosome - a promising anti-cancer target. Biologics. 2016;10:167-76.
31. Fu J, Hagan IM, Glover DM. The centrosome and its duplication cycle. Cold Spring Harb Perspect Biol. 2015;7(2):a015800.
32. Sato N, Mizumoto K, Nakamura M, Nakamura K, Kusumoto M, Niiyama H, et al. Centrosome abnormalities in pancreatic ductal carcinoma. Clin Cancer Res. 1999;5(5):963-70.
33. Pihan GA, Purohit A, Wallace J, Knecht H, Woda B, Quesenberry P, et al. Centrosome defects and genetic instability in malignant tumors. Cancer Res. 1998;58(17):3974-85.
34. Kinoshita K, Noetzel TL, Pelletier L, Mechtler K, Drechsel DN, Schwager A, et al. Aurora A phosphorylation of TACC3/maskin is required for centrosome-dependent microtubule assembly in mitosis. J Cell Biol. 2005;170(7):1047-55.
35. Bruinsma W, Macurek L, Freire R, Lindqvist A, Medema RH. Bora and Aurora-A continue to activate Plk1 in mitosis. J Cell Sci. 2014;127(Pt 4):801-11.
36. Gheghiani L, Loew D, Lombard B, Mansfeld J, Gavet O. PLK1 Activation in Late G2 Sets Up Commitment to Mitosis. Cell Rep. 2017;19(10):2060-73.
37. Dutertre S, Cazales M, Quaranta M, Froment C, Trabut V, Dozier C, et al. Phosphorylation of CDC25B by Aurora-A at the centrosome contributes to the G2-M transition. J Cell Sci. 2004;117(Pt 12):2523-31.
38. Timofeev O, Cizmecioglu O, Settele F, Kempf T, Hoffmann I. Cdc25 phosphatases are required for timely assembly of CDK1-cyclin B at the G2/M transition. J Biol Chem. 2010;285(22):16978-90.

39. Ghadimi BM, Sackett DL, Difilippantonio MJ, Schrock E, Neumann T, Jauho A, et al. Centrosome amplification and instability occurs exclusively in aneuploid, but not in diploid colorectal cancer cell lines, and correlates with numerical chromosomal aberrations. Genes Chromosomes Cancer. 2000;27(2):183-90.
40. Jusino S, Fernandez-Padin FM, Saavedra HI. Centrosome aberrations and chromosome instability contribute to tumorigenesis and intra-tumor heterogeneity. J Cancer Metastasis Treat. 2018;4.
41. Meraldi P, Honda R, Nigg EA. Aurora-A overexpression reveals tetraploidization as a major route to centrosome amplification in p53-/- cells. EMBO J. 2002;21(4):483-92.
42. Rivlin N, Brosh R, Oren M, Rotter V. Mutations in the p53 Tumor Suppressor Gene: Important Milestones at the Various Steps of Tumorigenesis. Genes Cancer. 2011;2(4):466-74.
43. Lin X, Xiang X, Hao L, Wang T, Lai Y, Abudoureyimu M, et al. The role of Aurora-A in human cancers and future therapeutics. Am J Cancer Res. 2020;10(9):2705-29.
44. Asteriti IA, Giubettini M, Lavia P, Guarguaglini G. Aurora-A inactivation causes mitotic spindle pole fragmentation by unbalancing microtubule-generated forces. Mol Cancer. 2011;10:131.
45. Ferrari S, Marin O, Pagano MA, Meggio F, Hess D, El-Shemerly M, et al. Aurora-A site specificity: a study with synthetic peptide substrates. Biochem J. 2005;390(Pt 1):293-302.
46. Wang J, Nikhil K, Viccaro K, Chang L, Jacobsen M, Sandusky G, et al. The Aurora-A-Twist1 axis promotes highly aggressive phenotypes in pancreatic carcinoma. J Cell Sci. 2017;130(6):1078-93.
47. Mani RS. The emerging role of speckle-type POZ protein (SPOP) in cancer development. Drug Discov Today. 2014;19(9):1498-502.
48. Shi Q, Zhu Y, Ma J, Chang K, Ding D, Bai Y, et al. Prostate Cancer-associated SPOP mutations enhance cancer cell survival and docetaxel resistance by upregulating Caprin1-dependent stress granule assembly. Mol Cancer. 2019;18(1):170.
49. Nikhil K, Kamra M, Raza A, Haymour HS, Shah K. Molecular Interplay between AURKA and SPOP Dictates CRPC Pathogenesis via Androgen Receptor. Cancers (Basel). 2020;12(11).

50. Wang J, Nikhil K, Viccaro K, Chang L, White J, Shah K. Phosphorylation-dependent regulation of ALDH1A1 by Aurora kinase A: insights on their synergistic relationship in pancreatic cancer. BMC Biol. 2017;15(1):10.
51. Nikhil K, Raza A, Haymour HS, Flueckiger BV, Chu J, Shah K. Aurora Kinase A-YBX1 Synergy Fuels Aggressive Oncogenic Phenotypes and Chemoresistance in Castration-Resistant Prostate Cancer. Cancers (Basel). 2020;12(3).
52. Johnson EO, Chang KH, de Pablo Y, Ghosh S, Mehta R, Badve S, et al. PHLDA1 is a crucial negative regulator and effector of Aurora A kinase in breast cancer. J Cell Sci. 2011;124(16):2711-22.
53. Karthigeyan D, Prasad SB, Shandilya J, Agrawal S, Kundu TK. Biology of Aurora A kinase: implications in cancer manifestation and therapy. Med Res Rev. 2011;31(5):757-93.
54. Cheng A, Zhang P, Wang B, Yang D, Duan X, Jiang Y, et al. Aurora-A mediated phosphorylation of LDHB promotes glycolysis and tumor progression by relieving the substrate-inhibition effect. Nat Commun. 2019;10(1):5566.
55. Zhong Y, Yang J, Xu WW, Wang Y, Zheng CC, Li B, et al. KCTD12 promotes tumorigenesis by facilitating CDC25B/CDK1/Aurora A-dependent G2/M transition. Oncogene. 2017;36(44):6177-89.
56. Johnson EO, Chang K-H, Ghosh S, Venkatesh C, Giger K, Low PS, et al. LIMK2 is a crucial regulator and effector of Aurora-A-kinase-mediated malignancy. J Cell Sci. 2012;125(Pt 5):1204-16.
57. Shah K, Shokat KM. A chemical genetic approach for the identification of direct substrates of protein kinases. Methods Mol Biol. 2003;233:253-71.
58. Forgacs G, Yook SH, Janmey PA, Jeong H, Burd CG. Role of the cytoskeleton in signaling networks. J Cell Sci. 2004;117(Pt 13):2769-75.
59. Mizuno K, Okano I, Ohashi K, Nunoue K, Kuma K, Miyata T, et al. Identification of a Human Cdna-Encoding a Novel Protein-Kinase with 2 Repeats of the Lim Double Zinc-Finger Motif. Oncogene. 1994;9(6):1605-12.
60. Hanks SK, Quinn AM, Hunter T. The Protein-Kinase Family - Conserved Features and Deduced Phylogeny of the Catalytic Domains. Science. 1988;241(4861):42-52.
61. Nunoue K, Ohashi K, Okano I, Mizuno K. LIMK-1 and LIMK-2, two members of a LIM motif-containing protein kinase family. Oncogene. 1995;11(4):701-10.

62. Koshimizu U, Takahashi H, Yoshida MC, Nakamura T. cDNA cloning, genomic organization, and chromosomal localization of the mouse LIM motif-containing kinase gene, Limk2. Biochem Biophys Res Commun. 1997;241(2):243-50.
63. Okano I, Hiraoka J, Otera H, Nunoue K, Ohashi K, Iwashita S, et al. Identification and characterization of a novel family of serine threonine kinases containing two N-terminal LIM motifs. J Biol Chem. 1995;270(52):31321-30.
64. Ray S, Fanti JA, Macedo DP, Larsen M. LIM kinase regulation of cytoskeletal dynamics is required for salivary gland branching morphogenesis. Mol Biol Cell. 2014;25(16):2393-407.
65. Nomoto S, Tatematsu Y, Takahashi T, Osada H. Cloning and characterization of the alternative promoter regions of the human LIMK2 gene responsible for alternative transcripts with tissue-specific expression. Gene. 1999;236(2):259-71.
66. Osada H, Hasada K, Inazawa J, Uchida K, Ueda R, Takahashi T, et al. Subcellular localization and protein interaction of the human LIMK2 gene expressing alternative transcripts with tissue-specific regulation. Biochem Biophys Res Commun. 1996;229(2):582-9.
67. Vallee B, Cuberos H, Doudeau M, Godin F, Gosset D, Vourc'h P, et al. LIMK2-1, a new isoform of human LIMK2, regulates actin cytoskeleton remodeling via a different signaling pathway than that of its two homologs, LIMK2a and LIMK2b. Biochem J. 2018;475(23):3745-61.
68. Tastet J, Cuberos H, Vallee B, Toutain A, Raynaud M, Marouillat S, et al. LIMK2-1 is a Hominidae-Specific Isoform of LIMK2 Expressed in Central Nervous System and Associated with Intellectual Disability. Neuroscience. 2019;399:199-210.
69. Saito I, Ozawa H, Aono H, Ikebe T, Yamashita T, Makino Y. Trends in fatal coronary heart disease among people aged 25-74 years in Oita City, Japan, from 1987-1998. J Clin Epidemiol. 2002;55(5):469-76.
70. Gamell C, Schofield AV, Suryadinata R, Sarcevic B, Bernard O. LIMK2 mediates resistance to chemotherapeutic drugs in neuroblastoma cells through regulation of drug-induced cell cycle arrest. PLoS One. 2013;8(8):e72850.
71. Croft DR, Crighton D, Samuel MS, Lourenco FC, Munro J, Wood J, et al. p53-mediated transcriptional regulation and activation of the actin cytoskeleton regulatory RhoC to LIMK2 signaling pathway promotes cell survival. Cell Res. 2011;21(4):666-82.

72. Brown S, Coghill ID, McGrath MJ, Robinson PA. Role of LIM domains in mediating signaling protein interactions. IUBMB Life. 2001;51(6):359-64.
73. Hamill S, Lou HJ, Turk BE, Boggon TJ. Structural Basis for Noncanonical Substrate Recognition of Cofilin/ADF Proteins by LIM Kinases. Mol Cell. 2016;62(3):397-408.
74. Goyal P, Pandey D, Behring A, Siess W. Inhibition of nuclear import of LIMK2 in endothelial cells by protein kinase C-dependent phosphorylation at Ser-283. J Biol Chem. 2005;280(30):27569-77.
75. Hiraoka J, Okano I, Higuchi O, Yang N, Mizuno K. Self-association of LIM-kinase 1 mediated by the interaction between an N-terminal LIM domain and a C-terminal kinase domain. Febs Lett. 1996;399(1-2):117-21.
76. Harris BZ, Lim WA. Mechanism and role of PDZ domains in signaling complex assembly. J Cell Sci. 2001;114(18):3219-31.
77. Endicott JA, Noble MEM, Johnson LN. The Structural Basis for Control of Eukaryotic Protein Kinases. Annu Rev Biochem. 2012;81:587-613.
78. McClendon CL, Kornev AP, Gilson MK, Taylor SS. Dynamic architecture of a protein kinase (vol 111, pg E4623, 2014). P Natl Acad Sci USA. 2014;111(47):16973-.
79. Etienne-Manneville S, Hall A. Rho GTPases in cell biology. Nature. 2002;420(6916):629-35.
80. Maekawa M, Ishizaki T, Boku S, Watanabe N, Fujita A, Iwamatsu A, et al. Signaling from rho to the actin cytoskeleton through protein kinases ROCK and LIM-kinase. Science. 1999;285(5429):895-8.
81. Ohashi K, Nagata K, Maekawa M, Ishizaki T, Narumiya S, Mizuno K. Rho-associated kinase ROCK activates LIM-kinase 1 by phosphorylation at threonine 508 within the activation loop. J Biol Chem. 2000;275(5):3577-82.
82. Sumi T, Matsumoto K, Takai Y, Nakamura T. Cofilin phosphorylation and actin cytoskeletal dynamics regulated by Rho- and Cdc42-activated LIM-kinase 2. J Cell Biol. 1999;147(7):1519-32.
83. Goyal P, Pandey D, Siess W. Phosphorylation-dependent regulation of unique nuclear and nucleolar localization signals of LIM kinase 2 in endothelial cells. J Biol Chem. 2006;281(35):25223-30.

84. Yin JW, Wang G. The Mediator complex: a master coordinator of transcription and cell lineage development. Development. 2014;141(5):977-87.
85. Malik S, Roeder RG. The metazoan Mediator co-activator complex as an integrative hub for transcriptional regulation. Nat Rev Genet. 2010;11(11):761-72.
86. Huehn A, Cao WX, Elam WA, Liu XQ, De La Cruz EM, Sindelar CV. The actin filament twist changes abruptly at boundaries between bare and cofilin-decorated segments. J Biol Chem. 2018;293(15):5377-83.
87. DesMarais V, Ghosh M, Eddy R, Condeelis J. Cofilin takes the lead. J Cell Sci. 2005;118(1):19-26.
88. Moriyama K, Iida K, Yahara I. Phosphorylation of Ser-3 of cofilin regulates its essential function on actin. Genes Cells. 1996;1(1):73-86.
89. Scott RW, Olson MF. LIM kinases: function, regulation and association with human disease. J Mol Med (Berl). 2007;85(6):555-68.
90. Mikheeva SA, Mikheev AM, Petit A, Beyer R, Oxford RG, Khorasani L, et al. TWIST1 promotes invasion through mesenchymal change in human glioblastoma. Mol Cancer. 2010;9:194.
91. Qin Q, Xu Y, He T, Qin C, Xu J. Normal and disease-related biological functions of Twist1 and underlying molecular mechanisms. Cell Res. 2012;22(1):90-106.
92. Leptin M. Twist and Snail as Positive and Negative Regulators during Drosophila Mesoderm Development. Gene Dev. 1991;5(9):1568-76.
93. Nikhil K, Chang L, Viccaro K, Jacobsen M, McGuire C, Satapathy SR, et al. Identification of LIMK2 as a therapeutic target in castration resistant prostate cancer. Cancer Lett. 2019;448:182-96.
94. Nikhil K, Kamra M, Raza A, Shah K. Negative cross talk between LIMK2 and PTEN promotes castration resistant prostate cancer pathogenesis in cells and in vivo. Cancer Lett. 2021;498:1-18.
95. Nikhil K, Haymour HS, Kamra M, Shah K. Phosphorylation-dependent regulation of SPOP by LIMK2 promotes castration-resistant prostate cancer. Brit J Cancer. 2020.
96. Gebert LFR, MacRae IJ. Regulation of microRNA function in animals. Nat Rev Mol Cell Biol. 2019;20(1):21-37.

97. Liu M, Bi F, Zhou X, Zheng Y. Rho GTPase regulation by miRNAs and covalent modifications. Trends Cell Biol. 2012;22(7):365-73.
98. Chapnik E, Rivkin N, Mildner A, Beck G, Pasvolsky R, Metzl-Raz E, et al. miR-142 orchestrates a network of actin cytoskeleton regulators during megakaryopoiesis. Elife. 2014;3:e01964.
99. Wang W, Yang C, Nie H, Qiu X, Zhang L, Xiao Y, et al. LIMK2 acts as an oncogene in bladder cancer and its functional SNP in the microRNA-135a binding site affects bladder cancer risk. Int J Cancer. 2019;144(6):1345-55.
100. Huang YL, Li XH, Ma H, Yue HY, Hu XY. Metabolites of intestinal microflora upregulate miR-192-5p to suppress proliferation of colon cancer cells via RhoA-ROCK-LIMK2 pathway. Eur Rev Med Pharmacol Sci. 2020;24(4):1794-806.
101. Chen J, Ananthanarayanan B, Springer KS, Wolf KJ, Sheyman SM, Tran VD, et al. Suppression of LIM Kinase 1 and LIM Kinase 2 Limits Glioblastoma Invasion. Cancer Res. 2020;80(1):69-78.
102. Manetti F. LIM kinases are attractive targets with many macromolecular partners and only a few small molecule regulators. Med Res Rev. 2012;32(5):968-98.
103. Sleebs BE, Nikolakopoulos G, Street IP, Falk H, Baell JB. Identification of 5,6-substituted 4-aminothieno[2,3-d]pyrimidines as LIMK1 inhibitors. Bioorg Med Chem Lett. 2011;21(19):5992-4.
104. Ross-Macdonald P, de Silva H, Guo Q, Xiao H, Hung CY, Penhallow B, et al. Identification of a nonkinase target mediating cytotoxicity of novel kinase inhibitors. Mol Cancer Ther. 2008;7(11):3490-8.
105. Harrison BA, Almstead ZY, Burgoon H, Gardyan M, Goodwin NC, Healy J, et al. Discovery and Development of LX7101, a Dual LIM-Kinase and ROCK Inhibitor for the Treatment of Glaucoma. Acs Med Chem Lett. 2015;6(1):84-8.
106. Harrison BA, Whitlock NA, Voronkov MV, Almstead ZY, Gu KJ, Mabon R, et al. Novel Class of LIM-Kinase 2 Inhibitors for the Treatment of Ocular Hypertension and Associated Glaucoma. J Med Chem. 2009;52(21):6515-8.
107. Shen MY, Zhou SY, Li YY, Li D, Hou TJ. Theoretical study on the interaction of pyrrolopyrimidine derivatives as LIMK2 inhibitors: insight into structure-based inhibitor design. Mol Biosyst. 2013;9(10):2435-46.

108. Goodwin NC, Cianchetta G, Burgoon HA, Healy J, Mabon R, Strobel ED, et al. Discovery of a Type III Inhibitor of LIM Kinase 2 That Binds in a DFG-Out Conformation. ACS Med Chem Lett. 2015;6(1):53-7.
109. Rawla P. Epidemiology of Prostate Cancer. World J Oncol. 2019;10(2):63-89.
110. Pollock PA, Ludgate A, Wassersug RJ. In 2124, half of all men can count on developing prostate cancer. Curr Oncol. 2015;22(1):10-2.
111. Saramaki O, Visakorpi T. Chromosomal aberrations in prostate cancer. Front Biosci-Landmrk. 2007;12:3287-301.
112. Hubbard GK, Mutton LN, Khalili M, McMullin RP, Hicks JL, Bianchi-Frias D, et al. Combined MYC Activation and Pten Loss Are Sufficient to Create Genomic Instability and Lethal Metastatic Prostate Cancer. Cancer Res. 2016;76(2):283-92.
113. Banerjee-Basu S, Baxevanis AD. Molecular evolution of the homeodomain family of transcription factors. Nucleic Acids Res. 2001;29(15):3258-69.
114. Gurel B, Ali TZ, Montgomery EA, Begum S, Hicks J, Goggins M, et al. NKX3.1 as a Marker of Prostatic Origin in Metastatic Tumors. Am J Surg Pathol. 2010;34(8):1097-105.
115. Lei QY, Jiao J, Xin L, Chang CJ, Wang SY, Gao J, et al. NKX3.1 stabilizes p53, inhibits AKT activation, and blocks prostate cancer initiation caused by PTEN loss. Cancer Cell. 2006;9(5):367-78.
116. Tan PY, Chang CW, Chng KR, Wansa KDSA, Sung W-K, Cheung E. Integration of regulatory networks by NKX3-1 promotes androgen-dependent prostate cancer survival. Mol Cell Biol. 2012;32(2):399-414.
117. Kim MJ, Cardiff RD, Desai N, Banach-Petrosky WA, Parsons R, Shen MM, et al. Cooperativity of Nkx3.1 and Pten loss of function in a mouse model of prostate carcinogenesis. Proc Natl Acad Sci U S A. 2002;99(5):2884-9.
118. Zhang P, Liu W, Zhang J, Guan H, Chen W, Cui X, et al. Gene expression profiles in the PC-3 human prostate cancer cells induced by NKX3.1. Mol Biol Rep. 2010;37(3):1505-12.
119. Ren S, Kang MR, Wang J, Huang V, Place RF, Sun Y, et al. Targeted induction of endogenous NKX3-1 by small activating RNA inhibits prostate tumor growth. Prostate. 2013;73(14):1591-601.
120. Rawla P. Epidemiology of Prostate Cancer. World J Oncol. 2019;10(2):63-89.

121. Wang Y, Qin Z, Wang Y, Chen C, Wang Y, Meng X, et al. The role of radical prostatectomy for the treatment of metastatic prostate cancer: a systematic review and meta-analysis. Biosci Rep. 2018;38(1).
122. Mizokami A, Namiki M. Reconsideration of progression to CRPC during androgen deprivation therapy. J Steroid Biochem Mol Biol. 2015;145:164-71.
123. Hu R, Denmeade SR, Luo J. Molecular processes leading to aberrant androgen receptor signaling and castration resistance in prostate cancer. Expert Rev Endocrinol Metab. 2010;5(5):753-64.
124. Toren PJ, Gleave ME. Novel non-AR therapeutic targets in castrate resistant prostate cancer. Transl Androl Urol. 2013;2(3):265-77.
125. Beltran H, Rickman DS, Park K, Chae SS, Sboner A, MacDonald TY, et al. Molecular characterization of neuroendocrine prostate cancer and identification of new drug targets. Cancer Discov. 2011;1(6):487-95.
126. Tang A, Gao K, Chu L, Zhang R, Yang J, Zheng J. Aurora kinases: novel therapy targets in cancers. Oncotarget. 2017;8(14):23937-54.
127. Abate-Shen C, Shen MM, Gelmann E. Integrating differentiation and cancer: the Nkx3.1 homeobox gene in prostate organogenesis and carcinogenesis. Differentiation. 2008;76(6):717-27.
128. Song LN, Silva J, Koller A, Rosenthal A, Chen EI, Gelmann EP. The Tumor Suppressor NKX3.1 Is Targeted for Degradation by DYRK1B Kinase. Mol Cancer Res. 2015;13(5):913-22.
129. Bhatia-Gaur R, Donjacour AA, Sciavolino PJ, Kim M, Desai N, Young P, et al. Roles for Nkx3.1 in prostate development and cancer. Genes Dev. 1999;13(8):966-77.
130. Gurel B, Ali TZ, Montgomery EA, Begum S, Hicks J, Goggins M, et al. NKX3.1 as a marker of prostatic origin in metastatic tumors. Am J Surg Pathol. 2010;34(8):1097-105.
131. Kivinummi K, Urbanucci A, Leinonen K, Tammela TLJ, Annala M, Isaacs WB, et al. The expression of AURKA is androgen regulated in castration-resistant prostate cancer. Sci Rep. 2017;7(1):17978.